

NASA CONTRACTOR REPORT



NASA CR-1

0060384



TECH LIBRARY KAFB, NM

NASA CR-1097

LOAN COPY: RETURN TO
AFWL (WLIL-2)
KIRTLAND AFB, N MEX

Cb-I_{Zr} SODIUM THERMAL CONVECTION LOOP

by E. E. Hoffman and J. Holowach

Prepared by

GENERAL ELECTRIC COMPANY

Cincinnati, Ohio

for Lewis Research Center

NATIONAL AERONAUTICS AND SPACE ADMINISTRATION • WASHINGTON, D. C. • SEPTEMBER 1968



0060384

NASA CR-1097

Cb-1Zr SODIUM THERMAL CONVECTION LOOP

By **E. E. Hoffman** and **J. Holowach**

Distribution of this report is provided in the interest of information exchange. Responsibility for the contents resides in the author or organization that prepared it.

Prepared under Contract No. NAS 3-2547 by
GENERAL ELECTRIC COMPANY
Cincinnati, Ohio

for Lewis Research Center

NATIONAL AERONAUTICS AND SPACE ADMINISTRATION

For sale by the Clearinghouse for Federal Scientific and Technical Information
Springfield, Virginia 22151 - CFSTI price \$3.00

FOREWORD

The work described herein was performed by the General Electric Company under NASA Contract NAS 3-2547. The purpose was to design, construct, test, and evaluate a Cb-1Zr loop in which sodium was circulated by thermal convection for 1000 hours. Components to be evaluated in this experiment included electrical power vacuum feedthroughs, thermocouples, the method of attaching heater electrodes, the electrical resistivity characteristics of the heater segment, and the use of thermal and electrical insulation. Mr. T. A. Moss and Mr. R. L. Davies, Space Power Systems Division, Lewis Research Center, were the Technical Managers for the National Aeronautics and Space Administration. The report was originally issued as General Electric Report R67SD3014.

ABSTRACT

A sodium thermal convection loop constructed of Cb-1Zr was tested for 1000 hours at temperatures up to 2380°F. The purpose of the experiment was to evaluate several of the components selected for subsequent use in a two-loop Cb-1Zr facility in which liquid sodium was to circulate in a primary loop and potassium was to circulate in a two-phase secondary loop. In general, the components tested performed satisfactorily. No significant corrosion of the Cb-1Zr by the high temperature sodium was observed and the level of the vacuum environment maintained during the experiment prevented deleterious contamination of the Cb-1Zr tubing. The results of chemical analysis indicated a migration of the oxygen in the Cb-1Zr tubing from the hottest regions of the loop to the cooler regions.

TABLE OF CONTENTS

<u>SECTION</u>		<u>PAGE</u>
	FOREWORD	iii
	ABSTRACT	v
I	INTRODUCTION	1
II	LOOP DESIGN.	4
III	MATERIAL PROCUREMENT	8
IV	LOOP FABRICATION	10
V	TEST EQUIPMENT	17
	A. Vacuum System.	17
	B. Heater Power Supply.	19
	C. Partial Pressure Gas Analyzer.	21
	D. Chamber Pressure Measurement	21
VI	SODIUM PURIFICATION AND FILLING OF THE LOOP.	22
VII	LOOP INSTALLATION AND INSTRUMENTATION.	24
	A. Installation	24
	B. Thermal Insulation	27
	C. Instrumentation.	29
VIII	TEST OPERATION	37
	A. Test Conditions.	41
	B. Test Chamber Environment	45
	1. Ionization Gauge Pressure Observations	45
	2. Partial Pressure Observations.	48
IX	TEST SHUTDOWN, DRAINING AND DISASSEMBLY OF THE LOOP.	55
X	CHEMICAL AND METALLURGICAL EVALUATION OF TEST COMPONENTS	61
	A. Results of Chemical Analysis of Cb-1Zr Tubing.	61
	B. Results of Examination of Cb-1Zr Components.	66
	C. Results of Bend Tests of Tube Specimens.	73
	D. Results of Microhardness Survey of Tube Specimens.	76

TABLE OF CONTENTS (Continued)

<u>SECTION</u>		<u>PAGE</u>
XI	EVALUATION OF COMPONENT PERFORMANCE AND INSTALLATION PROCEDURES	78
XII	SUMMARY AND CONCLUSIONS.	81
XIII	PUBLISHED REPORTS.	82
XIV	APPENDICES	
	A. Drawing List and Drawings of the Sodium Thermal Con- vection Loop Test.	83
	B. Loop Design.	101
	C. Grain Growth Studies on Cb-1Zr Tubing.	117
XV	REFERENCES	123

LIST OF ILLUSTRATIONS

<u>Figure No.</u>		<u>Page No.</u>
1	Cb-1Zr Sodium Thermal Convection Loop Test	5
2	Machined Parts of the Sodium Thermal Convection Loop Prior to Welding	11
3	Vacuum Purge Welding Chamber in Which the Cb-1Zr Sodium Thermal Convection Loop Was Welded	12
4	Refractory Metal Furnace Used to Perform Local Heat Treatments of Cb-1Zr Weldments in the Vacuum-Purge Welding Chamber.	13
5	Cb-1Zr Sodium Thermal Convection Loop Following Fabrication. .	15
6	Type 304L SS Support Structure for the Sodium Thermal Convection Loop	16
7	High Vacuum System (10^{-10} Torr Range) Used to Test the Sodium Thermal Convection Loop. The Chamber is 18 Inches in Diameter and 30 Inches High and Incorporates a 1000 l/sec Getter-Ion Pump and 3 Adsorption Pumps.	18
8	Water Cooled, 1000-Ampere Electrical Power Feedthrough	20
9	Sodium Thermal Convection Loop Purification and Fill System. .	23
10	Sodium Thermal Convection Loop Following Mounting of the Loop and the Support Structure in the Test Chamber.	25
11	Sodium Thermal Convection Loop Test Facility With Associated Instrumentation and Power Control Equipment.	26
12	Dimpling of 0.5-Inch Wide x 0.002-Inch Thick Cb-1Zr Foil for use in Insulating Loop Components. Enlarged View of Dimpled Foil Shown	28
13	Sodium Thermal Convection Loop Showing the Location and Number of Layers of Dimpled Cb-1Zr Foil Used to Insulate the Various Regions of the Loop. Nominal Temperatures of Several Regions of the Loop are also Indicated	30
14	Thermal emf of W-3%Re/W-25%Re Wire Used to Instrument the Sodium Thermal Convection Loop	32

LIST OF ILLUSTRATIONS (Cont)

<u>Figure No.</u>		<u>Page No.</u>
15	Thermocouple Circuit and Location of W-3%Re/W-25%Re Thermocouples on the Sodium Convection Loop.	33
16	Method Used to Install W-3%Re/W-25%Re Thermocouple Wires on Cb-1Zr Alloy Tubing.	35
17	Method Used to Install W-3%Re/W-25%Re Thermocouple Wires in High Vacuum Feedthrough Flanges.	36
18	Temperatures of the Sodium Thermal Convection Loop During the 0-to-509 Hour Test Period.	42
19	Temperatures of the Sodium Thermal Convection Loop During the 509-to-1000-Hour Test Period	43
20	Temperatures Along the Top Heater Electrode Bar of the Sodium Thermal Convection Loop	44
21	Pressure in Test Chamber During 1000-Hour Sodium Thermal Convection Loop Test as Indicated by Ionization Gauge. Test was Shutdown After 509-Hours Operation to Modify Instrumentation	47
22	Vacuum Chamber Pressures During the First Period (0-to-509 Hours) of Operation of the Sodium Thermal Convection Loop Test	53
23	Overall View of the Cb-1Zr Sodium Thermal Convection Loop Following Completion of the 1000-Hour Test. Photograph Taken Just After Removal of the Bell Jar Portion of the Vacuum Chamber	56
24	Top Heater Coil and Upper Portion of the Cb-1Zr Sodium Thermal Convection Loop Following the 1000-Hour Test and Prior to the Removal of Cb-1Zr Insulating Foil	57
25	Top Portion of the Cb-1Zr Sodium Thermal Convection Loop Following Completion of the 1000-Hour Test	58
26	Cb-1Zr Sodium Thermal Convection Loop Following 1000-Hour Test	60
27	Sodium Thermal Convection Loop Showing Location of the Cb-1Zr Specimens Taken for Metallurgical and Chemical Evaluation. Temperatures Indicated are Nominal Temperatures for the First Period (0-to-509 Hours) of Loop Operation.	62

LIST OF ILLUSTRATIONS (Cont)

<u>Figure No.</u>		<u>Page No.</u>
28	Microstructure of a Cross Section of the Cb-1Zr Tubing (0.375-Inch OD x 0.065-Inch Wall Thickness Before Test. . . .	67
29	Cross Sectional Photomicrographs of Cb-1Zr Tube From Region 4 Inches Below Middle Heater Electride (Near Region K in Figure 27).	68
30	Microstructure of a Cross Section of the Cb-1Zr Tube From the Middle of the Top Heater Coil (Region M in Figure 27)	70
31	Microstructure of a Cross Section of the Cb-1Zr Tube From the Heater Exit (Region O in Figure 27)	71
32	Microstructure of a Cross Section of the Cb-1Zr Tube From the Heater Inlet (Region H in Figure 27).	72
33	Cross Sections of Cb-1Zr Tube Bend Specimens From Various Regions of the Sodium Thermal Convection Loop. Temperatures Shown are the Temperatures of These Regions During the First Period (0-to-509 Hours) of Loop Operation	74
34	Cross Section of Cb-1Zr Tube Bend Specimen From Region O (2075°F) of the Loop. The Transgranular Nature of the Cracking is Very Evident in the Enlarged View	75
35	Microhardness Gradients of Cb-1Zr Tube Specimens from Various Regions of the Sodium Thermal Convection Loop	77
36	Sodium Thermal Convection Loop Assembly	84
37	Heater Coil Assembly.	85
38	Heater Coil Installation.	86
39	Tee	88
40	Surge Tank.	89
41	Valve Tube.	90
42	Bimetallic Joint Component (Surge Tank Tube).	91
43	Bimetallic Joint.	93
44	Support Structure Assembly.	94

LIST OF ILLUSTRATIONS (Cont)

<u>Figure No.</u>		<u>Page No.</u>
45	Electrical Connector.	96
46	Bus Bar	97
47	Washer.	98
48	Sleeve.	99
49	Assemble Special Electric Feedthrough	100
50	Schematic Diagram of Thermal Convection Loop.	104
51	Temperature Distribution of the Cold Leg of the 0.375-Inch Diameter Cb-1Zr Tube (Emittance = 0.5) of the Sodium Thermal Convection Loop as a Function of the Heat Rejection Length. .	107
52	Variation of Terminal Temperature Ratio with Fin Plate Length.	113
53	Variation of Radiating Effectiveness with Fin Plate Length. .	114
54	Effect of Bend Diameter on the Maximum Fiber Strain in 0.375-Inch OD x 0.065-Inch.	119
55	Cross Section of 0.375-Inch OD x 0.065-Inch Wall Cb-1Zr Tube. The Recrystallized Tube was Bent Around a 3.5-Inch Diameter Die and Subsequently Annealed for 165 Hours at 2200°F	120
56	Micrograph of a Cross Section of 0.375-Inch Diameter x 0.065-Inch Thick Wall Cb-1Zr Alloy Tubing. The Recrystallized Tubing was Bent Around a 2.6-Inch Diameter Die and Subsequently Annealed for 1 Hour at 2200°F	122

LIST OF TABLES

<u>Table No.</u>		<u>Page No.</u>
I	Comparison of the Design Data for the Cb-1Zr Sodium Thermal Convection Loop and the Sodium Circuit of the Cb-1Zr Rankine System Corrosion Test	7
II	Results of Chemical Analysis of Cb-1Zr Materials Used to Fabricate the Sodium Thermal Convection Loop.	9
III	Operation History of the Sodium Thermal Convection Loop . . .	39
IV	Principal Test Conditions During the Two Test Periods of Operation of the Sodium Thermal Convection Loop	46
V	Increase in Pressure in the Sodium Thermal Convection Loop Chamber	49
VI	Ion Gauge Pressure Readings and the True Partial Pressures of the Various Residual Gases in the Test Chamber During Startup of the Sodium Thermal Convection Loop on February 24, 1964.	50
VII	Results of Partial Pressure Scans Made at End of First Period (0 to 509 Hours) of Loop Operation	52
VIII	Chemical Analyses of Various Cb-1Zr Tube Specimens from the Sodium Thermal Convection Loop.	63
IX	Summary of the Performance of the Principal Components Being Evaluated in the 1000-Hour Sodium Thermal Convection Loop Test.	79

Cb-1Zr SODIUM THERMAL CONVECTION LOOP

I. INTRODUCTION

This report describes the design, fabrication, instrumentation, operation, and evaluation of a Cb-1Zr thermal convection loop in which sodium was circulated for 1000 hours. This loop was the first test in a series of three which were included in this program. The primary purpose of the Potassium Corrosion Test Loop Development Program was to develop a prototype corrosion test loop for the evaluation of refractory alloys in boiling and condensing potassium environments which simulate projected space electric power systems.

The Cb-1Zr Rankine System Corrosion Test Loop experiment, which will be described in a subsequent topical report in this series, was to consist of a two-loop Cb-1Zr facility in which liquid sodium was pumped in the primary circuit and potassium was pumped and boiled in a two-phase secondary loop. The required operational conditions initially specified for the potassium circuit of the loop are listed below:

- a. Boiling temperature ~ 1900°F
- b. Superheat temperature - 2000°F
- c. Condensing temperature - 1350°F
- d. Subcooling temperature - 800°F
- e. Mass flow rate - 20 to 40 lb/hr
- f. Vapor impingement velocity on blades - 1000 ft/sec
- g. Test duration - 2500 hr*

The method chosen to heat the boiler of the Cb-1Zr Rankine System Corrosion Test Loop was the use of a primary or heater loop in which I²R** heated sodium was to be pumped through the outer annulus of a tube-in-tube counterflow boiler where the required heat was to be transferred to the potassium in the secondary,

* Test duration subsequently was extended to 5000 hours.

** I²R will be used to designate the self-resistance heater in this report.

two-phase circuit. One of the principal goals of this test program was to incorporate as many components as required to assure an accurate determination of the test conditions and thereby minimize the possibility of undetected test variations, e.g., high frequency boiling instabilities, which might compromise loop operation or the post-test compatibility evaluation.

In order to assure the optimum performance and reliability of the individual components of the Cb-1Zr Rankine System Corrosion Test Loop, a plan was established to evaluate as many of the critical loop components as was practical in two preliminary loop tests. These two loop tests were to be designed and operated in a manner to evaluate primarily the critical components associated with the all-liquid sodium heater circuit. Several of the reasons for this approach are listed below:

1. The higher operating temperatures and electrical power requirements of the sodium heater circuit might result in malfunction or degradation of critical components such as the EM pump.
2. Many of the components required for the potassium circuit, e.g., valves, pressure transducers, could be adequately evaluated in the single phase sodium systems.

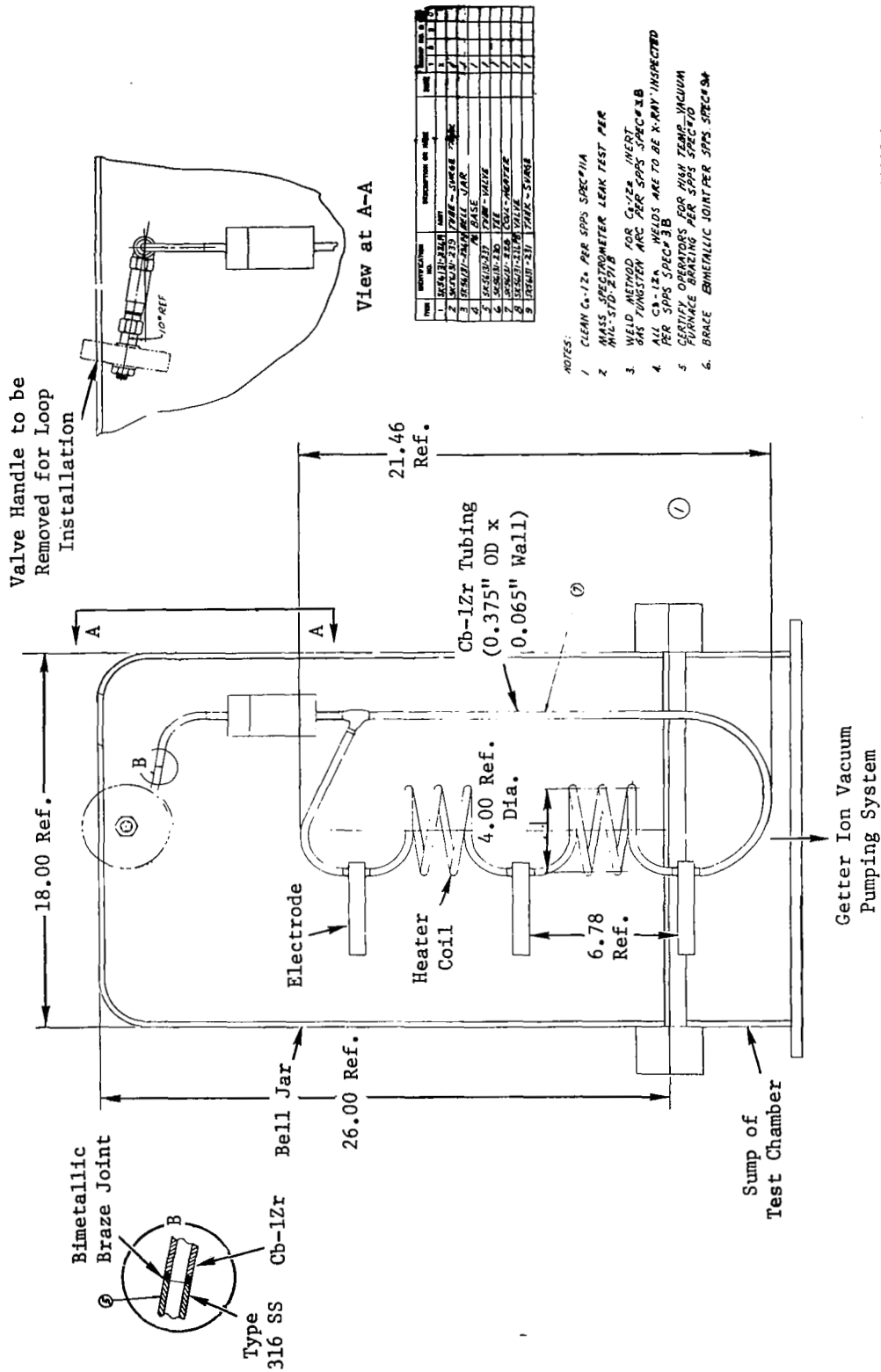
The two all-liquid sodium loops were originally designated Component Evaluation Test Loops I and II. These two loops will be referred to as the Cb-1Zr Sodium Thermal Convection Loop and the Cb-1Zr Pumped Sodium Loop in the topical reports covering these experiments. The thermal convection loop test is the subject of this report. It was specified that this loop was to be operated for 1000 hours at a maximum temperature of 2200°F to evaluate the electrical resistivity characteristics of the heater segment, the method of attaching the electrodes, the electrical power vacuum feedthroughs, thermocouple materials and procedures, and the performance of selected thermal and electrical insulation materials. In addition to these specific component evaluations, it was anticipated that the total pressure and partial pressure measuring instrumentation associated with the very low pressure test chamber environment (10^{-7} - 10^{-8} torr) would be evaluated and the extent of environmental contamination would be determined by post-test analysis of critical loop components.

The Cb-1Zr alloy was chosen by NASA as the primary material of loop construction for the entire Potassium Corrosion Test Loop Development Program based on its advanced state of commercial development and the indicated corrosion resistance of this alloy to high purity alkali metal environments. It was anticipated that subsequent to this program, refractory metal alloys having considerably greater high temperature strengths than Cb-1Zr could be evaluated in the two loop corrosion test system developed by this program.

II. LOOP DESIGN

The design of the Cb-1Zr Sodium Thermal Convection Loop was determined by a consideration of the Cb-1Zr Rankine System Corrosion Test Loop test components which could be evaluated in a test of this type and the test facilities available for such a loop. It was concluded that a thermal convection loop containing an I²R heater of the identical dimensions proposed for the sodium heater of the Rankine System Loop would be tested. The test loop would have overall dimensions, which could be accommodated in an available 26-inch high by 18-inch diameter getter-ion pumped high vacuum test chamber. These factors essentially determined the design of the test loop. Due to the limited heat rejection capabilities in a small, unpumped loop system of this type, it was realized that the sodium heater segment could not be operated at power levels comparable to those to be subsequently required for the Cb-1Zr Rankine System Corrosion Test Loop. On the other hand, the temperature levels to be required in the Cb-1Zr Corrosion Test Loop heater could easily be achieved in the low flow natural convection loop system. Although the I²R heater and the associated high electrical current vacuum feedthroughs associated with the heater were the principal components to be evaluated, this test also provided the opportunity to check out the instrumentation procedures associated with test loop temperature measurement and the techniques used to monitor the vacuum chamber total pressure and the partial pressures of the residual gases in the environment. This test was also to be useful in evaluating the effectiveness of the Cb-1Zr foil wrapping as a reflective insulating material as well as its usefulness in reducing possible contamination of the Cb-1Zr loop tubing by the test chamber environment.

The features of this loop are illustrated in Figure 1. The engineering drawings for the Cb-1Zr Sodium Thermal Convection Loop are included in Appendix A of this report. The flow circuit of the loop was constructed of Cb-1Zr. The heater consisted of two 4-inch diameter helical coils in series which formed the major portion of the hot leg of the loop. The heated sodium flowed upward through the heater coils and down the cold leg of the loop. Heat rejection from the cold leg was entirely by thermal radiation to the water-cooled walls of the vacuum chamber. A small surge tank at the top of the cold



C1218-1

Figure 1. Cb-12r Sodium Thermal Convection Loop Test.

leg served as an expansion chamber to accommodate the volumetric expansion of the sodium during the heating of the loop. A Type 316SS/Cb-1Zr bimetallic joint was located between the surge tank and the stainless steel bellows-type valve shown at the top of the loop. A gas pressurization line was attached to the surge tank which was used initially as the sodium fill line and during loop operation as an inert gas pressurization line to maintain the pressure in the loop above the saturation pressure of the sodium to prevent localized boiling in the heater. Boiling in the heater section was undesirable since it would result in unstable loop operation because of the change in the overall electrical resistance of the heater. Rapid changes in the resistance of the heater coils would result in severe power fluctuations. The change in density of sodium liquid to vapor would also affect the flow rate and contribute to loop instability. The stainless steel shut-off valve on the gas pressurization line was used during the initial installation and filling and was in the open position during loop operation.

The design calculations used to predict sodium flow rate, loop temperatures, power requirements, electrical characteristics of the I^2R heater and the internal pressure stresses in the loop are given in Appendix B. The design data resulting from this analysis are given in Table I. A listing of the design data for the sodium circuit of the Rankine System Corrosion Test Loop is also given for purpose of comparison.

TABLE I

COMPARISON OF THE DESIGN DATA FOR THE Cb-1Zr SODIUM THERMAL CONVECTION LOOP
AND THE SODIUM CIRCUIT OF THE Cb-1Zr RANKINE SYSTEM CORROSION TEST

	<u>Sodium Heater Circuit of the Cb-1Zr Rankine System Corrosion Test Loop</u>	<u>Cb-1Zr Sodium Thermal Convection Loop</u>
<u>Structural</u>		
Material	Cb-1Zr	Cb-1Zr
Tube diameter	0.375 inch*	0.375 inch
Wall thickness	0.065 inch*	0.065 inch
Flow area	0.00033 ft ²	0.00033 ft ²
<u>Fluid Flow</u>		
Coolant	Sodium	Sodium
Flow rate	824 lb/hr	16 lb/hr
Velocity in 0.25-inch ID tubing	16 ft/sec	0.3 ft/sec
Reynolds no.	159,000	3,100
Friction factor	0.0048	0.012
Pressure loss, total	15 psi	0.01 psi
<u>Heat Transfer - Heater</u>		
Heater length	73 in.	73 in.
Geometry	4 in. dia. coil	4 in. dia. coil
Temperature in	1950°F	1700°F
Temperature out	2100°F	2200°F
Power input	12 KW	0.7 KW
<u>Electrical</u>		
Current	2000 amp	650 amp
Potential	6 volts	2.7 volts
Power	12 KW	1.75 KW
<u>Stress</u>		
Internal pressure	190 psi	190 psia
Max. internal pressure stress	370 psi	370 psi

* Boiler portion of the sodium circuit, 1-inch OD x 0.1-inch wall thickness tubing.

III. MATERIAL PROCUREMENT

All portions of the Sodium Thermal Convection Loop which were to be in contact with sodium during the test were constructed of Cb-1Zr. The Cb-1Zr components were fabricated from 2-inch diameter bar (surge tank), 3-1/2-inch diameter bar (electrodes, fittings and bimetallic joint), and 3/8-inch OD x 0.065-inch wall tubing. With a few minor exceptions, the bar and tubing conformed to specifications used in procuring these materials. A more detailed discussion of the Quality Assurance Test Program and copies of the specifications used in procuring these materials may be found in the topical report which covered this phase of the Potassium Corrosion Test Loop Development Program⁽¹⁾. The results of chemical analyses of the various Cb-1Zr products used in the construction of the loop are given in Table II. As may be noted in Figure 1, the 3/8-inch OD tubing was used to form the entire loop circuit, with the exception of several small fittings. The tubing was received from the vendor in the recrystallized condition. The final annealing heat treatment of this material was 2200°F for one hour in vacuum.

(1) Frank, R. G., et al., Potassium Corrosion Test Loop Development Topical Report No. 2: Material and Process Specifications for Refractory Alloy and Alkali Metals, R66SD3007, December 13, 1965.

TABLE II
RESULTS OF CHEMICAL ANALYSIS OF Cb-1Zr MATERIALS USED
TO FABRICATE THE SODIUM THERMAL CONVECTION LOOP

	Chemical Analysis				w/o <u>Zr</u>
	ppm				
	<u>O</u>	<u>N</u>	<u>H</u>	<u>C</u>	
<u>Tubing, 3/8-Inch OD</u> <u>x 0.065-Inch Wall</u>					
Vendor ^a	123	15	6	46	1.0
GE-SPPS	114,136	1,9	1,4	20,30	---
<u>Bar, 2-Inch OD^b</u>					
Vendor	340	65	3,7	40	1.1,0.87 ^c
GE-SPPS	229,279	54,53	2,2	40,80	---
<u>Bar, 3-1/2-Inch OD</u>					
Vendor	340	65	3.7	40	1.1,0.87 ^c
GE-SPPS	306	58	3	130, <100	---

^a Analysis of 2-inch OD tube blank from which tubing was made.

^b 2-inch OD bar was formed by eloxing from 3-1/2-inch OD bar.

^c Ingot analysis.

IV. LOOP FABRICATION

The Sodium Thermal Convection Loop was made up principally of 3/8-inch OD x 0.065-inch wall Cb-1Zr tubing. Machined parts, including the surge tank and the fittings used to join the various tube segments, are shown in Figure 2. All the parts shown in the photograph are of Cb-1Zr, with the exception of the straight, grooved tube segments, which are the stainless steel portions of Cb-1Zr to Type 316SS bimetallic joints.

Assembly of the loop consisted of coiling and bending the tubing, joining the tube segments and the machined components by inert gas tungsten arc welding, heat treating the Cb-1Zr weldments, and brazing the Cb-1Zr to stainless steel bimetallic joint.

The equipment, operators and procedures used in the cleaning, welding, brazing, and heat treating operations were qualified in accordance with the applicable SPPS specifications prior to the initiation of loop fabrication. These specifications, which were included in an earlier topical report⁽¹⁾ on this program, are listed below.

- a. Chemical Cleaning of Columbium and Columbium Alloy Products, SPPS Specification No. 03-0010-00-B (SPPS-11A).
- b. Welding of Columbium-1% Zirconium Alloy by the Inert Gas Tungsten Arc Process, SPPS Specification No. 03-0004-00-B (SPPS-3B).
- c. Vacuum Brazing Bimetallic Tube Joints, SPPS Specification No. 03-0008-00-B (SPPS-9A).
- d. Operator Certification for High Temperature, Vacuum Furnace Brazing of Bimetallic Tube Joints, SPPS Specification No. 03-0009-00-A (SPPS-10).

The chamber in which the welding operations were performed is shown in Figure 3. This welding chamber and the post-weld heat treating furnace were qualified simultaneously in accordance to the welding specification listed above. The heat treatment of the weldments was done in the welding chamber using a specially constructed tungsten heater furnace of the type illustrated in Figure 4 or in a commercial vacuum furnace*. The brazing of the bimetallic joints was performed in the latter furnace.

* Richard D. Brew and Company, Incorporated, Model 424-B, Series 286.

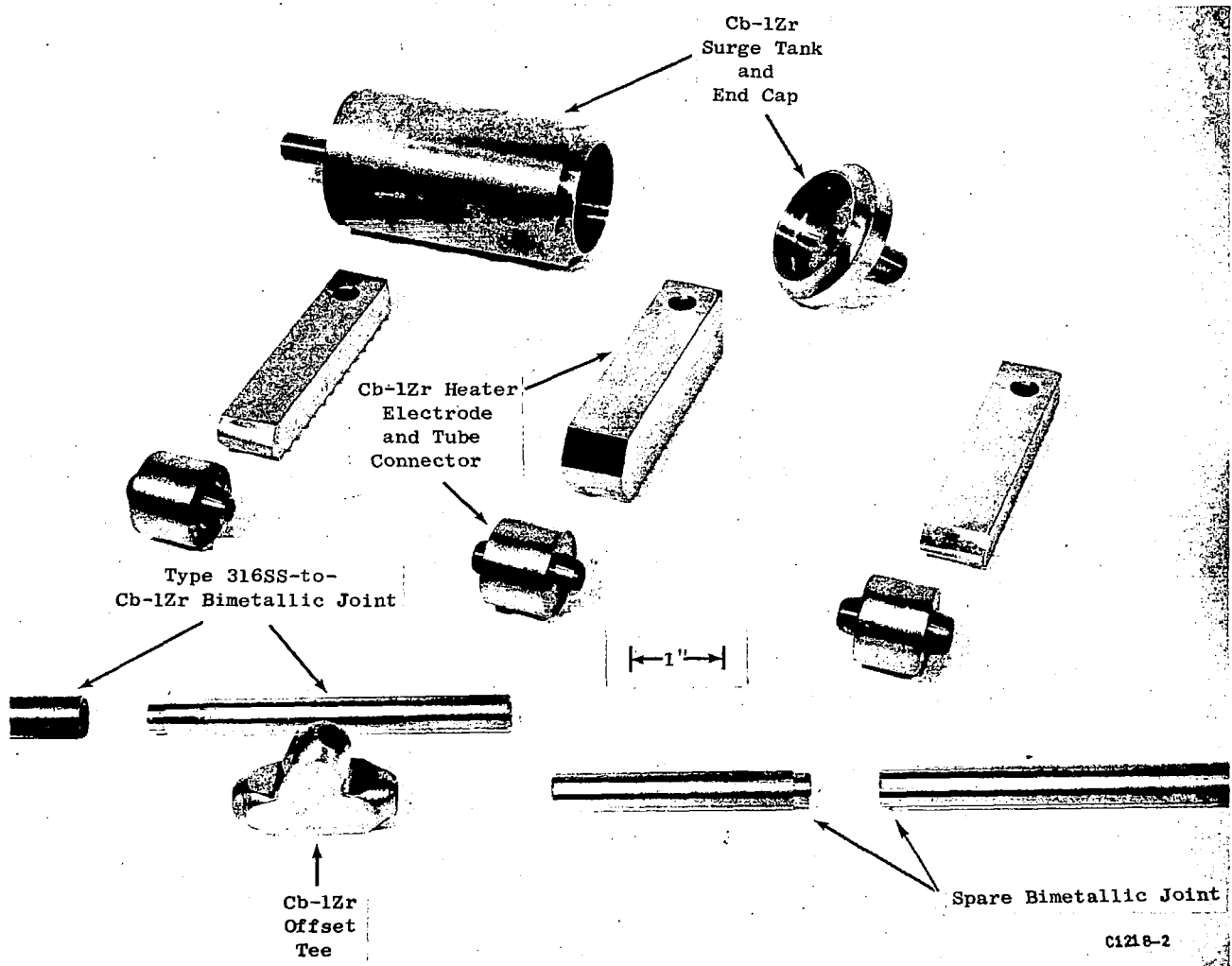


Figure 2. Machined Parts of the Sodium Thermal Convection Loop Prior to Welding.

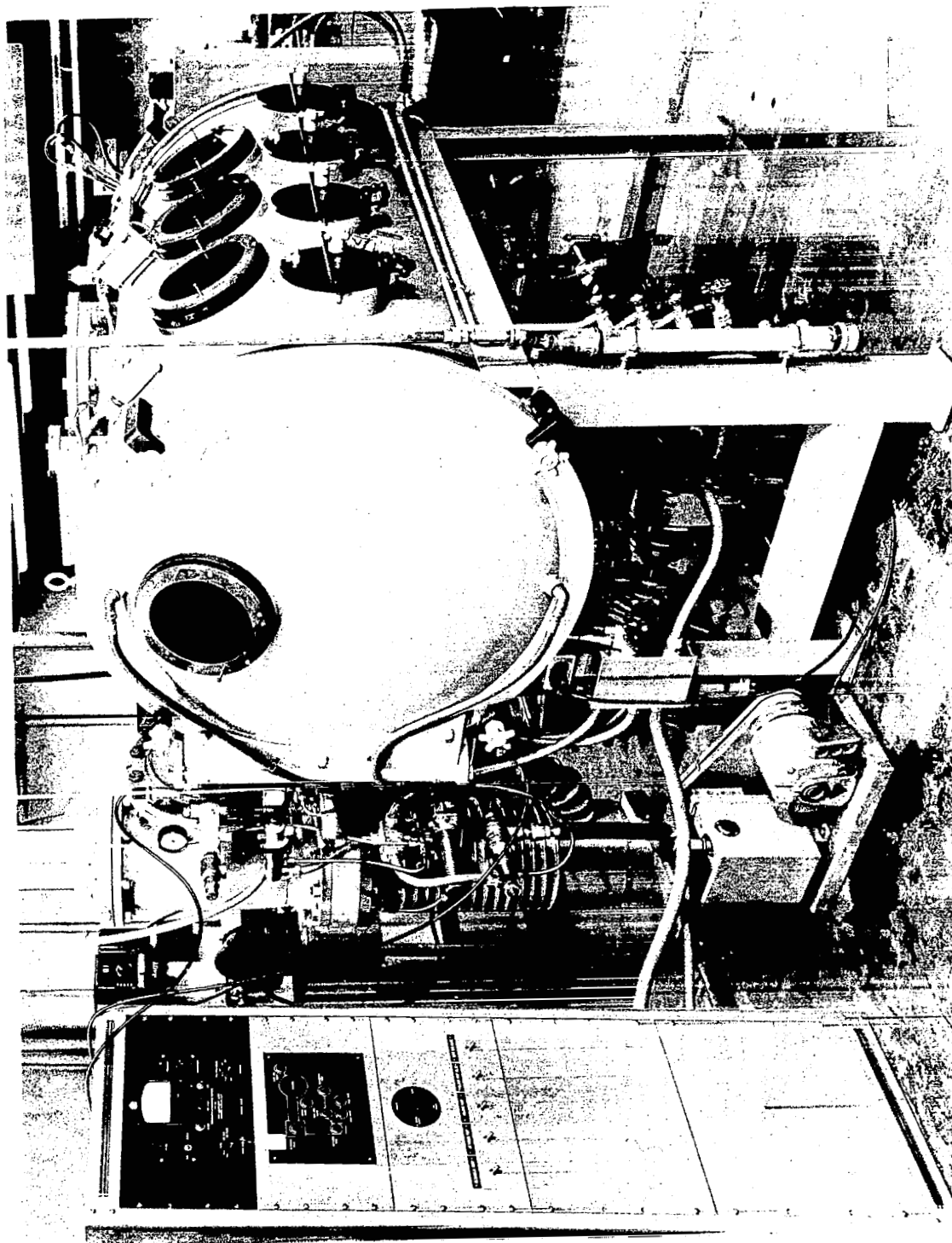
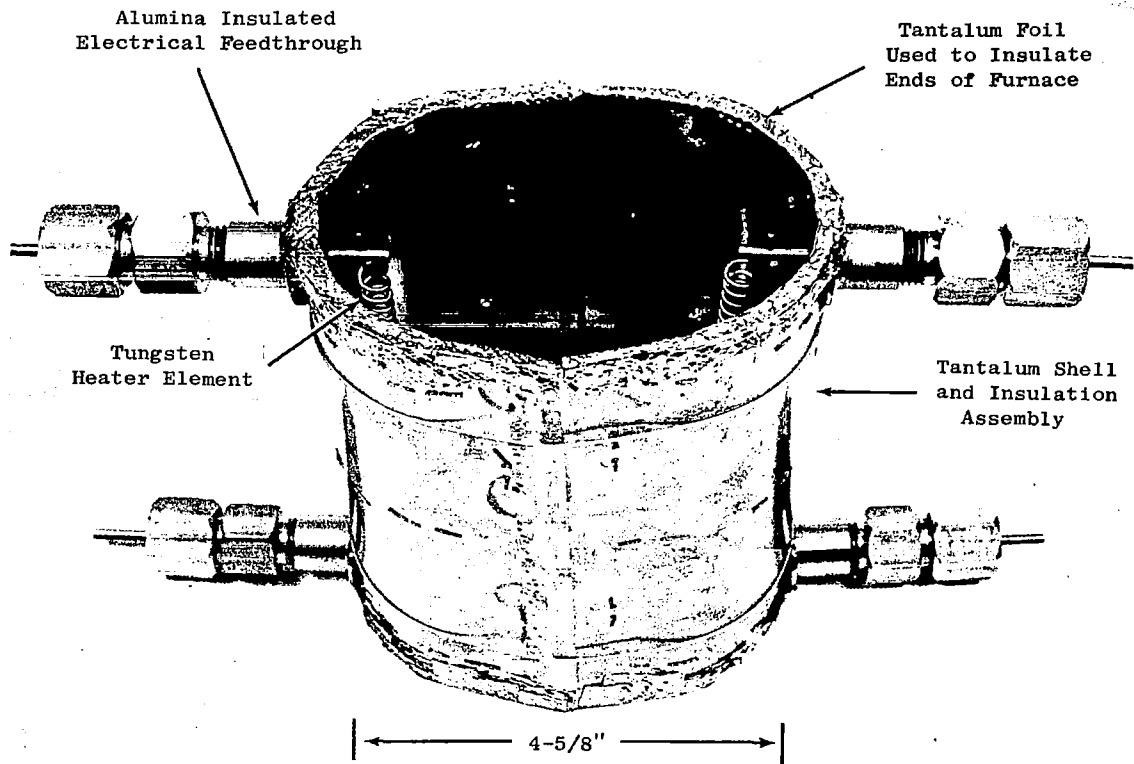


Figure 3. Vacuum Purge Welding Chamber in Which the Cb-12r Sodium Thermal Convection Loop Was Welded.



C1218-4

Figure 4. Refractory Metal Furnace Used to Perform Local Heat Treatments of Cb-1Zr Weldments in the Vacuum-Purge Welding Chamber.

All welded and brazed joints were inspected by X-ray and found to meet the specifications. The order of loop assembly was as follows:

- a. Three electrodes were welded to the tubing adaptors.
- b. The two halves of the surge tank were welded together, heat treated, and inspected.
- c. The bimetallic joint was brazed and inspected.
- d. The electrodes were welded to the tubing coils and loop legs and inspected.
- e. The offset tee fitting was welded to the bottom of the surge tank.
- f. The bimetallic joint was welded to the surge tank, and the weld was heat treated and inspected.
- g. The loop legs were welded to the tee fitting and inspected.
- h. The welds at the electrodes and tee were heat treated at the four locations using the tungsten heater furnace in the welding chamber.
- i. The stainless steel bellows isolation valve was joined to the stainless steel portion of the bimetallic joint by inert gas tungsten arc welding.

Following completion of fabrication, the loop was checked for leaks using a helium mass spectrometer leak detector with a sensitivity of 1.6×10^{-10} torr and no leaks were detected at maximum sensitivity. The completed loop ready for mounting on the loop support structure is shown in Figure 5. The upper portion of the loop was grit blasted with alumina to increase the emittance of this region to approximately 0.5. This was done to boost the radiation heat loss capability of this region of the loop. Grit blasting was performed in accordance with SPPS Specification No. 03-0011-00-A (SPPS-12), which was also included in the referenced topical report⁽¹⁾.

The support structure for the loop, which was constructed of Type 304L SS angle and plate, is shown in Figure 6. The stainless steel washers, nuts and bolts used to mount the various loop components were slotted to eliminate gas traps and aid in outgassing of the structure during test startup.

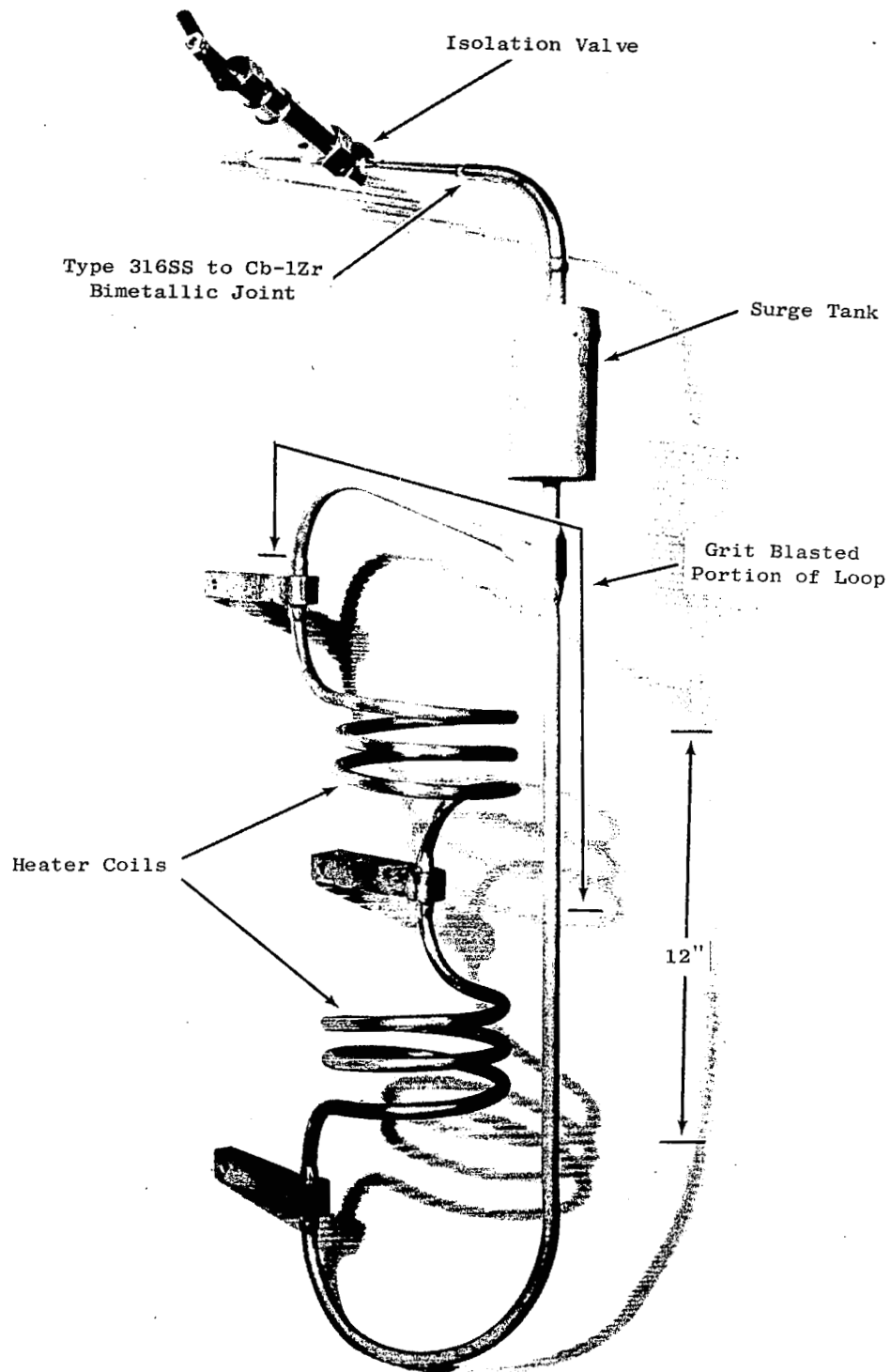


Figure 5. Cb-1Zr Sodium Thermal Convection Loop Following Fabrication.

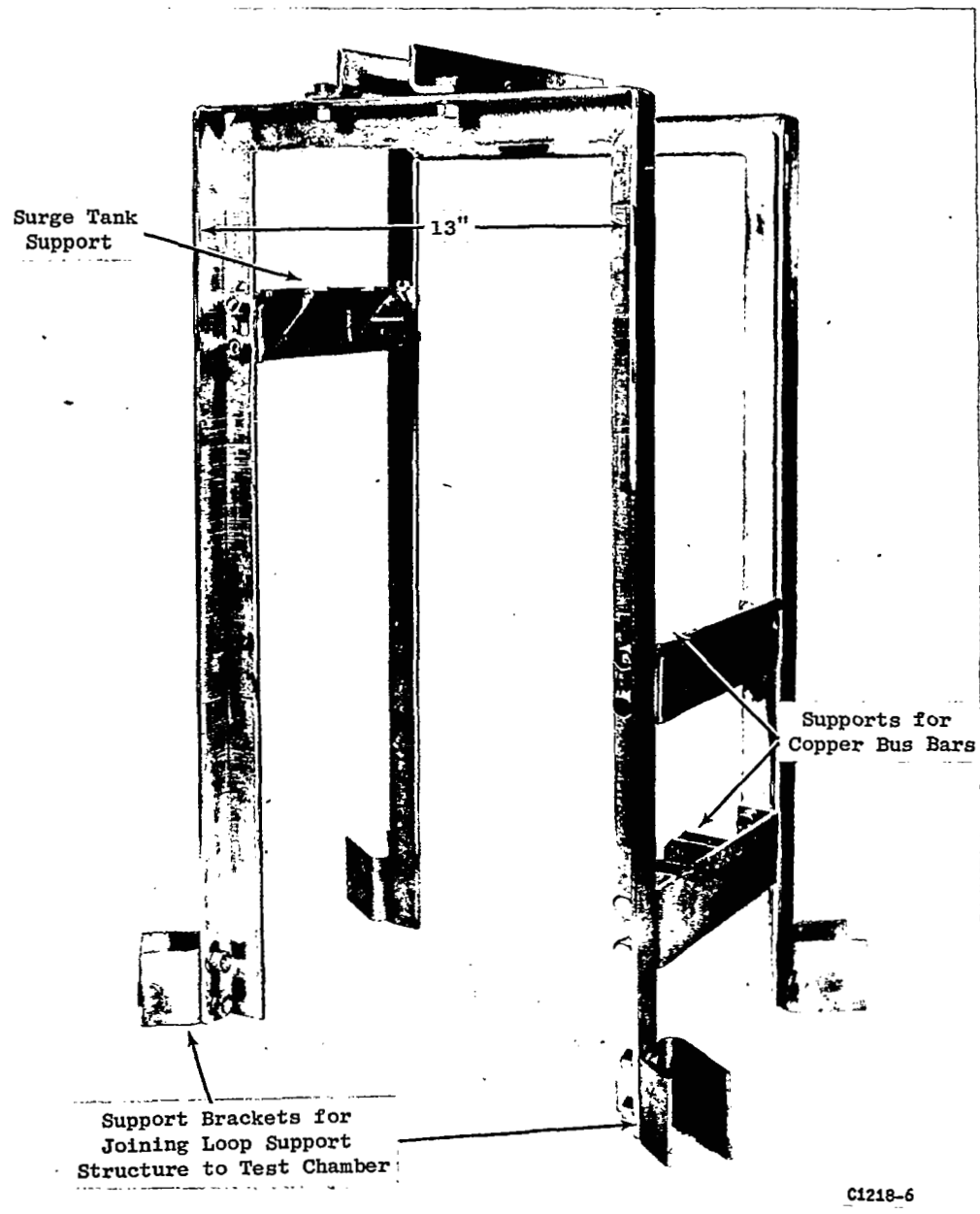


Figure 6. Type 304L SS Support Structure for the Sodium Thermal Convection Loop.

V. TEST EQUIPMENT

The principal items of test equipment used in operating the 1,000-hour Sodium Thermal Convection Loop Test included the vacuum chamber, the heater power and control system, and the partial pressure gas analyzer system.

A. Vacuum System

The vacuum chamber, shown in Figure 7, is of the bell jar construction fabricated by the Vacuum Products Section, General Electric Company. The chamber is thermally insulated with a polished aluminum shroud. Electrical resistance heating elements attached to the chamber wall permit continuous bakeout of the chamber to 500°F. The chamber also has sufficient water cooling coils welded to the wall to remove approximately 25 KW of heat during test operation.

Three molecular sieve sorption pumps are used to evacuate the chamber to the 1-10 micron range before the ion pumps can be turned on. The sorption pumps are equipped with an integral liquid nitrogen sump which is used to pre-chill the pumps before use. Prior to chilling, the sorption pumps are baked out to reactivate them. Heating of the sorption pumps after use accelerates the release of previously pumped gases from the molecular sieve to the atmosphere and readies them for the next pump-down cycle. A thermocouple gauge located on the sorption pump manifold is used to indicate the chamber pressure during sorption pumping. After rough pumping the system to less than 10 microns, a bakeable stainless steel valve is closed which isolates the sorption pumping manifold from the chamber proper.

The high vacuum pumping system consists of a 1,000 liter per second triode-type getter-ion pump and is capable of operating in the 10^{-3} to 10^{-10} torr range. The triode-type pumps have superior pumping speed for the rare gases and do not exhibit the argon instability sometimes observed in diode-type ion pumped systems. The pumping speed characteristics of the triode pump are given below. The pumping speeds for various gases are relative to air taken as 100%.

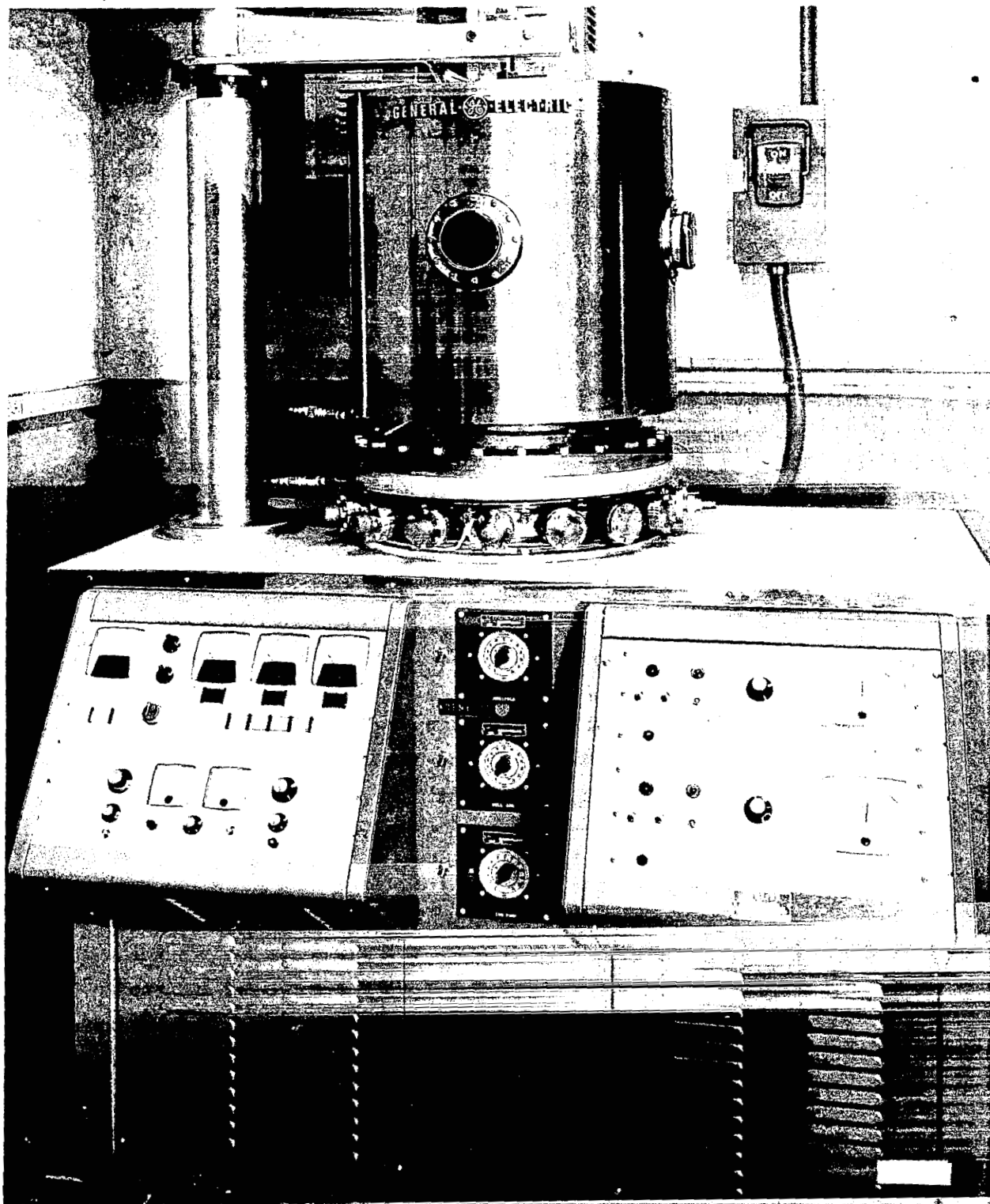


Figure 7. High Vacuum System (10^{-10} Torr Range) Used to Test the Sodium Thermal Convection Loop. The Chamber is 18 Inches in Diameter and 30 Inches High and Incorporates a 1000 l/sec Getter-Ion Pump and 3 Adsorption Pumps.

Hydrogen	200%	Light hydrocarbons	95-105%
Nitrogen	95%	Water vapor	100%
Oxygen	57%	Helium	30%
Carbon dioxide	100%	Argon	30%

The bell jar section of the chamber is raised and lowered by a motor driven screw jack. A bakeable glass viewing port is mounted on the bell jar. The glass face is made from optically flat plate 1/4-inch thick which made it possible to obtain high quality color photographs of the loop during test operation.

Twelve 2-3/4-inch OD instrumentation penetrations are located circumferentially around the base plate. These include six octal tube thermocouple feedthroughs^{*}, two 1,000-ampere electrical power feedthroughs^{**}, and an argon pressurization line for the loop. A photograph of the water-cooled, electrical power feedthrough is shown in Figure 8. All flanges are sealed with flat OFHC copper gaskets and are capable of withstanding prolonged bakeouts at 800°F.

B. Heater Power Supply

The heater power supply consisted of a combined temperature controller and stepless power regulator system with a stepdown current transformer. The system had a continuous power rating of 20 KW with an input power of single phase 440 volt AC. The combined temperature controller and power regulator include:

1. A manual power adjustment
2. Automatic set point control
3. Current limiter control

The system included a single pen, 1/4 percent, null balance, servo operated recording potentiometer with a GE Model 524 controller (3-mode proportional control, with rate action and automatic reset) and an amplistat plus a saturable core reactor and current transformer. The system functioned as follows:

* Varian Associates, Vacuum Products Division, Model 954-5015

** Varian Associates, Vacuum Products Division, Dwg. No. 608907

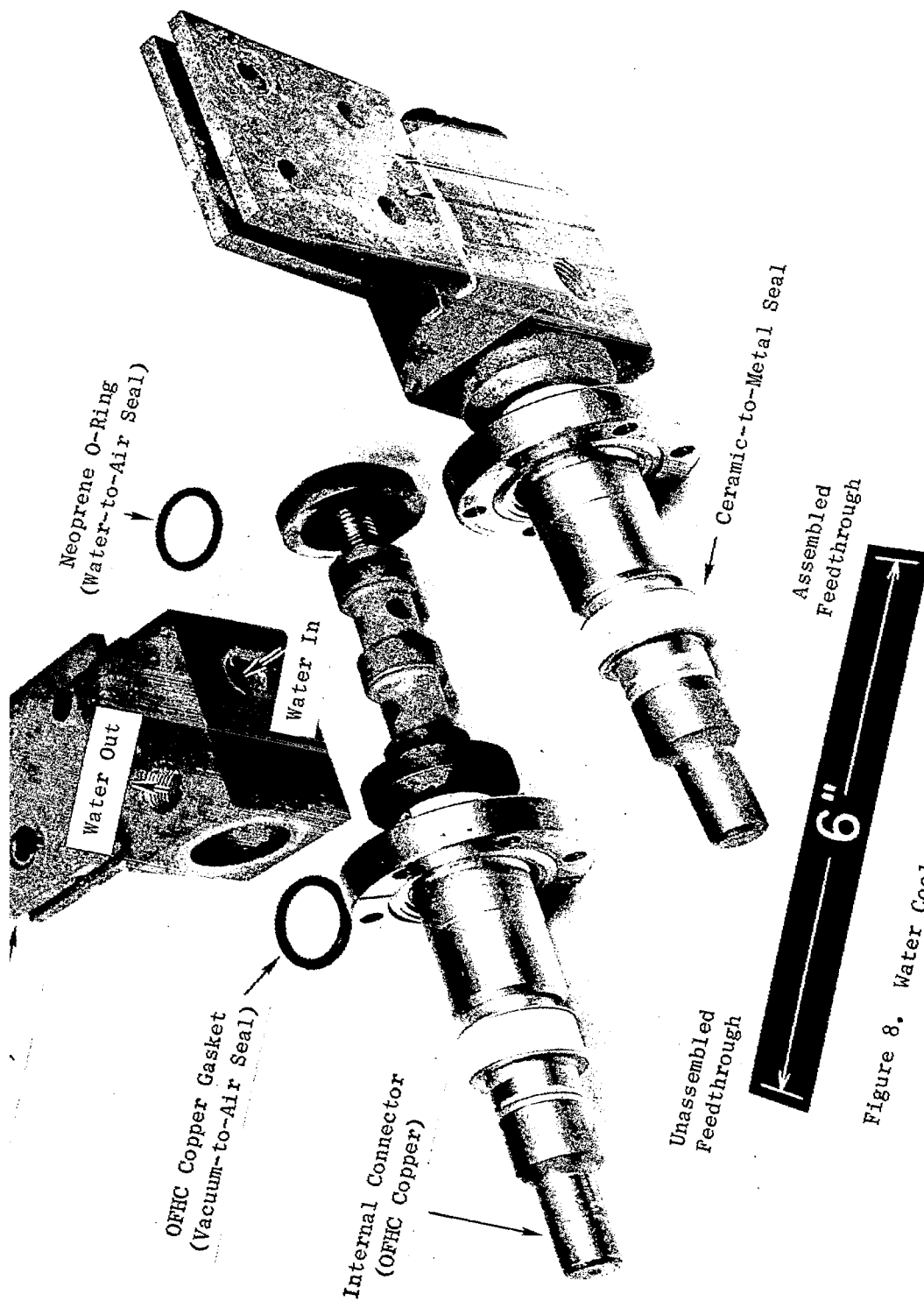


Figure 8. Water Cooled, 1000-Ampere Electrical Power Feedthrough.

An input signal to the recorder is obtained from the heater control thermocouple and is measured by the recorder. This input signal is compared to a known voltage developed across the measurement slidewire. The slidewire is part of a bridge circuit, the other part of which is located in the 3-mode controller. The output of the controller is directly proportional to the unbalance of the bridge circuit and provides a DC control signal to an amplistat. The control signal is amplified by the amplistat to a sufficient level to operate a saturable reactor. The output of the saturable reactor is connected to a stepdown transformer rated at 5,000 amperes continuous duty. The high current is fed through the vacuum chamber to the loop heater by water-cooled 1,000-ampere feedthroughs.

C. Partial Pressure Gas Analyzer

A partial pressure gas analyzer^a was used to monitor the concentration of the residual gases in the test chamber. The analyzer tube^b of the partial pressure analyzer was of glass-metal construction. It consisted of a Nier-type, electron-multiplier ion detector entirely enclosed in a glass-metal envelope. The analyzer tube was designed to operate at total pressure up to 10^{-5} torr, with the capability of detecting partial pressures of 10^{-12} torr. A three-kilogauss Alnico permanent magnet was mounted on the analyzer tube to achieve ion beam deflection, and with this tube and magnet system, resolution of adjacent peaks in the 2-50 AMU (atomic mass units) range could be achieved.

D. Chamber Pressure Measurement

The pressure in the test chamber was measured by means of an ionization gauge^c which contained two separate filaments, one of burn-out resistant thoriated iridium and one of tungsten. The gauge and associated power supply^d were capable of measuring pressure between 250 microns of mercury and 10^{-10} torr.

^aGeneral Electric Partial Pressure Analyzer Model 514

^bGeneral Electric Type ZS-8001

^cGeneral Electric Miniature Ionization Gauge, Model No. 22GT 102

^dGeneral Electric Ionization Gauge Supply, Model No. 22GC100

VI. SODIUM PURIFICATION AND FILLING OF THE LOOP

The sodium to be used in the filling of the Sodium Thermal Convection Loop was initially purchased as reactor grade sodium metal to SPPS Specification No. 01-0031-00-B (SPPS-45-I). This specification is included in an earlier topical report⁽¹⁾. The sodium was subsequently hot trapped in contact with zirconium foil in the 1200°-1300°F temperature range for approximately 150 hours. The handling operations involving the purifying and filling of the loop included: sampling and analyzing the sodium to be purified; filling the hot trap and analyzing the purified product; and filling the loop and analyzing the fill sodium. A schematic diagram of the filling and sampling system is shown in Figure 9. The sodium used to fill the loop system (112 grams) contained less than 20 ppm oxygen following the hot trap purification treatment. A detailed description of the hot trapping procedure, the sodium transfer system (hot trap to loop), the sampling procedures and the complete analytical results are given in a topical report⁽²⁾ describing this phase of the Potassium Corrosion Test Loop Development Program. The vacuum-inert gas amalgamation analytical procedure used to determine the oxygen concentration of the sodium which was used to fill the Sodium Thermal Convection Loop is also described in detail in an earlier topical report of the program⁽¹⁾.

(2) Dotson, L. E. and Hand, R. B., Potassium Corrosion Test Loop Development Topical Report No. 4: Purification Analysis and Handling of Sodium and Potassium, R66SD3012, June 13, 1966.

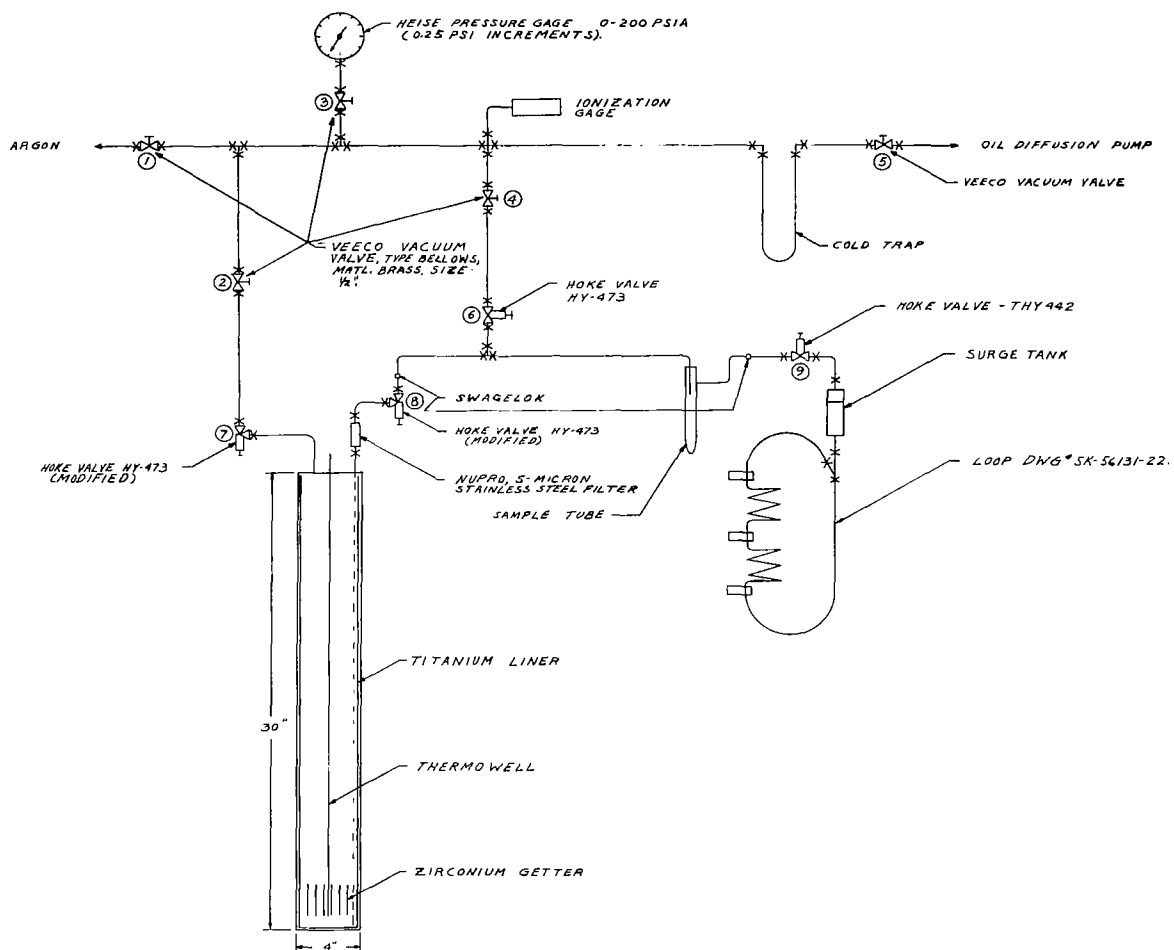


Figure 9. Sodium Thermal Convection Loop Purification and Fill System.

VII. LOOP INSTALLATION AND INSTRUMENTATION

A. Installation

Upon completion of the loop filling operation, the loop was installed in a support structure constructed of Type 304 SS which was welded to the base plate of the vacuum chamber. The support structure, previously illustrated in Figure 6, had been carefully polished to remove all grit or dirt to achieve a low outgassing surface. All nuts used in assembling the support structure were slotted with a 0.031-inch wide by 0.062-inch deep axial saw cut and each washer was cut radially to eliminate possible gas traps and thereby reduce the time required for effective outgassing.

The loop itself was primarily supported by the heater electrodes which were bolted to 2-inch wide x 0.25-inch thick OFHC copper bus bars which were fastened to the support structure. The bus bars were electrically insulated from the support structure by 99.7% alumina insulators. An additional support was placed under the surge tank to reduce the weight load of the cold leg on the electrodes. The loop and support structure are shown mounted in the test chamber in Figure 10. An overall view of the test facility is shown in Figure 11.

A 3/8-inch OD Type 304 SS tube was welded to the stainless steel Hoke valve^{*} using the inert gas tungsten arc process, and run out through an all welded, stainless steel vacuum feedthrough to a 99.9% high purity argon gas supply. The argon gas supply analyzed^{**} as follows:

Ar	-	99.997%	CO	-	1 ppm
O ₂	-	5 ppm	CO ₂	-	1 ppm
N ₂	-	5 ppm	H ₂	-	0.25 ppm
CH ₄	-	2 ppm	H ₂ O	-	4.5 ppm

* Model THY 442, Hoke, Inc., Cresskill, N. J.

** Vendor Analysis - Matheson Company, Inc.

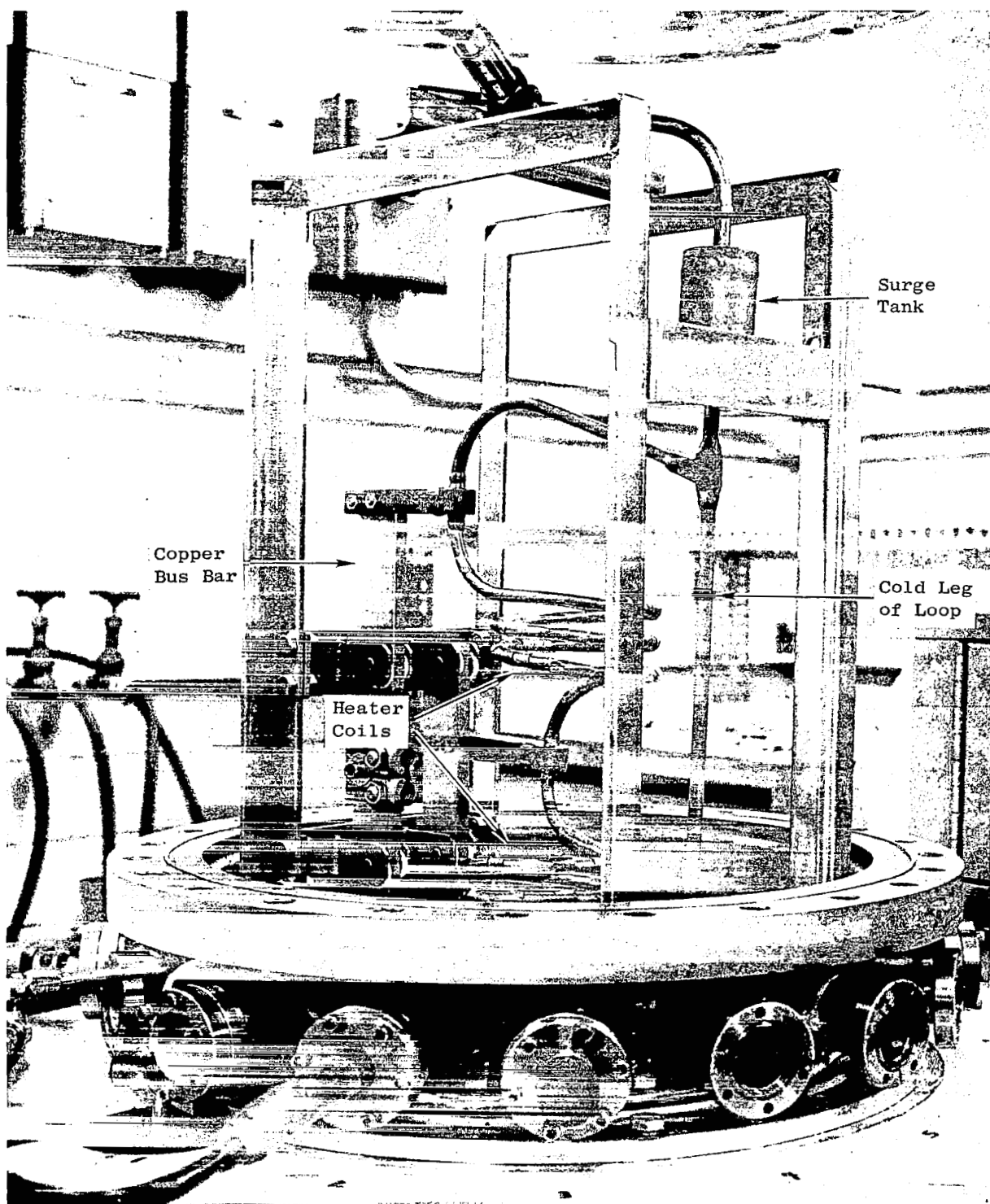


Figure 10. Sodium Thermal Convection Loop Following Mounting of the Loop and the Support Structure in the Test Chamber.

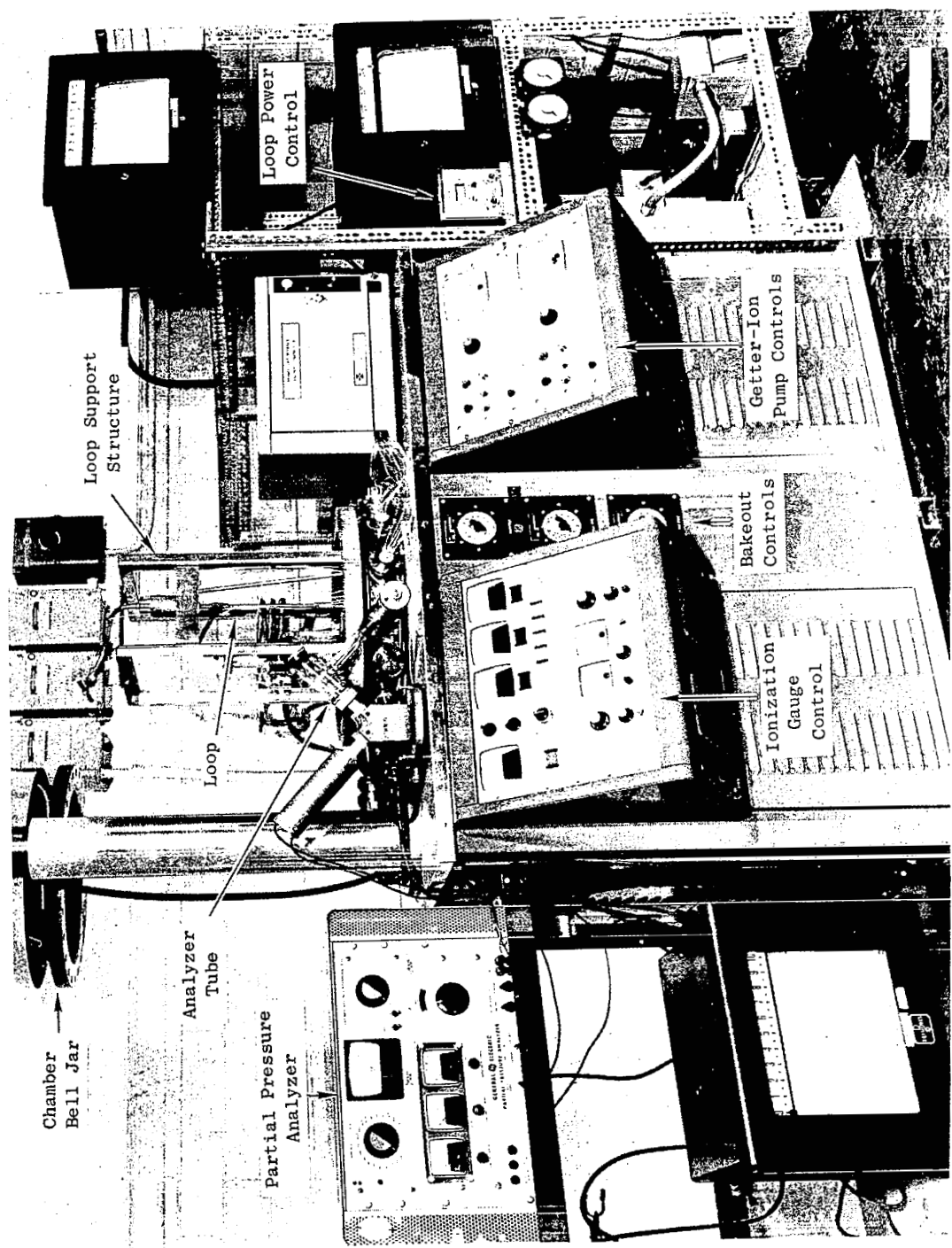


Figure 11. Sodium Thermal Convection Loop Test Facility With Associated Instrumentation and Power Control Equipment.

The external argon gas supply system was of all welded stainless steel construction with bellows-sealed valves and a metal diaphragm pressure regulator*. The argon system was used to pressurize the sodium and thereby prevent boiling in the heater coils during loop operation. The entire system was helium leak checked after assembly and all components were baked out at 300°F under vacuum. A schematic of the argon gas supply system was previously shown in Figure 9.

B. Thermal Insulation

Dimpled foil made from 0.002-inch thick by 0.5-inch wide Cb-1Zr strip was selected as the reflective insulating material for the Sodium Thermal Convection Loop. This approach was chosen for the following reasons:

1. The narrow strip could easily be wrapped around components of odd shapes and sizes, e.g., heater coils, to give any desired number of layers of insulation.
2. The dimpled foil with its self-spacing feature and minimum thermal conductive path (point contact between successive layers) yielded an insulation assembly of minimum mass and surface area which, in turn, would reduce out-gassing loads and radiation losses.

The dimpling of the foil was accomplished by passing the foil through the manually operated rolls shown in Figure 12. The Cb-1Zr foil and a sheet of plasticized polyvinylchloride** were passed through the rolls together. The hardened steel, coarse knurler roller embossed the foil with the indentations which spaced the successive layers of foil during subsequent application on the loop components. As the foil was removed from the rolls, it was thoroughly cleaned with ethyl alcohol. Dimpling the foil increased its thickness from 0.002 inch to approximately 0.010 inch.

* Thermco Company, LaPorte, Indiana, 0-400 psig.

** Kayflex L-10; Source: S&C Mfg. Company, Cincinnati, Ohio

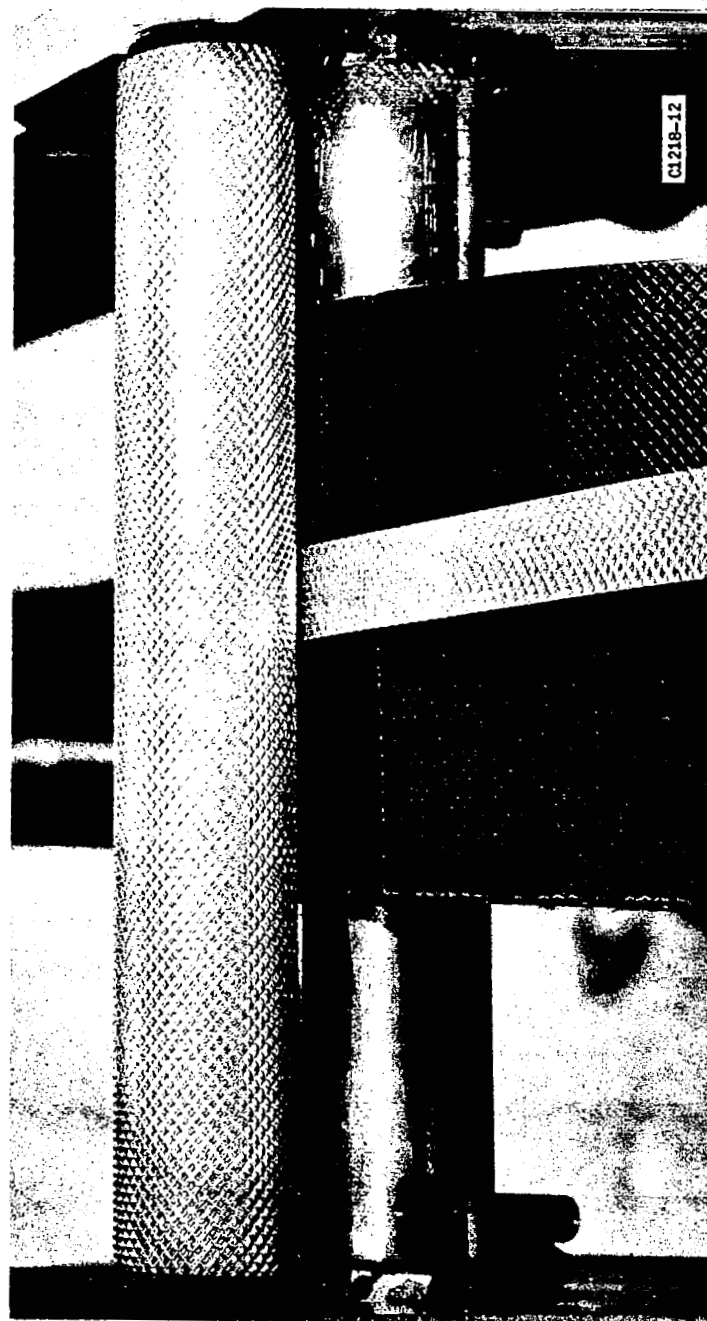
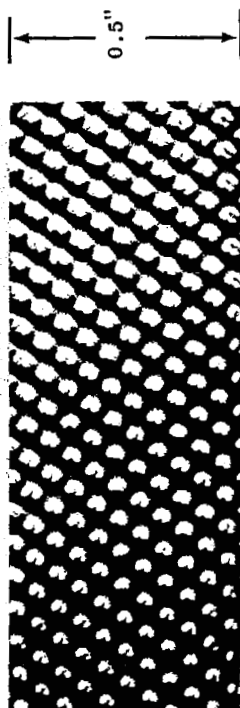


Figure 12. Dimpling of 0.5-Inch Wide x 0.002-Inch Thick Cb-12r Foil for use in Insulating Loop Components. Enlarged View of Dimpled Foil Shown.

The location and number of layers of foil used to insulate the loop are illustrated in Figure 13. The number of layers of foil selected was determined by a consideration of the allowable heat loss. For the heater coils, it was necessary to consider both the allowable heat loss and the allowable decrease in electrical resistivity. The layers of foil on the heater coils provide additional current flow paths, but this is not enough to significantly lower the resistance because of the relatively high resistance of the point contact path through the layers of foil.

The foil was applied to the tubing by continuously wrapping the strip on the tube in a spiral manner with approximately 10% (0.050-inch) overlap. The foil was fixed to the tube and to itself by spot welds made under a flowing argon atmosphere to prevent atmospheric contamination on the refractory alloy. Great care was taken in applying the foil over thermocouples attached directly to the tube walls to minimize the possibility of foil-to-thermocouple wire contact during test which might result from slight movement of either material. The approach used is further described in the section below covering the thermocouple installation procedures used.

C. Instrumentation

The temperature of the loop was measured by sixteen W-3%Re/W-25%Re thermocouples. Tungsten-3% rhenium/tungsten-25% rhenium was selected as the basic thermocouple alloy combination for instrumenting all alkali metal loops in the Potassium Corrosion Test Loop Program. The selection was based on its compatibility with the test loop alloy (Cb-1Zr), its high and fairly linear thermal emf and its reported excellent stability over extended periods of time in vacuum at elevated temperatures⁽³⁾.

The tungsten-3% rhenium leg was selected in preference to the pure tungsten leg because of its superior handling properties, i.e., less breakage during installation and operation. Even with the increased ductility of the W-3% wire over unalloyed tungsten wire, fractures of the W-3% Re leg of thermocouples, particularly near the brazed joint between the thermocouple wire and

(3) Hendricks, J. W. and McElroy, D. L., High Temperature High Vacuum Thermocouple Drift Tests, ORNL-TM-833, August 1964.

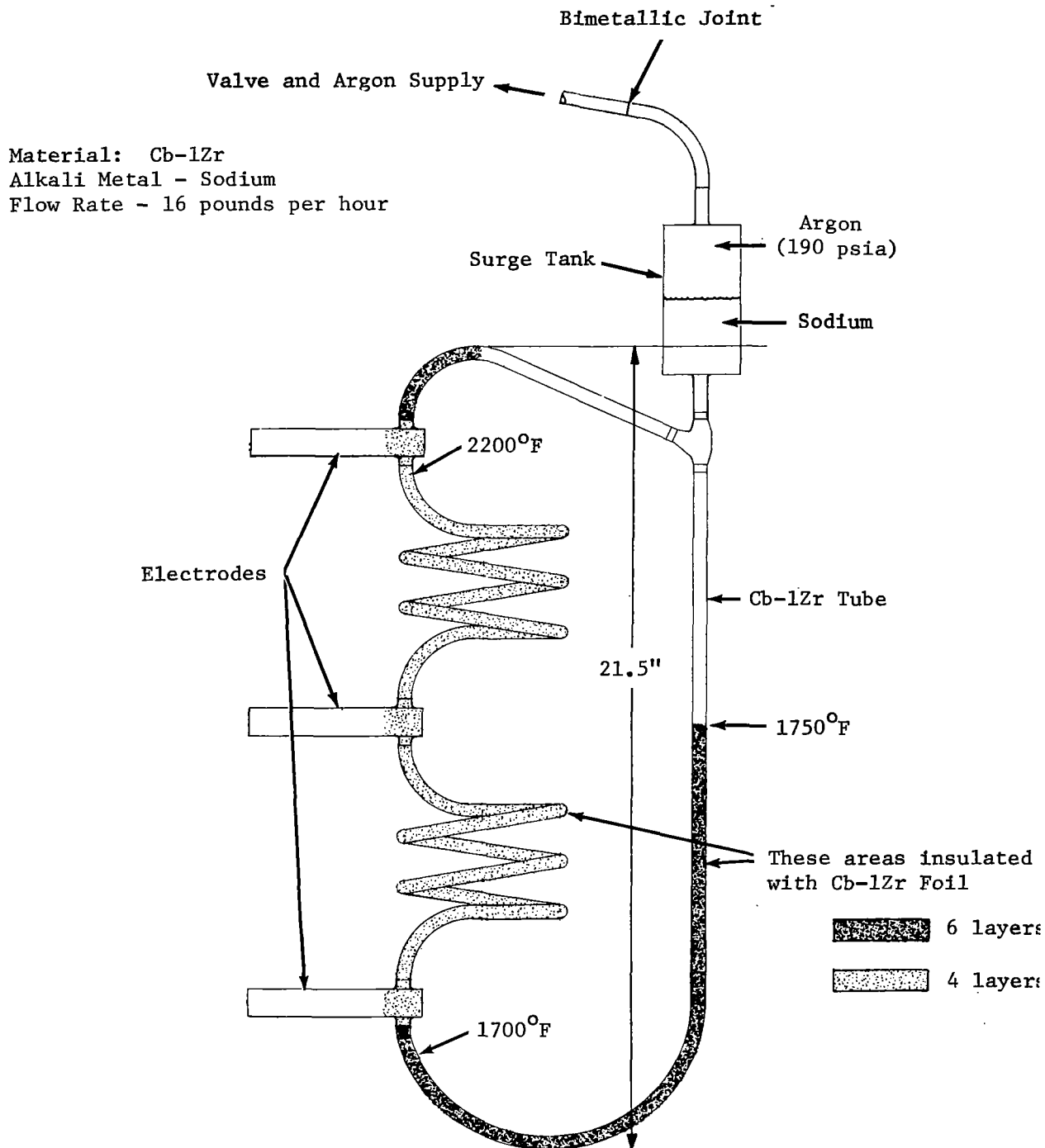


Figure 13. Design of the Cb-1Zr Sodium Thermal Convection Loop Showing the Location and Number of Layers of Dimpled Cb-1Zr Foil Used to Insulate the Various Regions of the Loop. Nominal Calculated Temperatures of Several Regions of the Loop are Also Indicated.

the nickel vacuum feedthrough tube, were one of the chief sources of thermocouple difficulties.

Although various tungsten-rhenium alloy combinations have been used for a number of years, a national standard has not as yet been adopted. Matched tungsten-rhenium thermocouple wire of various alloy combinations, however, can be purchased with a specified accuracy to tentative calibration tables adopted by the thermocouple wire suppliers. The policy adopted for this program is to purchase wire to a chemical or material specification and conduct calibration tests at General Electric on the thermocouple wire in accordance with the overall quality control plan. The W-3%Re wire was purchased from the Lamp Metals Components Department of the General Electric Company and the W-25%Re wire was purchased from Hoskins Manufacturing Company. All thermocouple wire used in a specific loop test is supplied from one matched lot with its own calibration.

The results of the calibration of the thermocouple wire used to instrument the loop are shown in Figure 14. The calibration test was originally run in an argon atmosphere at 5 psig using a certified platinum/platinum-10% rhodium thermocouple as the calibration standard. (Subsequent thermocouple calibrations for other loop tests of this program were performed in a high vacuum thermocouple test facility.)

The location of the loop thermocouples and a typical thermocouple circuit are shown in Figure 15. Starting at the hot junction of the thermocouple, the wires were routed along the support structure through a thermocouple vacuum feedthrough to a 150°F constant temperature reference junction. At the reference junction a transition from the W-Re thermocouple wire to copper lead wire was made which connected to the 24-point recording potentiometer.

The thermocouple wires inside the chamber were electrically insulated with high purity, 99.7% two hole alumina insulators to the point of contact with the Cb-1Zr tubing. Beryllium oxide insulators (99.5%) were used in contact with the regions of the loop designed to operate at temperatures in excess of 2000°F. The insulators are supported at frequent intervals by small straps of Cb-1Zr foil spot welded to the support structure. A foil strap near the junction is required to remove all possible strain on the spot welded junction.

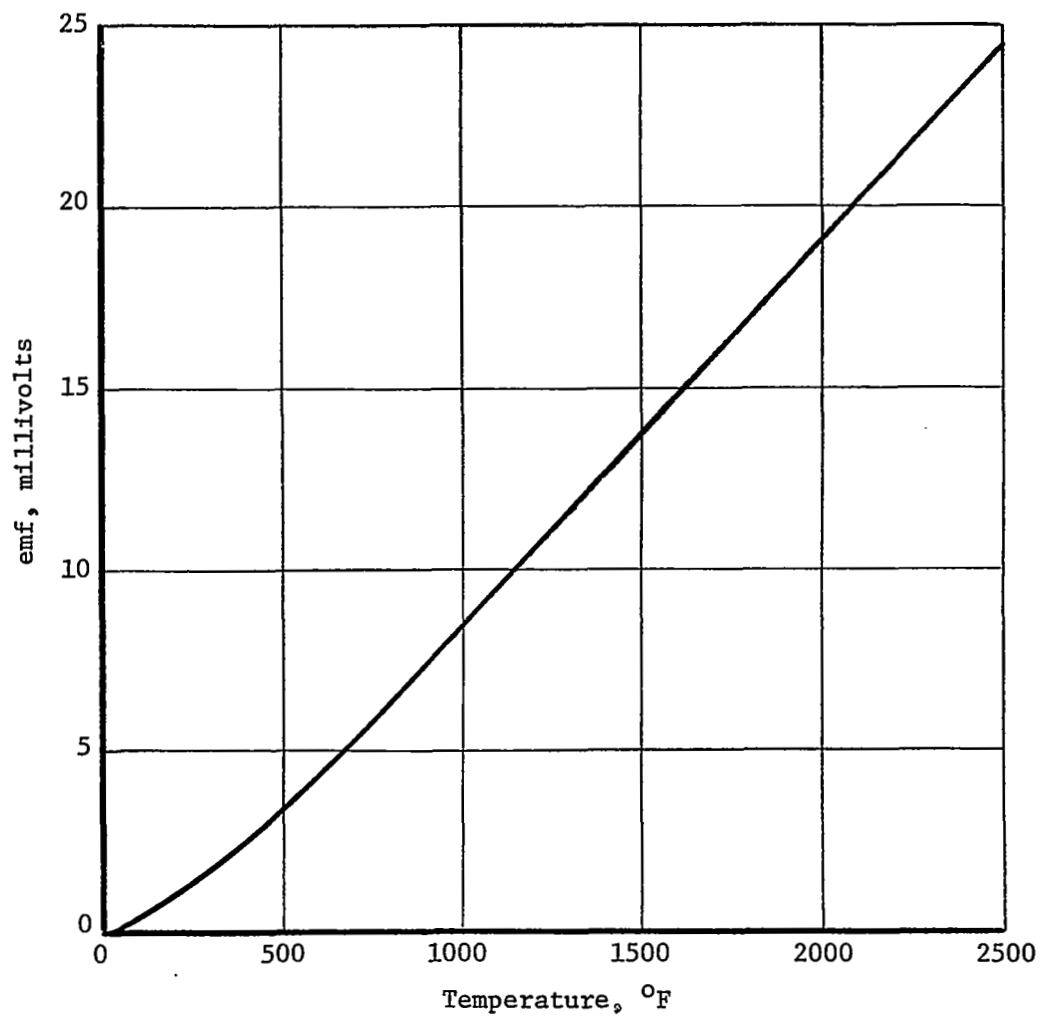


Figure 14. Thermal emf of W-3%Re/W-25%Re Wire Used to Instrument the Sodium Thermal Convection Loop.

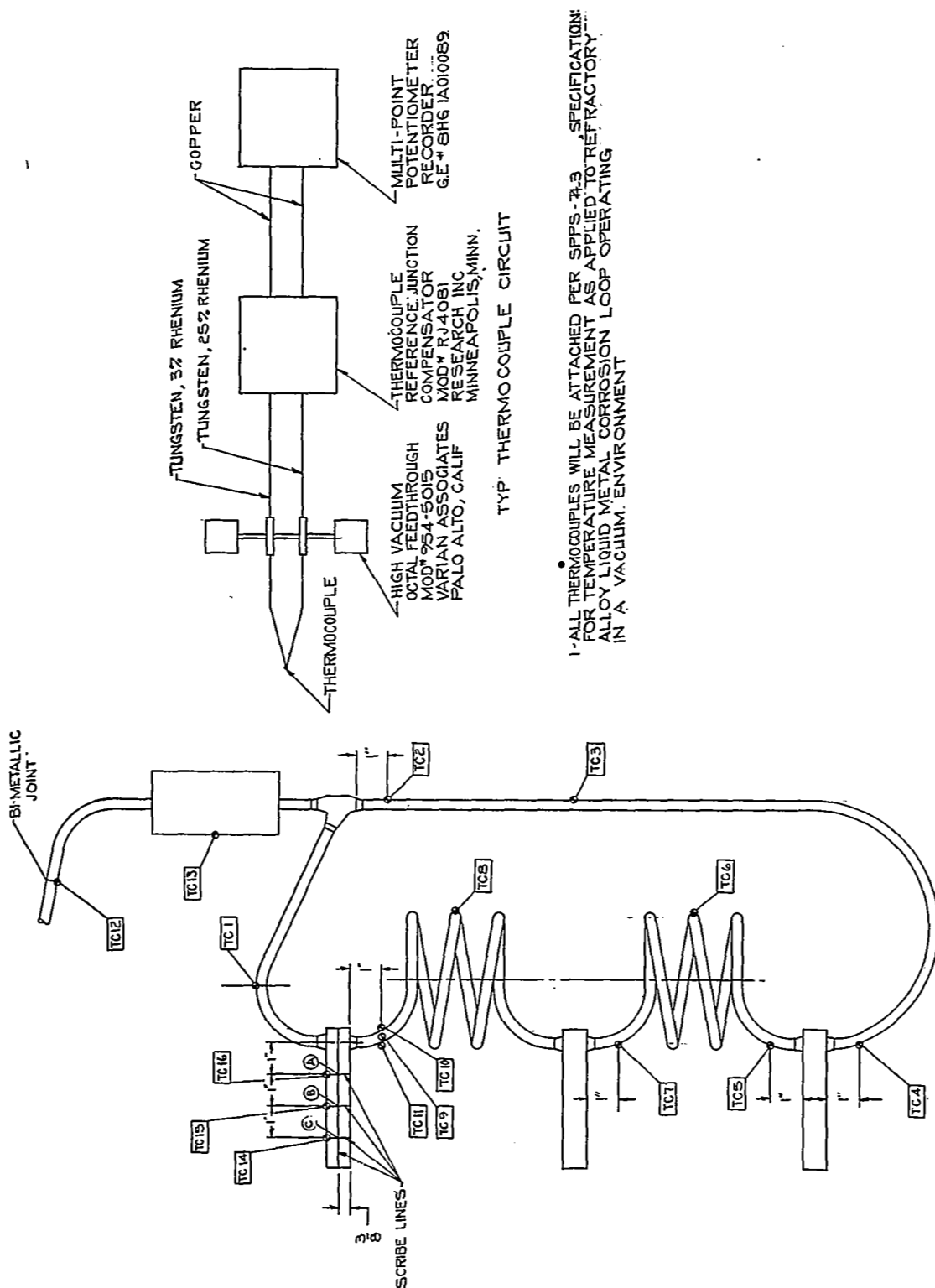


Figure 15. Thermocouple Circuit and Location of W-3%Re/W-25%Re Thermocouples on the Sodium Convection Loop.

A typical split spot-welded thermocouple junction is shown in Figure 16. Each wire is laid parallel to the other approximately 0.10 inch apart. Two consecutive spot welds are applied to each wire so that in the event the first spot weld breaks away from the surface without breakage of the wire, the thermocouple will continue to function. The active spot weld connection nearest to the measuring instrument will always be the actual hot junction. A small thermal shield is fixed around the junction to reduce heat radiation losses from the junction and to prevent thermocouple wire shorts when foil insulation is wrapped on the tube.

The thermocouple vacuum feedthrough with eight thermocouple wires and a schematic showing one pair of wires is shown in Figure 17. The feedthrough assembly* is completely bakeable to 500°F and has a flat copper gasket seal. The W-3%Re and W-25%Re wires were brazed into the 0.050-inch diameter nickel tubes with Premabraz 615 (61.5Ag-24Cu-14.5In) in an argon atmosphere using a local electrical resistance heat source. Single hole alumina ceramic insulators were used to electrically insulate the thermocouple wire from the nickel tube except for the brazed junction as shown in Figure 17, since the thermal gradient in the nickel tube would result in spurious thermal emf's if multiple electrical junctions were formed.

* Varian Associates, Model 954-0055, Palo Alto, California

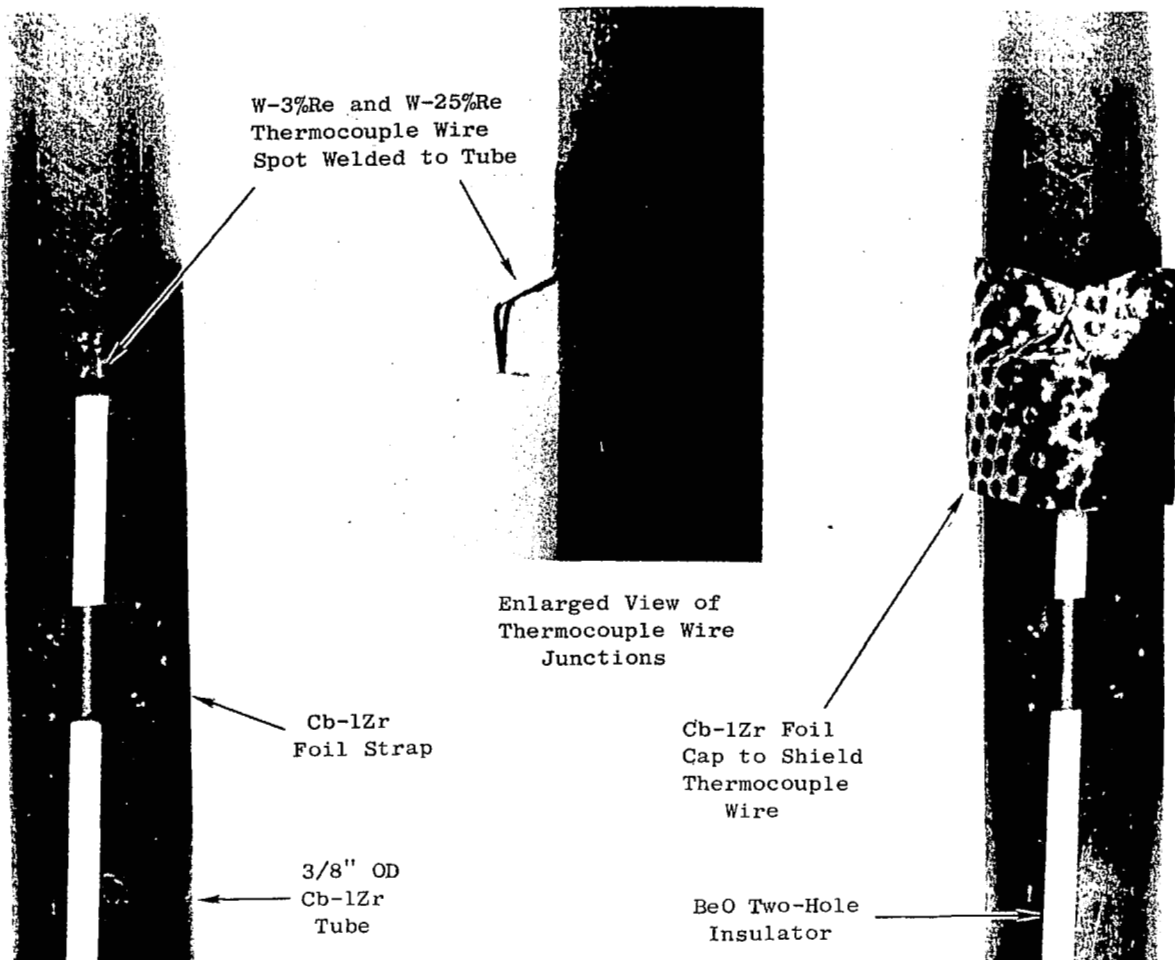
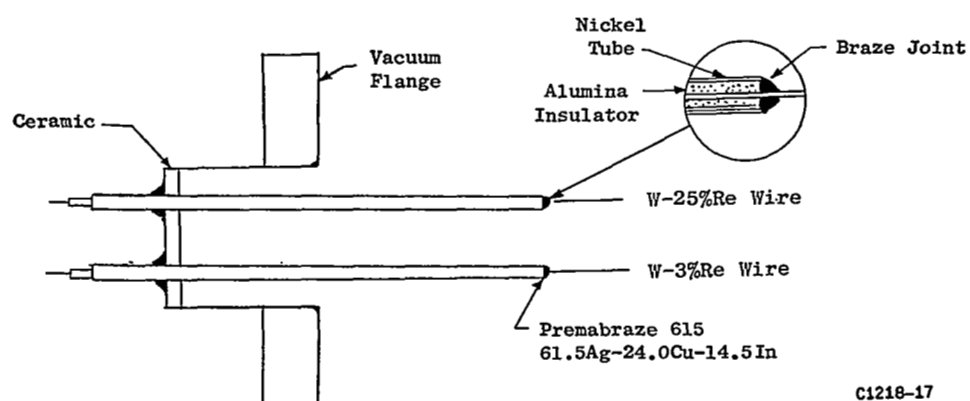
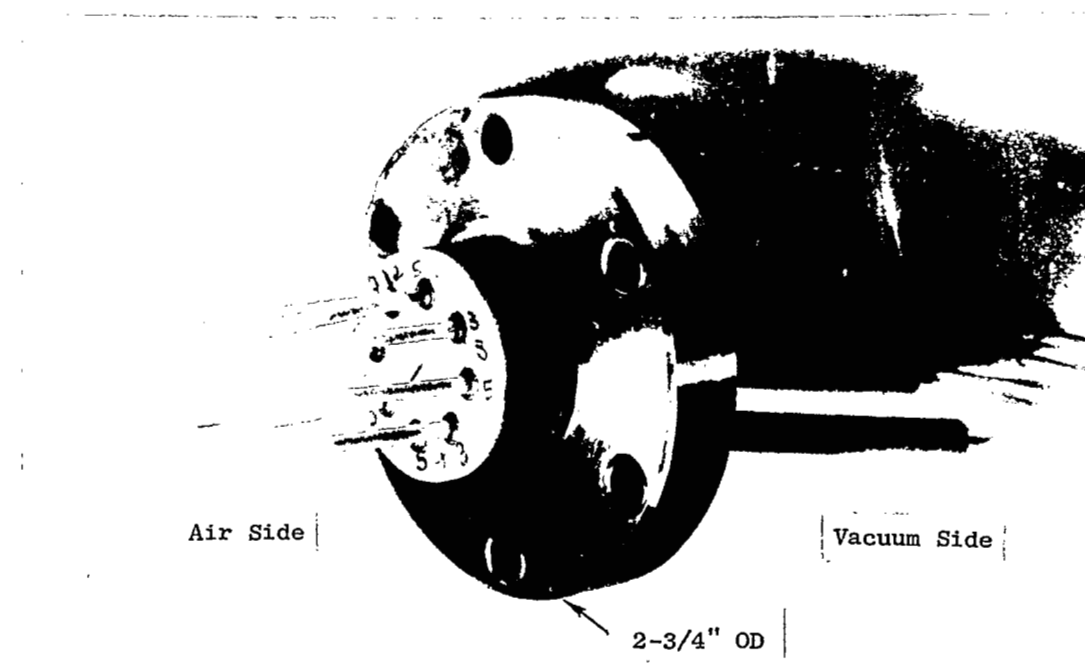


Figure 16. Method Used to Install W-3%Re/W-25%Re Thermocouple Wires on Cb-1Zr Alloy Tubing.



C1218-17

Figure 17. Method Used to Install W-3%Re/W-25%Re Thermocouple Wire in High Vacuum Feedthrough Flanges.

VIII. TEST OPERATION

The installation and instrumentation of the Sodium Thermal Convection Loop in the 18-inch diameter vacuum chamber was completed on January 23, 1964. The bell jar was then lowered and bolted to the sump flange and rough pumped by liquid nitrogen-chilled sorption pumps to less than 10 microns. The roughing pump was then valved off from the test chamber by an ultrahigh vacuum bakeable valve and the getter-ion pump was turned on. When the pressure reached 1×10^{-7} torr, the partial pressure gas analyzer was used to perform a helium leak check of all flanges, ports, and feedthroughs. No leaks were found and the system was then baked out at 200° to 300°F for 72 hours. The chamber pressure after bakeout was 6.6×10^{-8} torr.

A low power run was started on January 28, 1964 to outgas the loop components and the Cb-1Zr foil thermal insulation which was probably the major source of outgassing in the chamber because of its large surface area and its multilayer construction. During the low power runs, the loop temperature was carefully increased so that the pressure would not exceed 1.0×10^{-6} torr. A typical increase of 100°F in the loop temperature would increase the pressure by a full decade and require several hours to return to the original base pressure.

A complete check of the loop thermocouples at 1400°F showed that 5 of the 16 loop thermocouples were lost during the bakeout and the low power run. The test was stopped and an examination of the thermocouples showed that the major type of failure was open W-3%Re wires. This lot of W-3%Re wire had exhibited low reverse bend ductility and required extremely careful handling in instrumenting the loop. The combination of thermal cycling and slight loop vibrations (due to 60 cycle AC power) was apparently sufficient to fracture the leads, especially at the braze joint in the nickel tubulation of the vacuum feedthrough.

The loop thermocouples were replaced with grades of W-3%Re and W-25%Re wire which had more satisfactory handling properties, and low power testing was resumed on February 10, 1964. These replacement thermocouple wires were calibrated in argon. During the low power run, erratic fluctuations in the ion pump current were observed and the low power testing was stopped. The erratic pumping behavior of the getter-ion pump continued with the loop at

room temperature. An electrical check of the power supply showed that a defective resistor and relay were responsible for the malfunction and a replacement power supply was installed. Low power testing was again resumed on February 20, 1964 but high ion pump current required that the testing again be stopped and the loop was returned to room temperature. The high ion pump current resulted from the electrical shorting of two of the five pump cells by metallic whiskers formed during the test. All attempts to melt or vaporize the whiskers by high electrical current resistance heating were only temporarily successful and after a few hours of operation, the original high current condition would return. The two defective getter-ion pump cells were disconnected from the power supply and the test was resumed using the three remaining pump cells.

Although the overall pumping speed of the system had been considerably reduced, a pressure of 4×10^{-7} torr was reached after a 43-hour bakeout at 200° to 300°F. Power to the loop was steadily increased during a 4-hour period and on February 24, 1964 a maximum loop operating temperature of 2380°F was achieved. The test was continued uninterrupted for 509 hours and was shut down on March 16, 1964 for a mid-test inspection and replacement of the loop thermocouple feedthroughs with a modified design to eliminate spurious emf's generated by multiple junctions between the thermocouple wire and the nickel tubulation.

The thermocouple replacement was completed on March 20, 1964 and after an 18-hour bakeout, the loop was returned to full power at a maximum temperature of 2260°F. The test was continued uninterrupted to April 10, 1964 for a total accumulated test time of 1,000 hours.

The complete chronological history of the operation of the Sodium Thermal Convection Loop is presented in Table III. The temperature conditions during the two periods of loop operation and both the ion gauge and partial pressure measurements of the test chamber vacuum environment are discussed in more detail in the following sections.

TABLE III

OPERATION HISTORY OF THE SODIUM THERMAL CONVECTION LOOP

January 6, 1964	Loop assembly completed
January 8, 1964	Loop filled with 112 grams of sodium
January 9, 1964	Loop installed in the vacuum chamber
January 10, 1964	Started instrumentation and insulation of loop
January 23, 1964	Completed loop instrumentation
January 24, 1964	Started pumpdown of vacuum chamber
January 24, 1964	Started bakeout of vacuum chamber
January 27, 1964	Bakeout off
January 27, 1964	Chamber pressure 6.6×10^{-8} torr with the chamber and loop at room temperature
January 28, 1964	Start of low power run to degas loop - maximum loop temperature 1400°F
January 29, 1964	Thermocouple readings erratic; turned off power to loop
January 30, 1964	Vacuum chamber released to air and started repair of thermocouples
February 8, 1964	Thermocouple repairs completed and started pumpdown of chamber
February 8, 1964	Started bakeout of chamber
February 10, 1964	Tank pressure 3.6×10^{-7} torr with the chamber and the loop at 200°-300°F
February 10, 1964	Start of low power run to degas loop - loop temperature to 1400°F
February 11, 1964	Ion pump stopped - power supply defective requiring loop shutdown - power off
February 20, 1964	New ion pump power supply installed - bakeable valve to roughing system repaired
February 20, 1964	Started pumpdown of chamber - ion pump performance erratic - circuit checking initiated
February 22, 1964	Ion pump protection circuit bypassed to permit operation - 2 of 5 pump cells are defective and bypassed - chamber bakeout restarted
February 24, 1964	Tank pressure 4×10^{-7} torr with the chamber and loop at 200°-300°F - began increasing power to loop
February 24, 1964	Full power to loop - maximum temperature 2380°F - chamber pressure 4.2×10^{-7} torr

TABLE III

(continued)

March 16, 1964	Completed 509 hours of loop operation; shut down for mid-test inspection, repair of thermocouples, and removal of partial pressure analyzer tube
March 20, 1964	Chamber sealed and pumpdown initiated
March 20, 1964	Bakeout of chamber started
March 21, 1964	Full power to loop - maximum temperature 2260°F
April 10, 1964	Test completed 1,000 hours of operation
April 10, 1964	Vacuum tank opened for loop inspection and test disassembly

A. Test Conditions

The loop operation was divided into two test periods. During the first period, 0 to 509 hours, the power input and loop temperatures were slightly higher than during the second period, 509 to 1,000 hours. The test was shut down after a nominal 500 hours of operation to repair or replace defective thermocouples and to remove the partial pressure analyzer tube from the chamber to prepare it for use with the second loop test of this program.

Loop temperature, power input and calculated mass flow of sodium for the first period of loop operation are listed in Figure 18. The maximum loop temperature was 2380°F during this period. Prior to restarting the loop test for the second 500-hour test period, a recommendation was made to and approved by the NASA Technical Manager to reduce the maximum loop temperature to approximately 2250°F. The loop conditions during the 509 to 1,000-hour test period are given in Figure 19. As may be noted in both Figure 18 and 19, the temperature rise in the lower heater coil is substantially higher than in the upper coil. This is attributed to a number of factors, including the higher current flow in the lower temperature coil because of its lower electrical resistance, and the higher radiation heat losses in the upper coil because of its higher average temperature. As previously indicated in Table I, the sodium temperature rise in the heater of the sodium circuit of the Prototype Corrosion Loop shall be only 150°F (1950° to 2100°F) and the flow velocity in the pumped system shall be quite high (approximately 16 fps) compared with the very low velocity (approximately 0.2 fps) of the thermal convection loop described in this report.

One of the purposes of this experiment was to determine the amount of I^2R and conduction heating of the Cb-1Zr electrodes. The temperature gradient along the top heater electrode is indicated in Figure 20. This electrode operated at a higher temperature than the other electrodes and was monitored for this reason. Although no operational difficulties were encountered because of the relatively high Cb-1Zr electrode temperature adjacent to the copper bus bar, the design of the electrodes for the subsequent loop tests of the program was modified to both minimize heat loss from the sodium near the electrodes and to decrease the thermal conduction from the active portion of the heater to the electrodes.

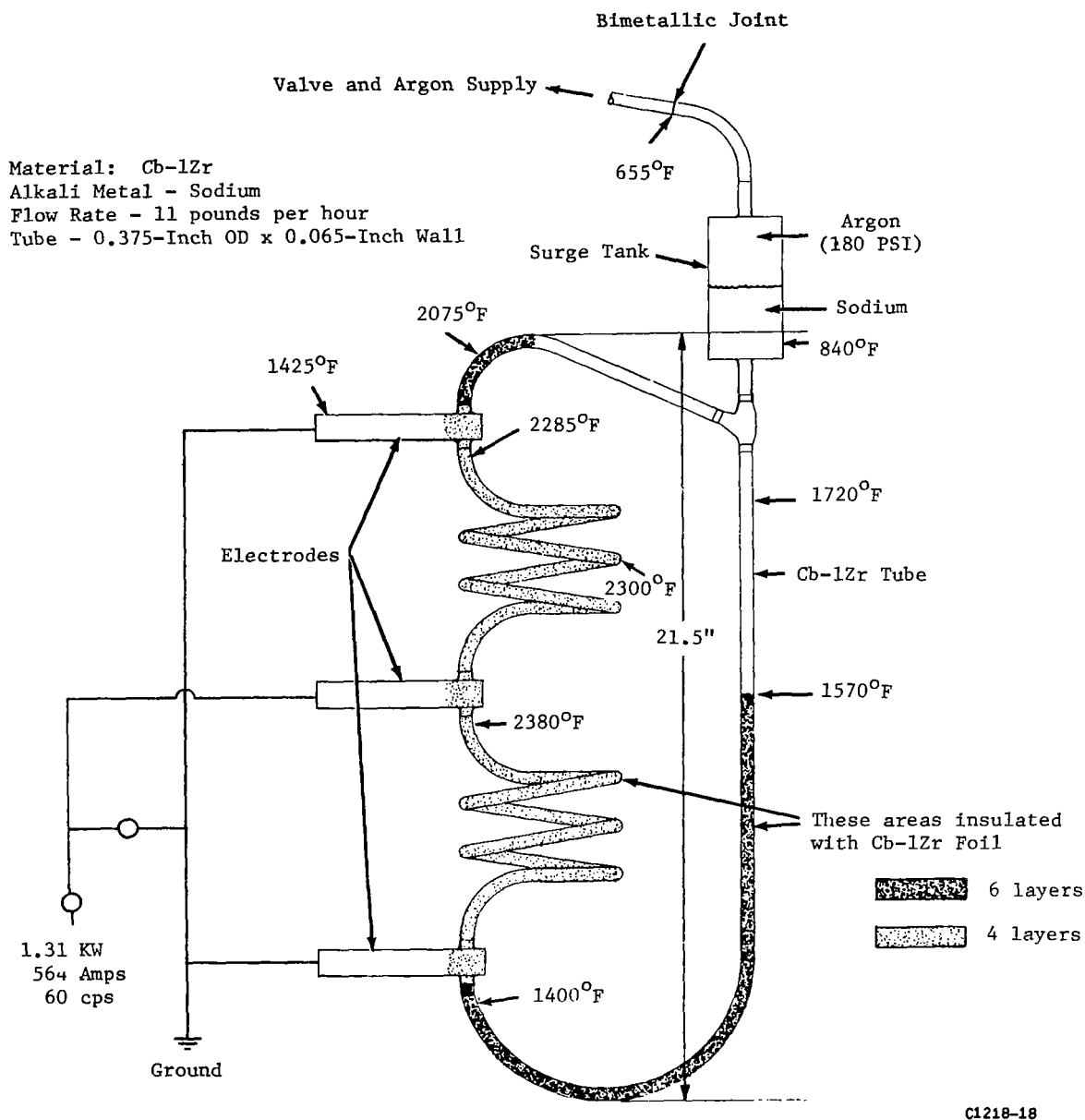


Figure 18. Temperatures of the Sodium Thermal Convection Loop During the 0-to-509 Hour Test Period.

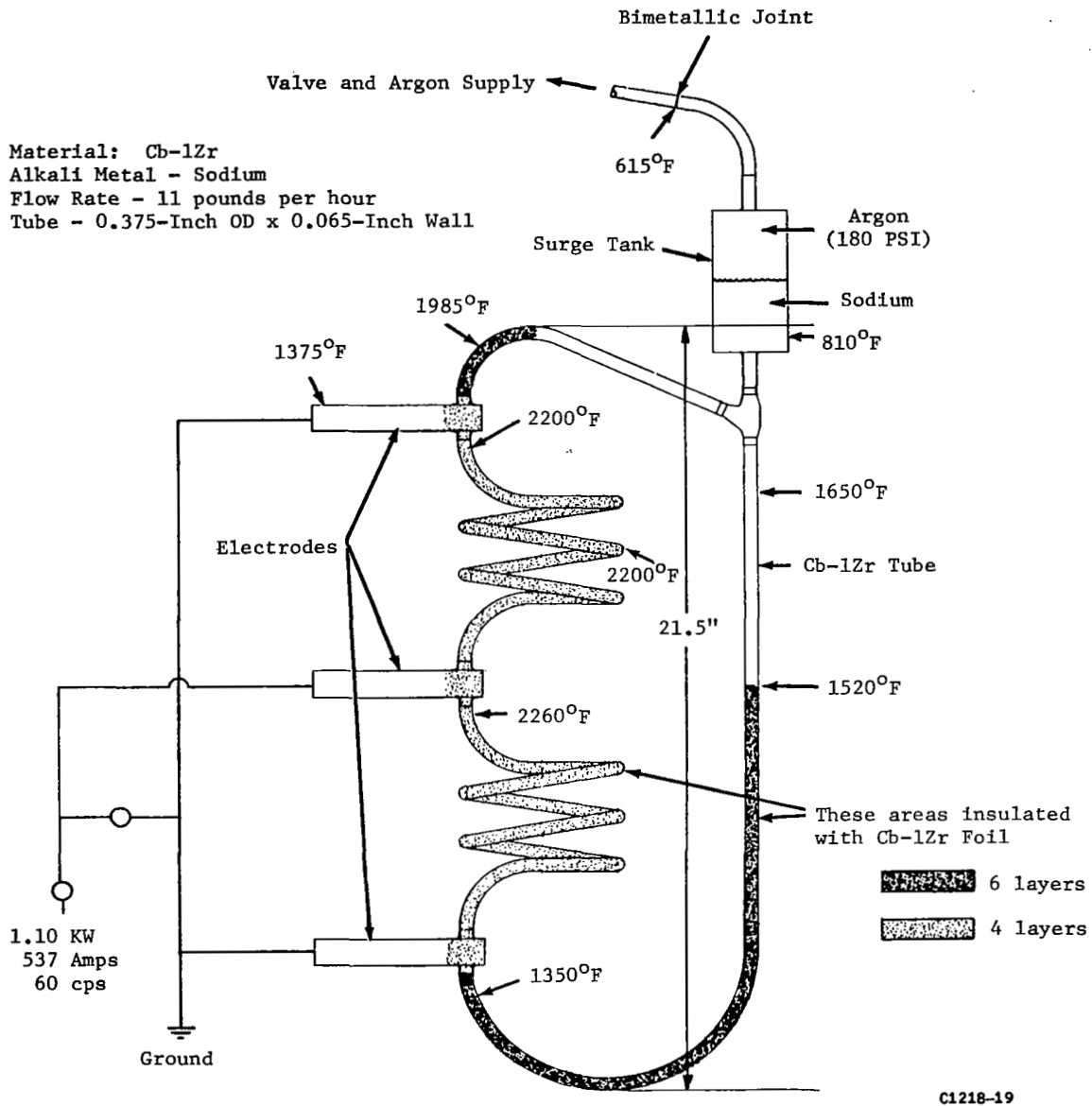


Figure 19. Temperatures of the Sodium Thermal Convection Loop During the 509-to 1000-Hour Test Period.

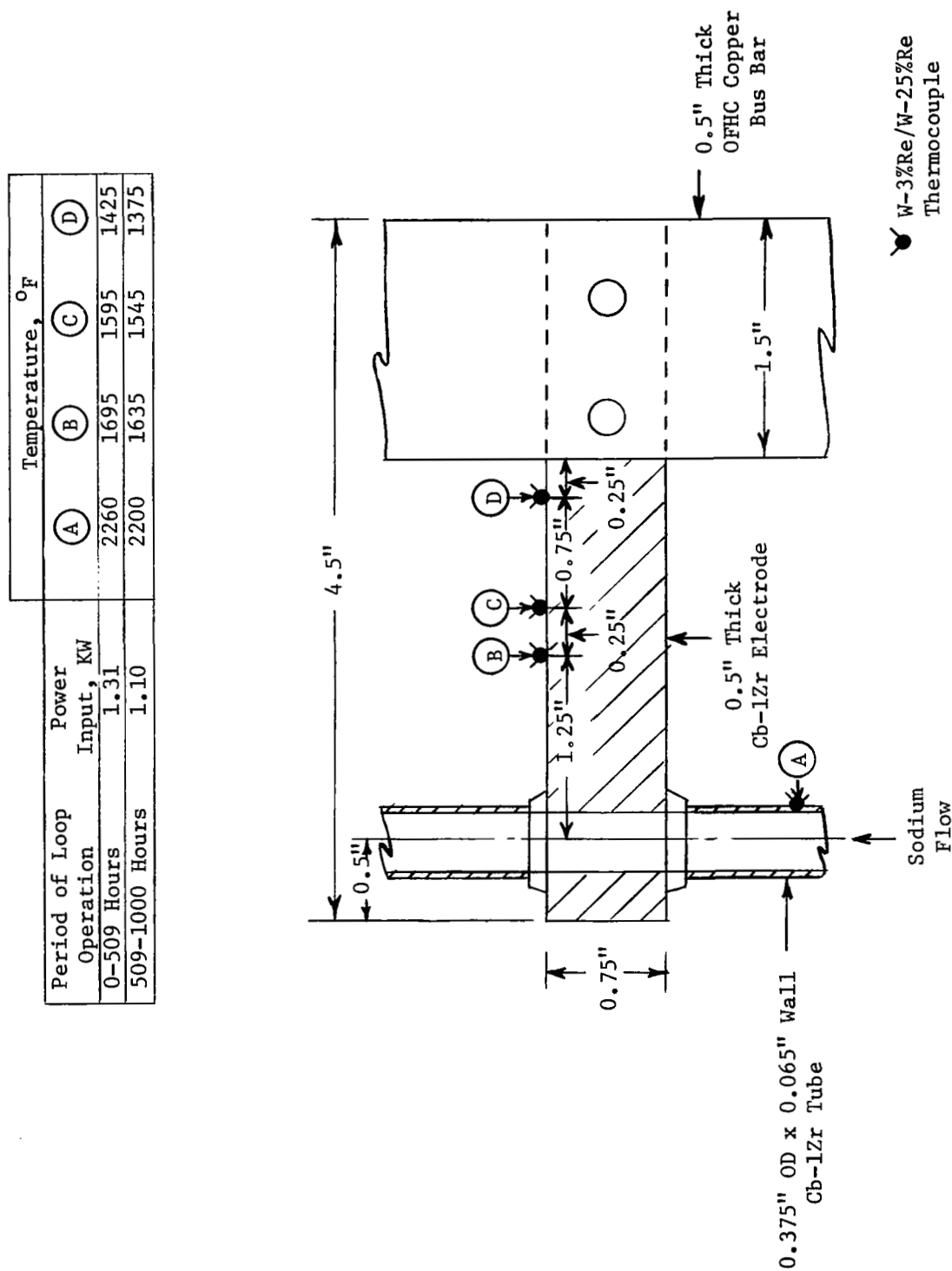


Figure 20. Temperatures Along the Top Heater Electrode Bar of the Sodium Thermal Convection Loop.

The most significant test conditions during the two periods of test operation are listed in Table IV. As may be noted in this table, a significant portion of the electrical power input to the copper bus bars is lost by radiation from heater components to the chamber walls and by conduction from the Cb-1Zr heater electrodes to the copper bus bars.

B. Test Chamber Environment

Continuous monitoring of the total pressure is the minimum requirement to assure that hot refractory alloy test components are not contaminated by the test chamber environment. In addition to monitoring the total pressure, it is desirable to determine the concentration of the residual gas species during test operation since it is the concentration of contaminating species, such as nitrogen and oxygen, which is generally most important. Great care was exercised in the design, assembly, and instrumentation of the test system to facilitate the achievement of a very low pressure in the test chamber with the loop at the operating conditions.

As indicated previously, the system was baked out for several time periods prior to the application of power to the loop heater circuit. A total bakeout time of approximately 100 hours was completed prior to the start of the first 500-hour operation period. During the bakeout, the temperatures of loop components and the test chamber were in the 200° to 300°F range.

1. Ionization Gauge Pressure Observations - The test chamber pressures during the 1000-hour test as indicated by the ionization gauge* are given in Figure 21. A more detailed discussion of the total pressure and partial pressure observations during test startup and shutdown is included in the section below. As may be noted in Figure 21, the total pressure during both the initial and second test startup dropped from the high to the low 10^{-7} torr range in less than five hours. During the first period of test operation (0 to 509 hours), the pressure held in the low 10^{-8} torr range for most of the time. During the 509 to 1000-hour test period, the ion gauge pressure was maintained in the high 10^{-9} torr range for the last 250 hours of test operation.

* Model 27GT104, glass miniature ionization gauge tube, General Electric Company, Vacuum Products Department, Schenectady, New York.

TABLE IV
 PRINCIPAL TEST CONDITIONS DURING THE TWO TEST
 PERIODS OF OPERATION OF THE SODIUM THERMAL CONVECTION LOOP

	<u>0-509 Hours</u>	<u>509-1000 Hours</u>
Flow rate	11 lb/hr	11 lb/hr
Flow velocity (0.25-inch ID, 2200°F region)	0.22 fps	0.22 fps
Sodium temperature, heater inlet	1400°F	1350°F
Sodium temperature, heater outlet	2075°F	1985°F
Sodium temperature, maximum	2380°F	2260°F
Current through heater coils	564 amps	537 amps
Potential across heater coils	2.32 volts	2.05 volts
Total power input to bus bars	1.31 KW	1.10 KW
Power input to sodium	0.68 KW	0.63 KW
Heat losses in heater coils and electrodes	0.63 KW	0.47 KW

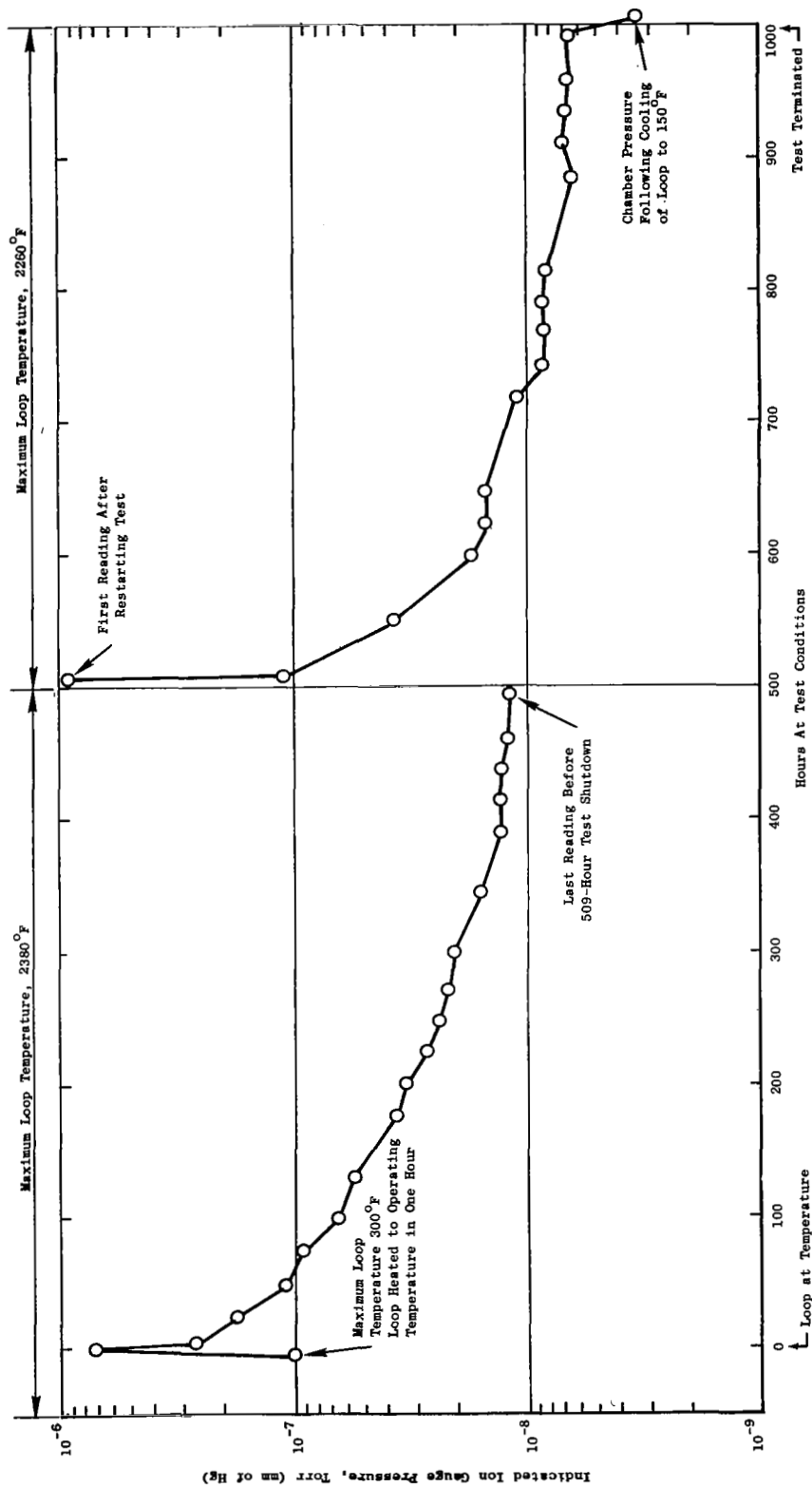


Figure 21. Pressure in Test Chamber During 1000-Hour Sodium Thermal Convection Loop Test as Indicated by Ionization Gauge. Test was Shutdown After 509-Hours Operation to Modify Instrumentation.

Following completion of the 1,000-hour test, the power to the loop was turned off and the loop was allowed to cool to room temperature. After three hours of cooling, with the loop at approximately 150°F, the chamber pressure had decreased to 3.4×10^{-9} torr.

The pressure rise rate with the getter-ion pumps turned off was obtained just before the test was terminated with the loop at the operating conditions and again after the loop had cooled to room temperature. Results of these pressure rise measurements are given in Table V. These results indicate that the pressure rise rates were essentially equal for the two loop conditions.

A 16-hour pressure rise test was also conducted after the 509-hour test shutdown with the loop at room temperature. During this period the chamber pressure increased from 3.5×10^{-9} torr to 4.8×10^{-6} torr. This pressure rise yields a pressure rise rate of 3.0×10^{-7} torr/hour, or approximately one-half the rate measured in the 20-minute test at the conclusion of the test after 1,000 hours of operation. Outgassing of the getter-ion pump is most probably responsible for the higher pressure rise rate for the 20-minute test.

2. Partial Pressure Observations - As indicated in Section V-C., a partial pressure analyzer* was used during the first period (0 to 509 hours) of loop operation to determine the concentration of the various residual gases in the test chamber environment.

The changes in ion gauge pressure and the pressure of the various gaseous species during the startup of the loop test are indicated in Table VI. With the chamber on bakeout and the maximum loop temperature at 300°F, the mass 28** peak (N₂, CO) was the major gas (48%) with significant concentrations of helium (25%) and hydrogen (18%). Several hours later with the loop at a maximum temperature of 2380°F, hydrogen was the major gas present. The hydrogen concentration increased by a factor of 10 when the maximum loop

* Model 514, Partial Pressure Gas Analyzer, General Electric Company, Power Tube Department, Schenectady, New York.

** Mass/charge

TABLE V

INCREASE IN PRESSURE IN THE
SODIUM THERMAL CONVECTION LOOP CHAMBER

<u>Time, Minutes</u>	<u>Loop at Temperature After 980 Hours of Test Operation</u>	<u>Following Termination of Test, Loop at Room Temperature</u>
0*	7.0×10^{-9}	3.4×10^{-9}
1	6.5×10^{-8}	9.9×10^{-9}
5	1.6×10^{-7}	9.2×10^{-8}
10	2.1×10^{-7}	1.4×10^{-7}
15	2.3×10^{-7}	1.9×10^{-7}
20	2.4×10^{-7}	2.4×10^{-7}
Pressure rise rate (0-20 minutes)	1.1×10^{-8} torr/min 6.6×10^{-7} torr/hr	1.2×10^{-8} torr/min 7.2×10^{-7} torr/hr

*Pressure just before getter-ion pumps turned off.

TABLE VI

ION GAUGE PRESSURE READINGS AND THE TRUE PARTIAL PRESSURES
OF THE VARIOUS RESIDUAL GASES IN THE TEST CHAMBER DURING STARTUP
OF THE SODIUM THERMAL CONVECTION LOOP ON FEBRUARY 24, 1964

Time	Max. Loop Temp., °F	Ion Gauge Pressure, Torr	True Partial Pressure, Torr x 10 ⁸						
			Mass/Charge						
			2 (H ₂)	4 (He)	18 (H ₂ O)	28 (N ₂ , CO)	32 (O ₂)	40 (Ar)	44 (CO ₂)
0755	300	2.6 x 10 ⁻⁸	1.4 (18%)*	1.9 (25%)	0.04 (0.5%)	3.7 (48%)	0.10 (1%)	0.35 (4%)	0.30 (4%)
1015	2150	3.0 x 10 ⁻⁷	10.6 (46%)	1.9 (8%)	0.04 (0.2%)	7.6 (33%)	0.03 (0.1%)	1.0 (4%)	1.4 (6%)
1430	2380	3.3 x 10 ⁻⁷	14.2 (55%)	4.9 (19%)	0.04 (2%)	4.7 (18%)	0.03 (1%)	0.87 (3%)	1.1 (4%)

* Percentage of the sum of the partial pressures of the individual gases.

temperature was increased from 300° to 2380°F and constituted 46% of the sum of the partial pressures. The next largest increase in the concentration of a major gas was noted for helium which increased from 1.9×10^{-8} torr to 4.9×10^{-8} torr during the same period. This increase in helium concentration is attributed to its release from the getter-ion pump elements as the total system pressure increased and the pump element temperature increased due to the higher current flow in the pumps.

The partial pressures of the various residual gases and the ion gauge pressure during the first 509 hours of loop operation are plotted in Figure 22. It may be noted that hydrogen was the major residual gas during this test period and constituted approximately 60 to 70% of the sum of the partial pressures. The mass 28 peak (N_2 , CO) was the second most abundant gas during the major portion of the test, increasing from approximately 20% of the sum of the partial pressures after 200 hours to approximately 30% after 500 hours of test operation.

Prior to shutting the loop test down to repair and modify thermocouples and remove the partial pressure analyzer, several analyzer scans were made to compare the concentration of the individual gases with the loop at temperature, with the loop at room temperature and after a 16-hour pressure rise test with the loop cold and the getter-ion pumps off. These results are listed in Table VII.

Cooling the loop from the test temperature (Scan No. 59) to room temperature (Scan No. 61) resulted in the following environmental changes:

- a. Ion gauge pressure decreased by factor of three.
- b. Hydrogen concentration decreased from 50% to 30% while the mass 28 peak (N_2 , CO) increased from 31% to 52%.

Comparison of Scans No. 61 and No. 62 indicates the changes in the chamber environment during a 16-hour pressure rise test with the loop at room temperature and the getter ion pumps off. The major changes were as follows:

- a. The ion gauge pressure increased by a factor of 1,300 which was equivalent to a pressure rise rate of 3×10^{-7} torr/hour.

TABLE VII

RESULTS OF PARTIAL PRESSURE SCANS MADE AT END OF FIRST PERIOD
(0 to 509 HOURS) OF LOOP OPERATION

Ion Gauge Pressure	Scan No. 59		Scan No. 61		Scan No. 62	
	Loop at Temperature After 503 Hours Operation	1.1 x 10 ⁻⁸ torr	Loop at Room Temperature After 509-Hour Shutdown	3.5 x 10 ⁻⁹ torr	Loop at Room Temperature Getter-Ion Pumps Off 16 Hours	4.8 x 10 ⁻⁶ torr
<u>Mass/Charge</u>						
2		6.0 x 10 ⁻⁹ (50%)*		1.2 x 10 ⁻⁹ (30%)		5.6 x 10 ⁻⁹ (0.1%)
4		1.4 x 10 ⁻⁹ (12%)		5.6 x 10 ⁻¹⁰ (14%)		3.2 x 10 ⁻⁶ (63%)
18		2.0 x 10 ⁻¹¹		1 x 10 ⁻¹¹		1 x 10 ⁻¹¹
28		3.8 x 10 ⁻⁹ (31%)		2.1 x 10 ⁻⁹ (52%)		1.3 x 10 ⁻⁶ (25%)
32		1 x 10 ⁻¹¹		1 x 10 ⁻¹¹		1 x 10 ⁻¹¹
40		2.9 x 10 ⁻¹⁰ (2%)		8.0 x 10 ⁻¹¹ (2%)		5.8 x 10 ⁻⁷ (11%)
44		5.5 x 10 ⁻¹⁰ (5%)		1.0 x 10 ⁻¹⁰ (2.5%)		4.2 x 10 ⁻⁸ (0.7%)
Total of Partial Pressures		1.2 x 10 ⁻⁸		4.0 x 10 ⁻⁹		5.1 x 10 ⁻⁶

* Percentage of the sum of the partial pressures of the individual gases.

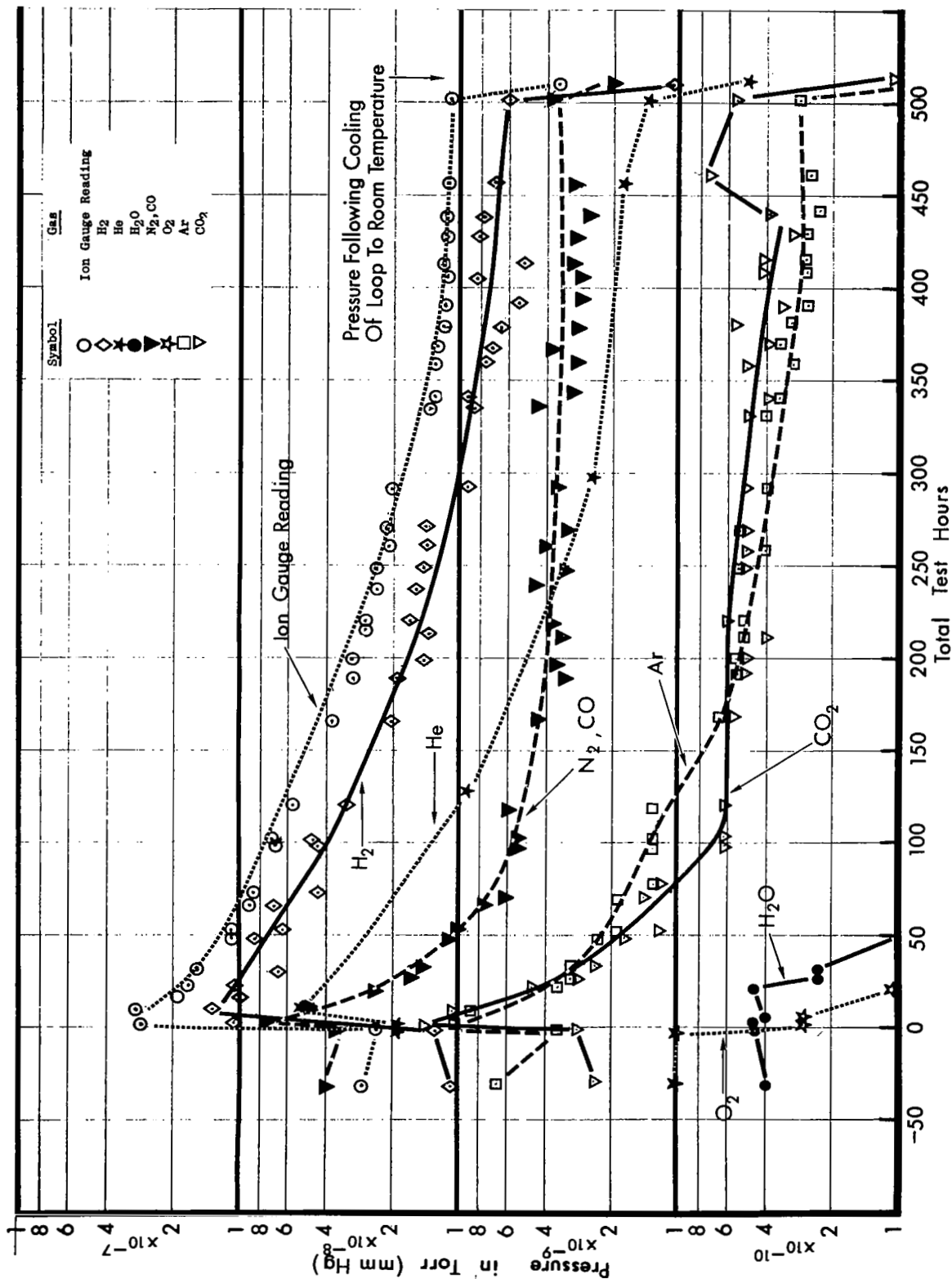


Figure 22. Vacuum Chamber Pressures During the First Period (0 to 509 Hours) of Operation of the Sodium Thermal Convection Loop Test.

b. Both the percentage and partial pressure of helium increased markedly during the pressure rise test.

c. The mass 28 peak (N_2 , CO) indicated a substantial increase in partial pressure (10^{-9} to 10^{-6} torr); however, its percentage of the total pressure actually decreased (52% to 25).

d. The hydrogen pressure did not change significantly during the pressure rise; therefore, the concentration of hydrogen showed a very large decrease (30% to 0.1%).

From the pressure rise rate measurements with the pumps off, it is fairly apparent that the ion pumps are a source of the inert gases (He and Ar) under these conditions. Changes in partial pressures of the other species are more difficult to explain due to the great variety of mechanisms by which these species might be introduced into or removed from the gas phase. For example, the hot elements of the ion gauge and partial pressure analyzer may act as either a source or a sink for the active gases and may actually pump one gas while evolving another or even convert one specie to another, e.g., O_2 to CO. The ion pumps could continue to pump active gases for some period of time after the voltage is removed. In addition, the chamber walls and the loop itself may act as either a source or sink for the active gases.

Several overall comments may be made concerning the partial pressure values obtained during loop operation. The hydrogen concentration was the major gas throughout the first 500 hours of the test and is attributed primarily to the relatively large amount of refractory metal in components such as electrodes, reflective foil insulation, and surge tank which operate at relatively low temperatures (500 to 1500°F), as well as possible hydrogen evolution from hot stainless steel and copper components in the chamber. The relatively high helium concentration during the test was not anticipated and must be attributed to an apparent high inventory of helium in the environment in equilibrium with the helium held by the pump elements.

It is significant that oxygen and water vapor partial pressure were extremely low during the test and following the 16-hour pressure rise test. This indicates that the test chamber was essentially free of air leaks. The results of chemical analyses of various loop components (described in Section X of this report) indicated no significant contamination during the test, and this is consistent with the ion gauge and partial pressure measurements made during the test.

IX. TEST SHUTDOWN, DRAINING AND DISASSEMBLY OF THE LOOP

Following completion of the room temperature pressure rise tests and partial pressure measurements on the test chamber described in the preceding section, the chamber was vented to air. The bell jar of the chamber was then removed and several views of the overall loop and closeup views of specific components are shown in Figures 23, 24, and 25. As may be noted in these photographs, all of the refractory alloy components were bright in appearance and looked very similar to the pretest appearance illustrated in Figure 10.

Some evidence of discoloration of the chamber walls in certain areas had been noted when the chamber was opened after the first period (0 to 509 hours) of loop operation. A slight amount of additional discoloration occurred during the second period of loop operation. The pattern of these discolorations suggested that they originated from the copper electrical connectors*. Chemical analyses performed on unused connectors and smears taken with filter paper moistened with a 10% nitric acid solution confirmed that the discolorations on the chamber walls were caused by the vaporization of volatile constituents from the connectors. Spectrographic analysis of the filter paper smears revealed that zinc and lead were the major elements present and wet chemical analysis of unused connector parts revealed 3-5% zinc and 2-4% lead. Although no contamination by these elements was detected on refractory metal components because of their relatively high operating temperature, the decision was made to use only high purity OFHC copper in the construction of connectors for future loop tests.

During the disassembly of the loop from the test support structure, samples of the 2-mil Cb-1Zr reflective insulating foil were taken from all regions and checked for appearance change and ductility. All the foil specimens were comparable in appearance and in reverse bend ductility to the before-test foil.

* Burndy, Catalog No. QA-26-B and Q2A28-2N (see Dwg. #10, Appendix A of this report).

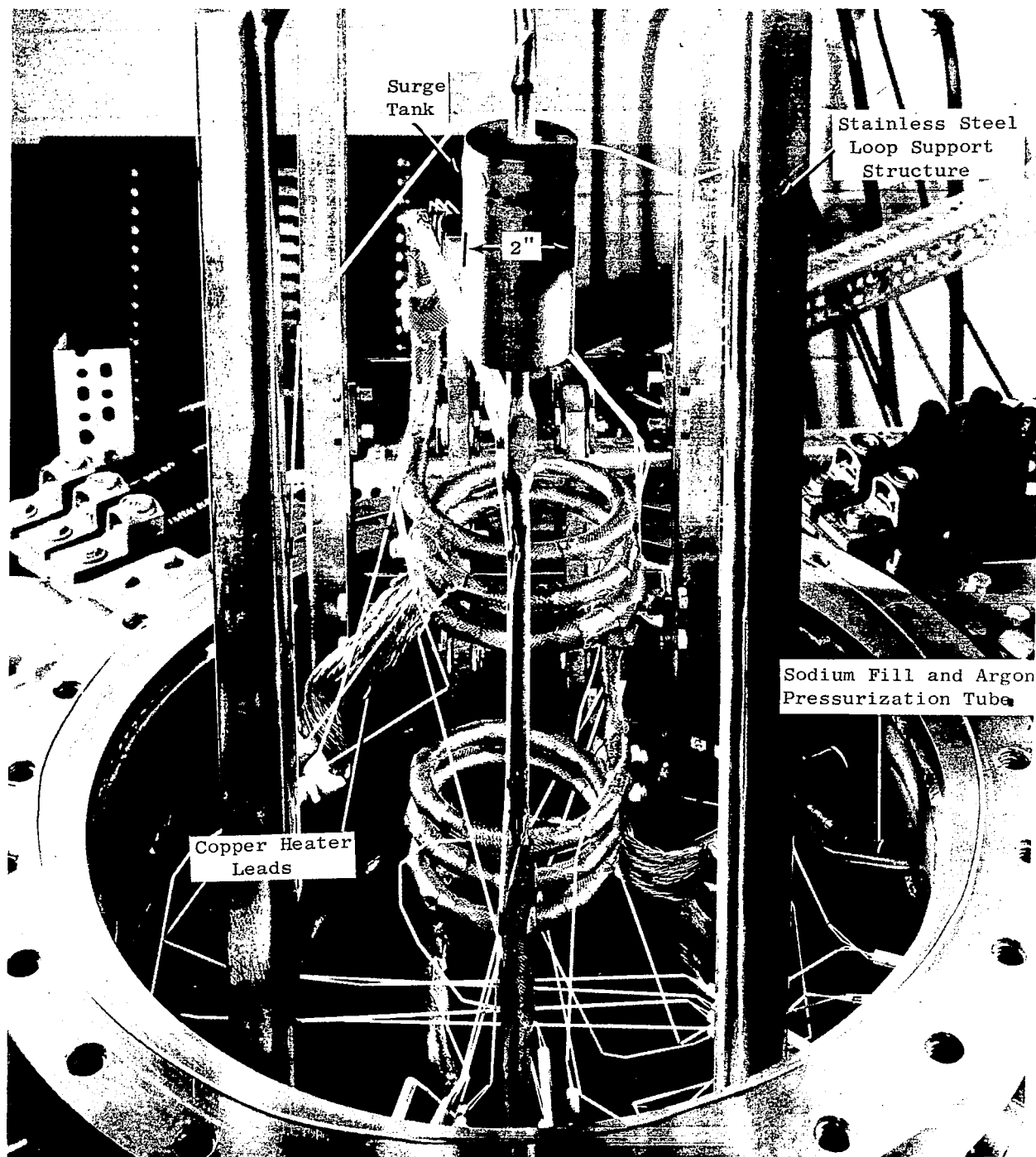


Figure 23. Overall View of the Cb-1Zr Sodium Thermal Convection Loop Following Completion of the 1000-Hour Test. Photograph Taken Just After Removal of the Bell Jar Portion of the Vacuum Chamber.

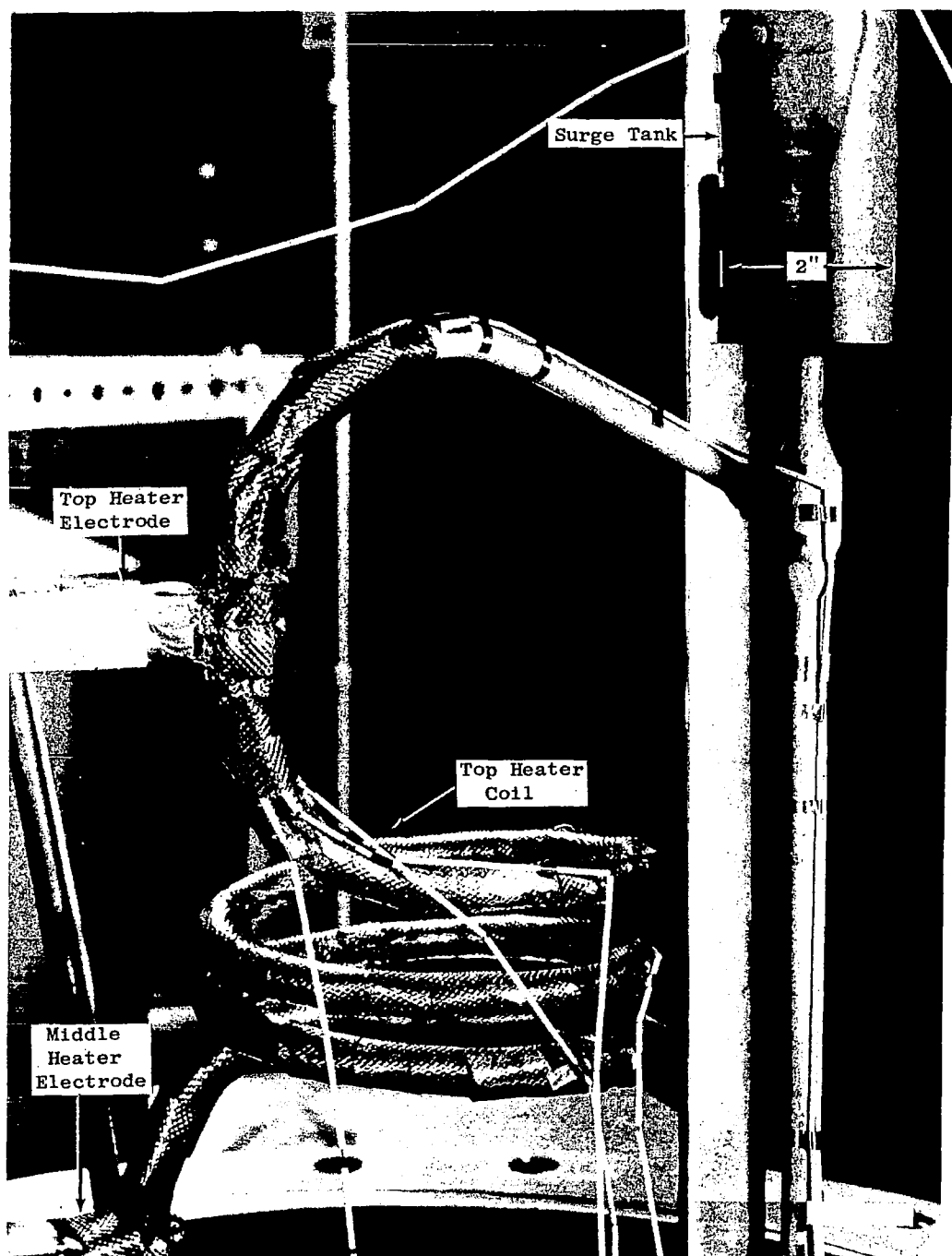


Figure 24. Top Heater Coil and Upper Portion of the Cb-1Zr Sodium Thermal Convection Loop Following the 1000-Hour Test and Prior to the Removal of Cb-1Zr Insulating Foil.

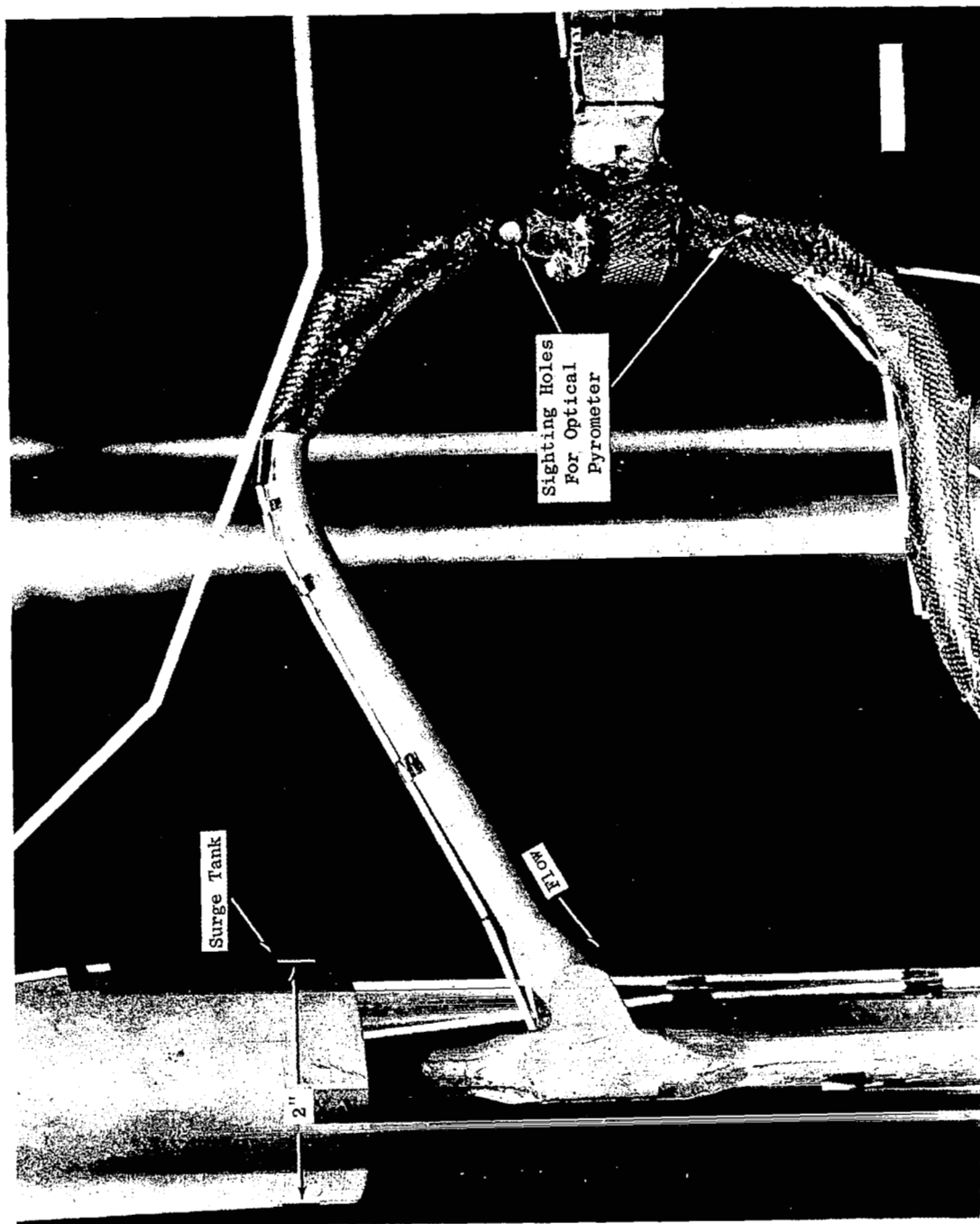


Figure 25. Top Portion of the Cb-12r - Sodium Thermal Convection Loop
Following Completion of the 1000-Hour Test.

The loop proper is shown in Figure 26 following removal from the test chamber. Comparison of this photograph with Figure 5, which showed the loop prior to test, indicates no significant change in the appearance of the loop.

The bulk of the sodium was removed by heating the inverted loop which allowed the sodium to flow into an evacuated stainless steel container which was attached to an argon gas pressurization tube following removal of the loop from the chamber. Following the initial draining, the loop was backfilled with inert gas several times and re-evacuated to sweep residual sodium into the stainless steel container. Heating of the loop was accomplished by means of heating tapes which were wrapped over two layers of aluminum foil which prevented direct contact of the heating tapes with the loop and resulted in more uniform heating.

The loop was cut into sections 6 to 8 inches in length and stripped of residual sodium in absolute ethyl alcohol in preparation for detailed chemical analysis and metallographic evaluation of the various portions of the loop.

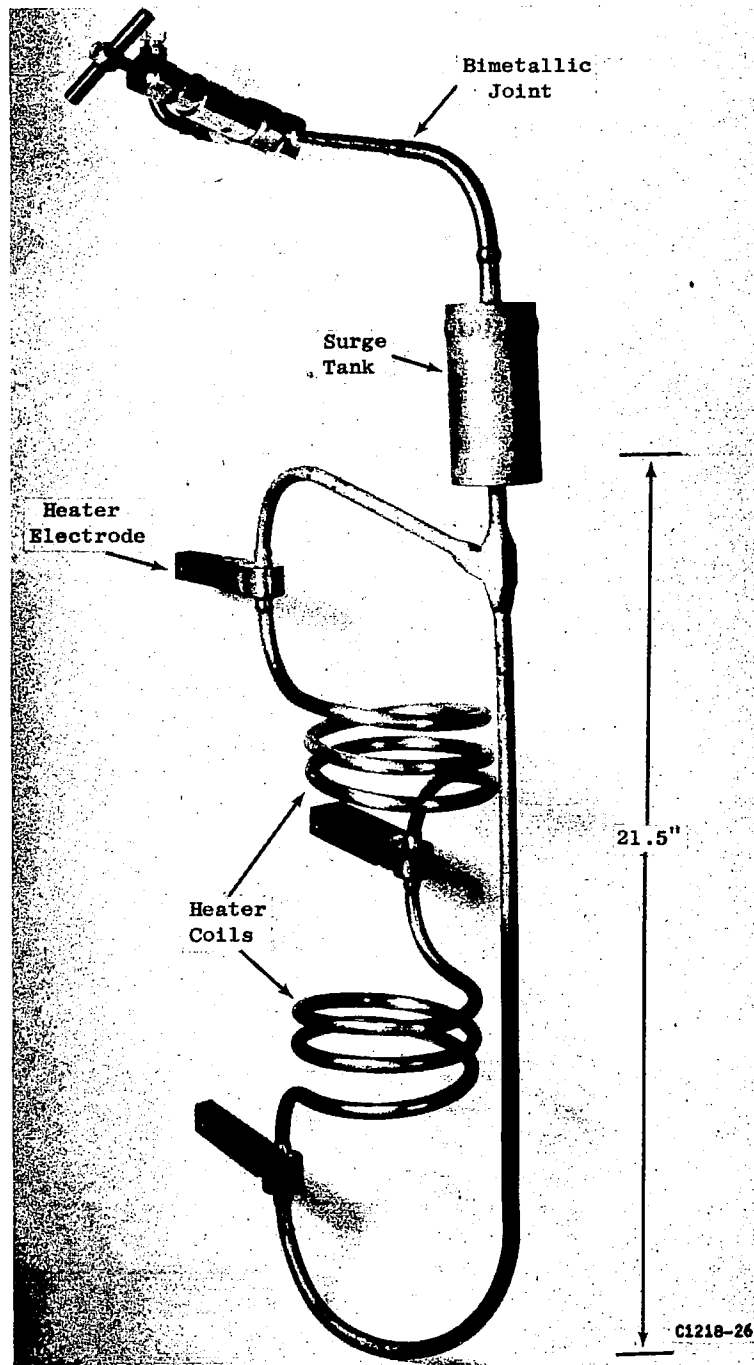


Figure 26. Cb-1Zr Sodium Thermal Convection Loop Following 1000 Hour Test.

X. CHEMICAL AND METALLURGICAL EVALUATION OF TEST COMPONENTS

The evaluation of the various portions of the loop consisted primarily of chemical analysis of the Cb-1Zr tubing, metallographic examination, bend testing, and microhardness surveys across tube walls. Various regions of the loop used in these evaluations are identified in Figure 27.

A. Results of Chemical Analysis of Cb-1Zr Tubing

The results of chemical analyses performed on various samples taken from the loop are given in Table VIII. No significant changes were noted in the nitrogen and carbon concentrations of the samples analyzed.

The oxygen concentrations of the various specimens indicated that oxygen pickup from the test environment was not-significant. The apparent high oxygen concentration of the outer portion of the wall of the Region A specimen is attributed to residual particles of alumina which were embedded in the outer surface as a result of the grit blasting of this area to increase the emittance of the tube. Metallographic detection of residual alumina particles in the outer surface and the low oxygen concentration of similar regions of the loop which were not grit blasted confirmed that the grit blasting treatment caused the high oxygen results. Limited tests were also conducted on control specimens to determine the oxygen increase in Cb-1Zr tubing resulting from the alumina grit blasting treatment used on certain regions of this loop. These results⁽⁴⁾ indicated that an oxygen increase of approximately 200 ppm would occur in Cb-1Zr tubing with 0.065-inch thick walls. The relatively low concentration of oxygen in the specimen from Region N, which was the hottest region of the loop, suggests that oxygen was depleted from this region.

Subsequent loop tests in this program which operated for longer periods of time and were analyzed in more detail confirmed the indication noted in this test, i.e., migration of oxygen from the hotter to the cooler regions of the loop with the sodium acting as the transport medium.

(4) Potassium Corrosion Test Loop Development, Quarterly Progress Report No. 4, for Period Ending June 15, 1964, NASA Contract NAS 3-2547, NASA-CR-54167, p. 65.

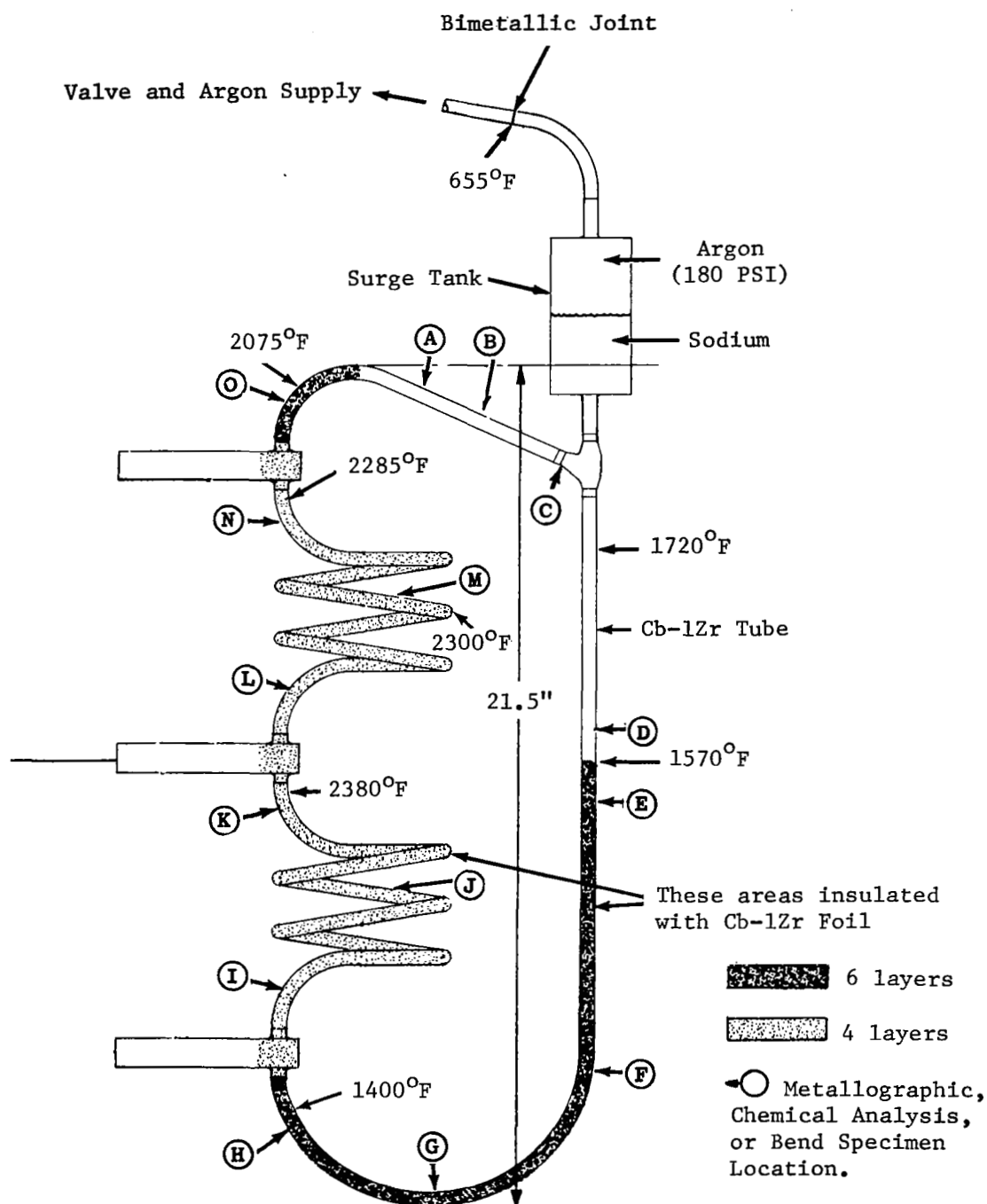


Figure 27. Sodium Thermal Convection Loop Showing Location of the Cb-1Zr Specimens Taken for Metallurgical and Chemical Evaluation. Temperatures Indicated are Nominal Temperatures for the First Period (0 to 509 Hours) of Loop Operation.

TABLE VIII

CHEMICAL ANALYSES OF VARIOUS Cb-1Zr TUBE
SPECIMENS FROM THE SODIUM THERMAL CONVECTION LOOP

Specimen Description	Chemical Analysis, ppm ^{a,b}			
	O	N	H	C
Region A ^c , (2000°F) ^d				
Outer 21 Mils ^e	310	11	50	-
Middle 21 Mils	171	1	79	-
Inner 21 Mils	199	5	62	-
Region H, (1400°F)				
Total Cross Section	190	3	37	40,50
Region M, (2300°F)				
Total Cross Section	69	3	13	-
Region O, (2074°F)				
Total Cross Section	194,216, 125,149	14,16, 13,9	173,174, 180,181	-
Before Test (MCN 404)	114,136	1,9	1,4	20,30

^aOxygen, nitrogen, and hydrogen concentrations determined by vacuum fusion analysis.

^bCarbon concentration determined using the conductimetric method.

^cLocation of the specimens indicated in Figure 27.

^dNominal temperature of region during first period (0 to 509 hours) of loop operation.

^eHigh oxygen concentration of this sample attributed to residual particles of alumina embedded in the outer surface during grit blasting to increase emittance.

The high hydrogen concentration detected in several regions of the loop was not anticipated. As indicated in the previous section, the loop was cut into sections 6 to 8 inches long with a tubing cutter, and the residual sodium which remained after the draining operation was removed by immersing these sections in absolute ethyl alcohol. It has been concluded from a number of subsequent tests that have been performed that the hydrogen pickup by the Cb-1Zr tubing occurred during the alcohol dissolution of the residual sodium from the tube walls. Although this phenomenon has been studied by other investigators⁽⁵⁾ in connection with the removal of lithium for refractory alloy tubing, it was not anticipated to be a problem for the specimens listed in Table VIII. Only a thin film of sodium remained on the walls of the specimen from Region O, which showed the highest hydrogen concentration, and the dissolution of this film by the alcohol was complete in a few seconds. In spite of the limited time required for the removal of the sodium, it appears that sufficient hydrogen was generated and diffused into the tube wall, substantially increasing its hydrogen concentration.

Previous investigations of the columbium-hydrogen system⁽⁶⁾ have indicated that increasing temperature and decreasing hydrogen pressure result in substantial decreases in the equilibrium hydrogen concentration of columbium.

The referenced study indicated hydrogen concentrations of less than 100 ppm in columbium following equilibration at 700°C (1292°F) in a hydrogen environment of 25 torr. The results of similar studies by Katz and Gulbransen⁽⁷⁾ on columbium containing 0.79 percent zirconium yielded similar results. These investigations indicate that the equilibrium hydrogen concentration of the Cb-1Zr loop tubing from the region of high post-test hydrogen concentration, Region O, where the operating temperature was in excess of 2000°F and the

(5) Personal communication, J. H. DeVan, Oak Ridge National Laboratory.

(6) Albrecht, W. M., Mallett, M. W., and Goode, W. D., "Equilibria in Niobium-Hydrogen System," J. Electrochemical Society, 105 (1958) 219, pp 461-453.

(7) Katz, O. M. and Gulbransen, E. A., Discussion Section, J. Electrochemical Society, 105/12 (1958) 756, p. 462.

hydrogen partial of the chamber was always less than 10^{-7} torr, should have been very much less than 100 ppm. To substantiate this conclusion, a test was conducted on a specimen of the Cb-1Zr loop tubing to assure that the high hydrogen concentration could not have been present in the tube wall at the completion of loop operation. A sample of the tubing from Region O, which previously analyzed 177 ppm hydrogen (average of four analyses listed in Table VIII) was heated for four hours at 2000°F in a 1×10^{-5} torr vacuum. Duplicate analyses of this Cb-1Zr tube specimen yielded a hydrogen concentration of 3 ppm. This rapid removal of hydrogen is additional evidence to support the conclusion that the hydrogen could not have been present in the tubing prior to the alcohol stripping procedure. Stripping experiments⁽⁸⁾ have subsequently shown that the alkali metal solvent, n-butyl cellosolve, does not result in hydrogen pickup by refractory alloys and this solvent or distillation will be employed in the cleaning of future loop test components to avoid the problem of possible hydrogen contamination.

(8) Personal Communication, C. E. Sessions, Oak Ridge National Laboratory.

B. Results of Metallographic Examination of Cb-1Zr Components

A total of 25 metallographic specimens were prepared from various regions of the loop. The microstructure of the Cb-1Zr tubing used to construct the loop is shown in Figure 28. As indicated previously in Section III of this report, the final annealing heat treatment of this tubing was one hour in vacuum at 2200°F. The grain size of the tubing before test was ASTM No. 6-7. The Cb-1Zr materials used to fabricate the loop were pickled in a solution of 60H₂O-20HF-20HNO₃ (percent by volume) to remove 0.2 to 0.4 mil of the surface prior to release for fabrication. The pickling was performed in accordance with SPPS Specification 03-0010-00-B, Chemical Cleaning of Columbium and Columbium Alloy Products⁽⁹⁾. The typical ID surface of the tubing had smooth, shallow irregularities with a maximum depth of 0.5 mil.

Metallographic examination of both longitudinal and transverse Cb-1Zr tubing from all regions of the loop revealed no evidence of corrosion of either the base material or the weldments used to join the various loop components. The most significant metallographic observation was the considerable amount of abnormal grain growth that occurred in those portions of the loop which were bent during loop fabrication (e.g., heater coils) and operated at temperatures in excess of 2000°F during the 1,000-hour test. This phenomenon is illustrated in Figure 29 which shows cross sectional views of two regions of the Cb-1Zr tube wall. Bending the tube on a 4-inch diameter during loop fabrication resulted in maximum strains of approximately 8% on both the compression and tension side of the tube. This well-known metallurgical phenomenon has been studied in many metals and alloys^(10,11). A small test program was conducted on the Cb-1Zr tubing used in the construction of the Sodium Thermal Convection Loop to determine the effect of the required bending and subsequent heating to the temperatures of interest on the grain size. The results obtained are

(9) Frank, R. G., et al., Potassium Corrosion Test Loop Development Topical Report No. 2, Material and Process Specifications for Refractory Alloy and Alkali Metals, R66SD3007, General Electric Company, Cincinnati, Ohio, December 13, 1965, p. 281.

(10) Murphy, D. J., et al., "Critical Strain in High Purity Tantalum and Tantalum-Tungsten Alloys," LA-2871, Los Alamos Scientific Laboratory, June 24, 1963.

(11) Rostoker, William and Dvorak, James R., "Interpretation of Metallographic Structures," Academic Press, New York, 1965, p. 28.

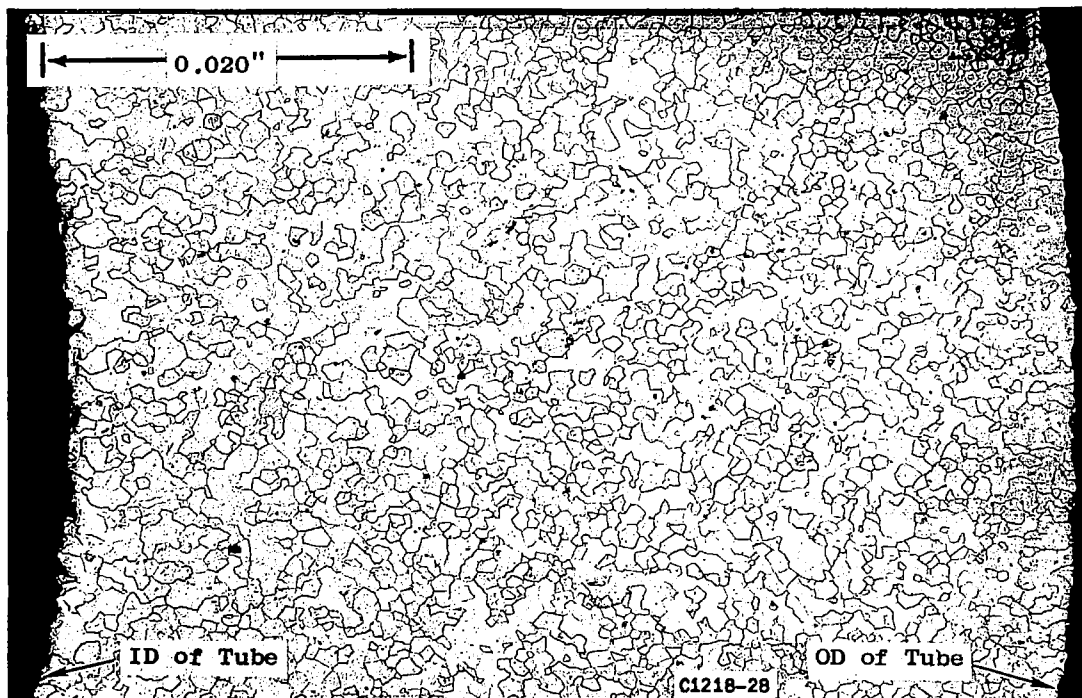


Figure 28. Microstructure of a Cross Section of the Cb-1Zr Tubing (0.375-Inch OD x 0.065-Inch Wall Thickness) Before Test.

Etchant: 60mlGlycerine-20mlHF-20mlHNO₃

Mag: 75X

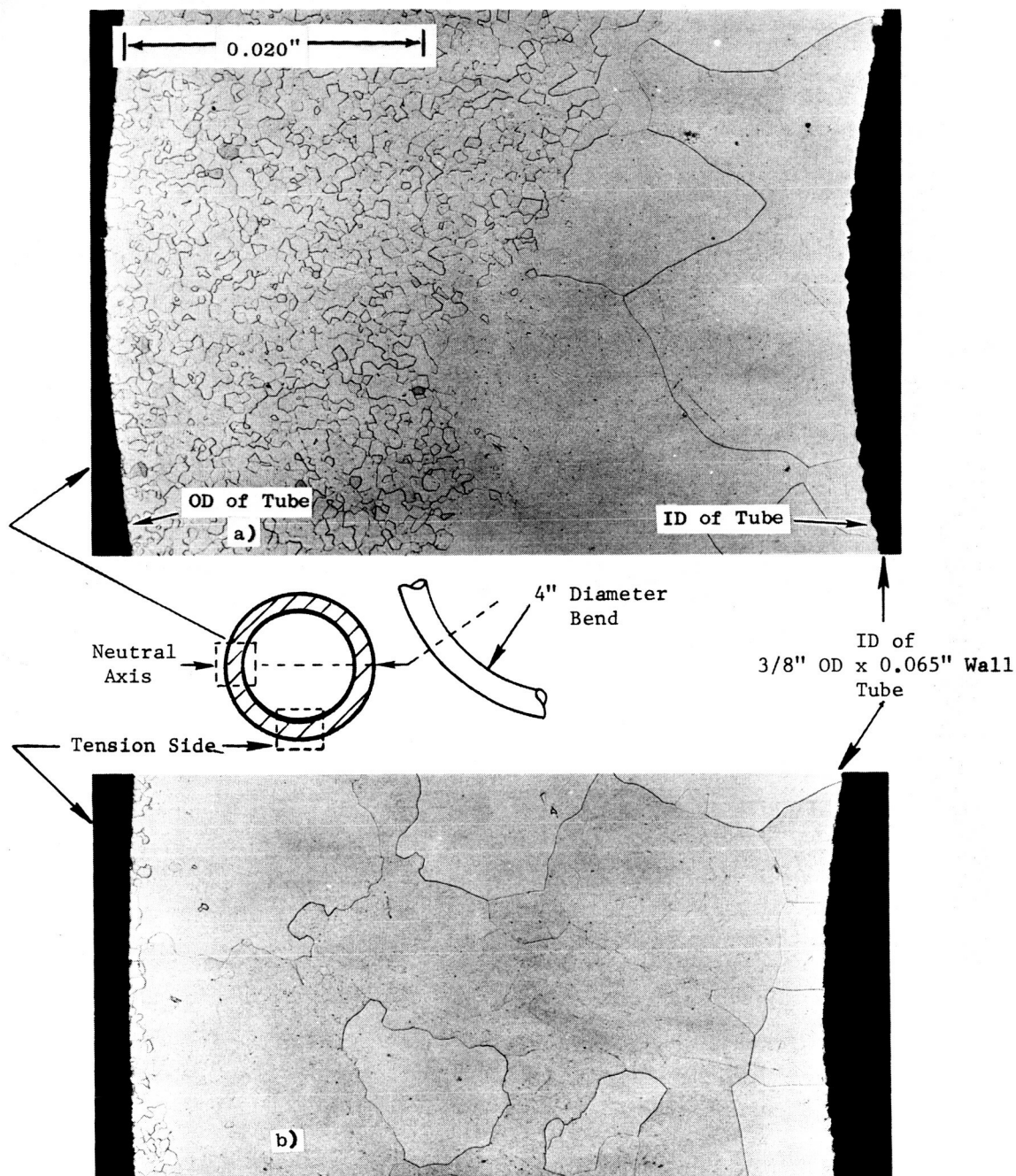


Figure 29. Cross Sectional Photomicrographs of Cb-1Zr Tube From Region 4 Inches Below Middle Heater Electride (Near Region K in Figure 27).

- a) Neutral Axis Area of Tube Bend Showing Partial Grain Growth.
- b) Tension Side of Tube Bend Showing Practically Complete Grain Growth.

Etchant: 60mlGlycerine-20mlHF-20mlHNO₃ Mag: 75X

described in detail in Appendix C and the grain growth obtained in the bent regions of the loop specimens following test are in good agreement with the pre-test observations described in Appendix C. The grain growth apparent in Figure 29 and in several of the photomicrographs described below is a result of the bending and thermal treatment and was not influenced by the sodium environment. The abnormal grain growth occurred to a limited degree in the neutral axis region of the 4-inch bend as illustrated in Figure 28a, but was essentially completed in the maximum strain area located 90 degrees from the neutral axis as shown in Figure 29b.

The typical metallographic appearance of tubing from the top heater coil is illustrated in Figure 30. The slight surface roughening which may be noted on the ID surface is typical of the 0.5 mil or less of surface irregularity observed in before test tube specimens. The metallographic appearance of specimens taken from the region just beyond the top heater electrode (Region O in Figure 27) is shown in Figure 31. This region had a high hydrogen concentration as described in the previous section, and had very little ductility after test. The bend results are described in detail in the next section.

Specimens taken from the cold leg of the loop (Regions A through F) were similar in metallographic appearance to the before test structure illustrated in Figure 28. Some evidence of possible oxygen pickup, presumably from transfer from the hotter regions of the loop was noted near the ID of the metallographic specimen which was taken from Region H, the minimum temperature region (1400°F) in the flow circuit. The microstructure of this specimen is shown in Figure 32. The slight increase in the oxygen concentration of the tube wall in this region (125 to 190 ppm) and the similar appearance of a fine precipitate located in the dark areas to ZrO_2 is the evidence for concluding that the dark region near the ID resulted from oxygen pickup from the flowing sodium. Unfortunately, there was not a sufficient length of straight tubing in this region to obtain meaningful gradient samples for chemical analysis.

In summary, the metallographic examination of specimens from all regions of the loop, including weldments, revealed no evidence of attack, and the grain growth observed in certain regions resulted from bending during loop fabrication and subsequent high temperature operation during the test.

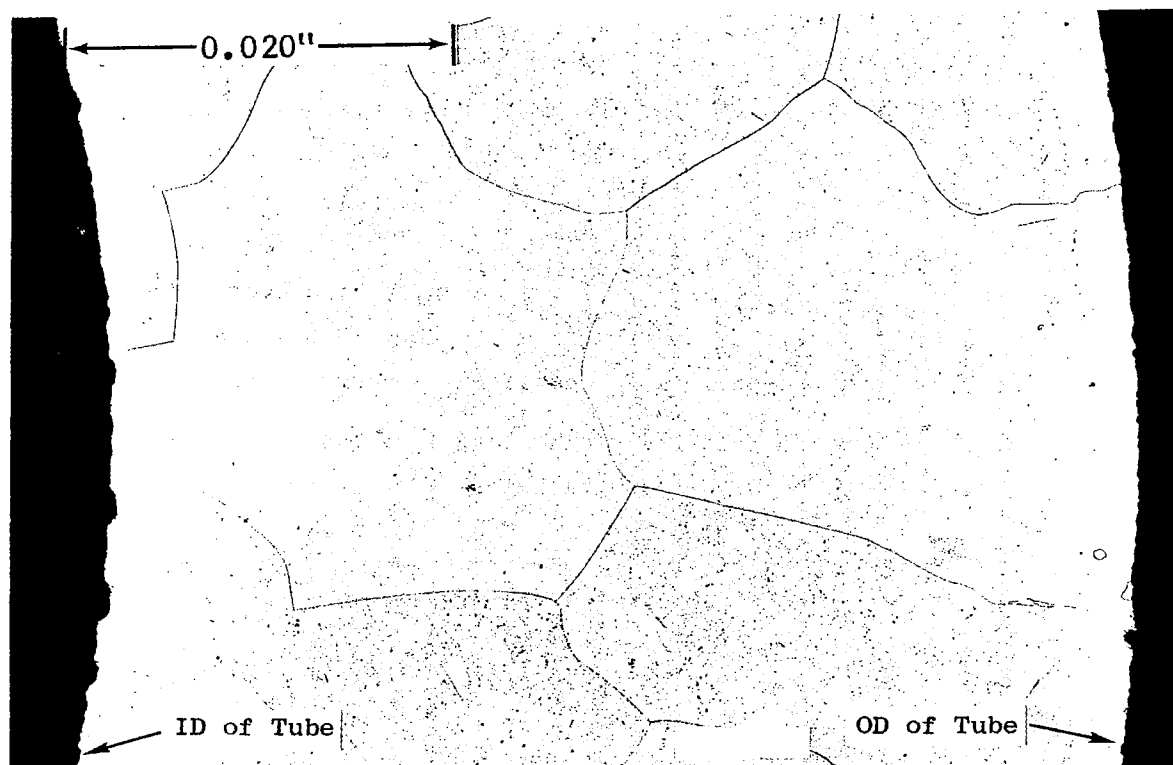


Figure 30. Microstructure of a Cross Section of the Cb-1Zr Tube From the Middle of the Top Heater Coil (Region M in Figure 27).

Etchant: 60mlGlycerine-20mlHF-20mlHNO₃

Mag: 75X

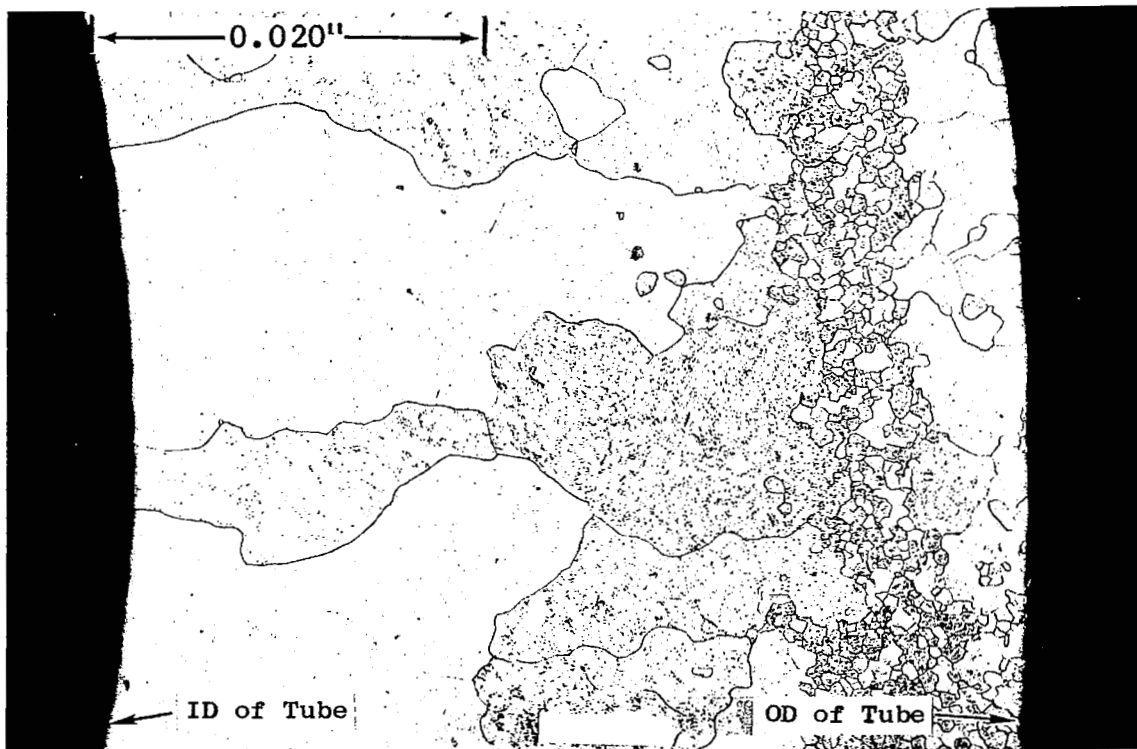


Figure 31. Microstructure of a Cross Section of the Cb-1Zr Tube From the Heater Exit (Region 0 in Figure 27).

Etchant: 60mlGlycerine-20mlHF-20mlHNO₃

Mag: 75X

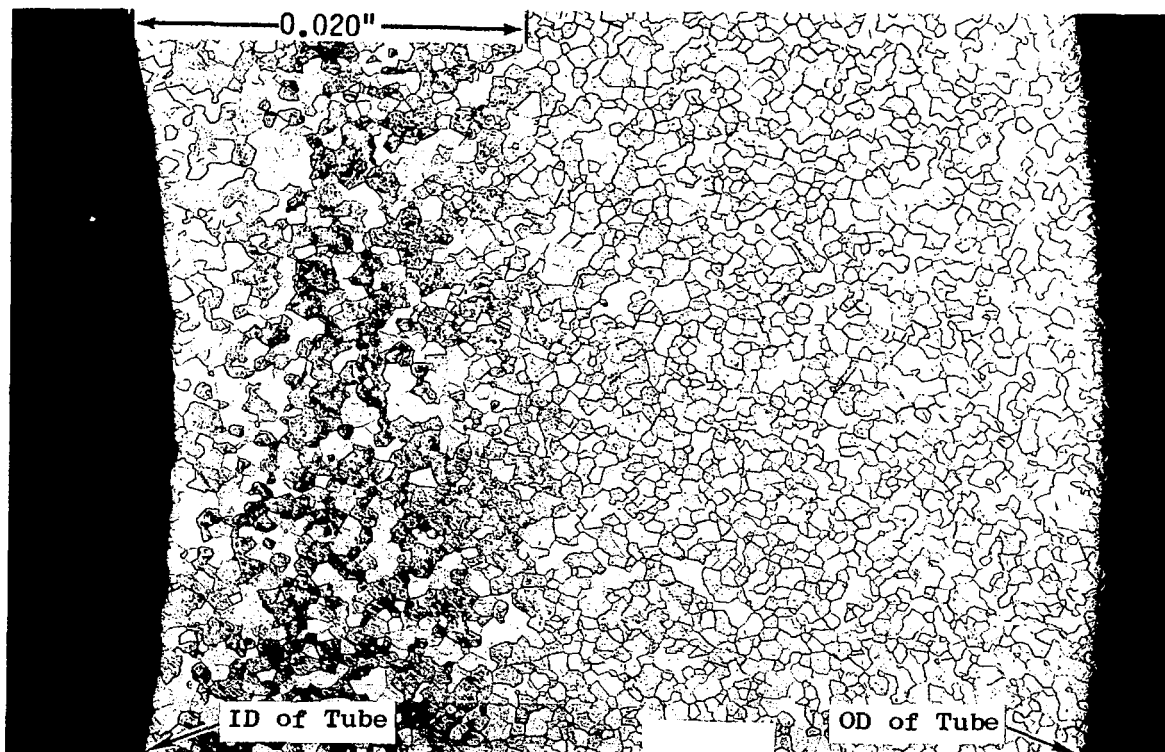


Figure 32. Microstructure of a Cross Section of the Cb-1Zr Tube From the Heater Inlet (Region H in Figure 27).

Etchant: 60mlGlycerine-20mlHF-20mlHNO₃

Mag: 75X

C. Results of Bend Tests of Tube Specimens

The post-test ductility of 1/2-inch long tube sections taken from eight regions of the loop was checked by flattening the tubes in a hydraulic press using a strip of 0.060-inch thick sheet as an internal support. Measurement of the specimens following flattening indicated a bend radius of 0.030 inch (one-half the tube wall thickness) for those specimens which could be completely flattened. Five of the specimens were found to be quite ductile, but duplicate specimens taken from Region O (Figure 27) and a single specimen from Region A cracked in an extremely brittle and transgranular manner. The ductility typical of all regions of the loop tubing, except Regions A and O, is illustrated by (a) and (b) in Figure 33. The dark band near the ID wall of the specimen illustrated in Figure 33a was previously shown at higher magnification in Figure 32. Although the size of the grains in the specimen from Region N (Figure 33b) was enormous, 10 to 40 mils in diameter, the specimen was completely ductile. The brittle nature of the specimens from Region O is illustrated in Figure 33c. A second bend specimen from Region O is shown in Figure 34. The transgranular nature of the cracking is quite apparent in the enlarged view in Figure 34b. Some evidence of deformation is apparent in the fine grained region of the tube wall. As indicated in the previous section, Region O was abnormally high in hydrogen concentration, approximately 180 ppm, and this fact plus the very large grain size in this region was no doubt responsible for the brittle behavior. Although the hydride phase could not be detected metallographically, the appearance of the cracks in Figure 34b suggests that the cracking may have occurred along very thin platelets of hydride phase⁽¹²⁾. The fact that hydrogen contamination was responsible for the cracking was confirmed by restoring completely ductile behavior to tube specimens from Region O by heat treating a vacuum at 2000°F for 4 hours. This heat treatment reduced the hydrogen concentration from 180 ppm to 3 ppm. Additional evidence to support the contention that hydrogen and not the

(12) McCoy, H. E. and Douglas, D. A., "Effect of Various Gaseous Contaminants on the Strength and Formability of Columbium," Columbium Metallurgy, Interscience Publishers, New York, 1961, page 112.

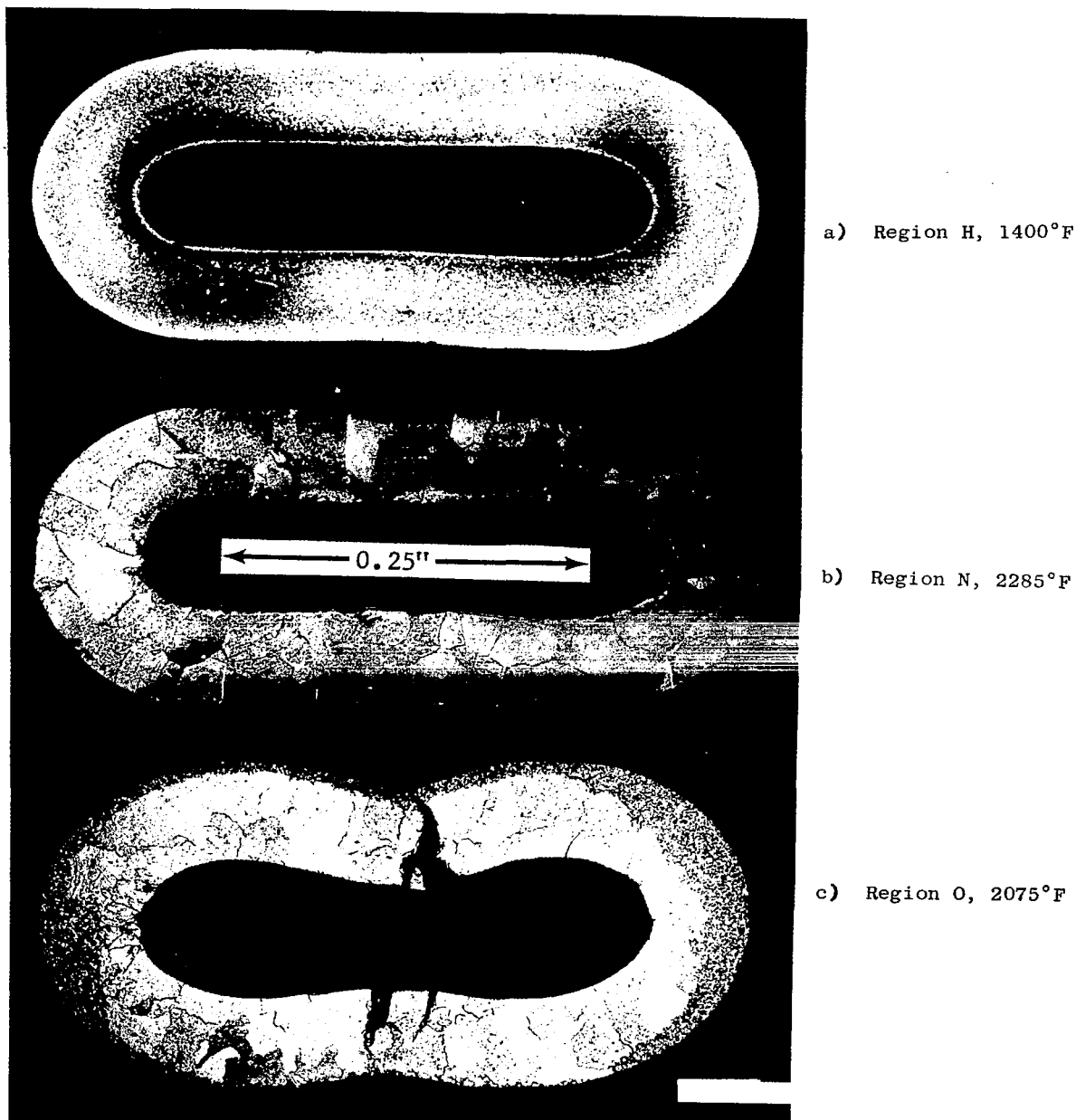


Figure 33. Cross Sections of Cb-1Zr Tube Bend Specimens From Various Regions of the Sodium Thermal Convection Loop. Temperatures Shown are the Temperatures of These Regions During the First Period (0 to 509 Hours) of Loop Operation.

Etchant: 60mlGlycerine-20mlHF-20mlHNO₃

Mag: 10X

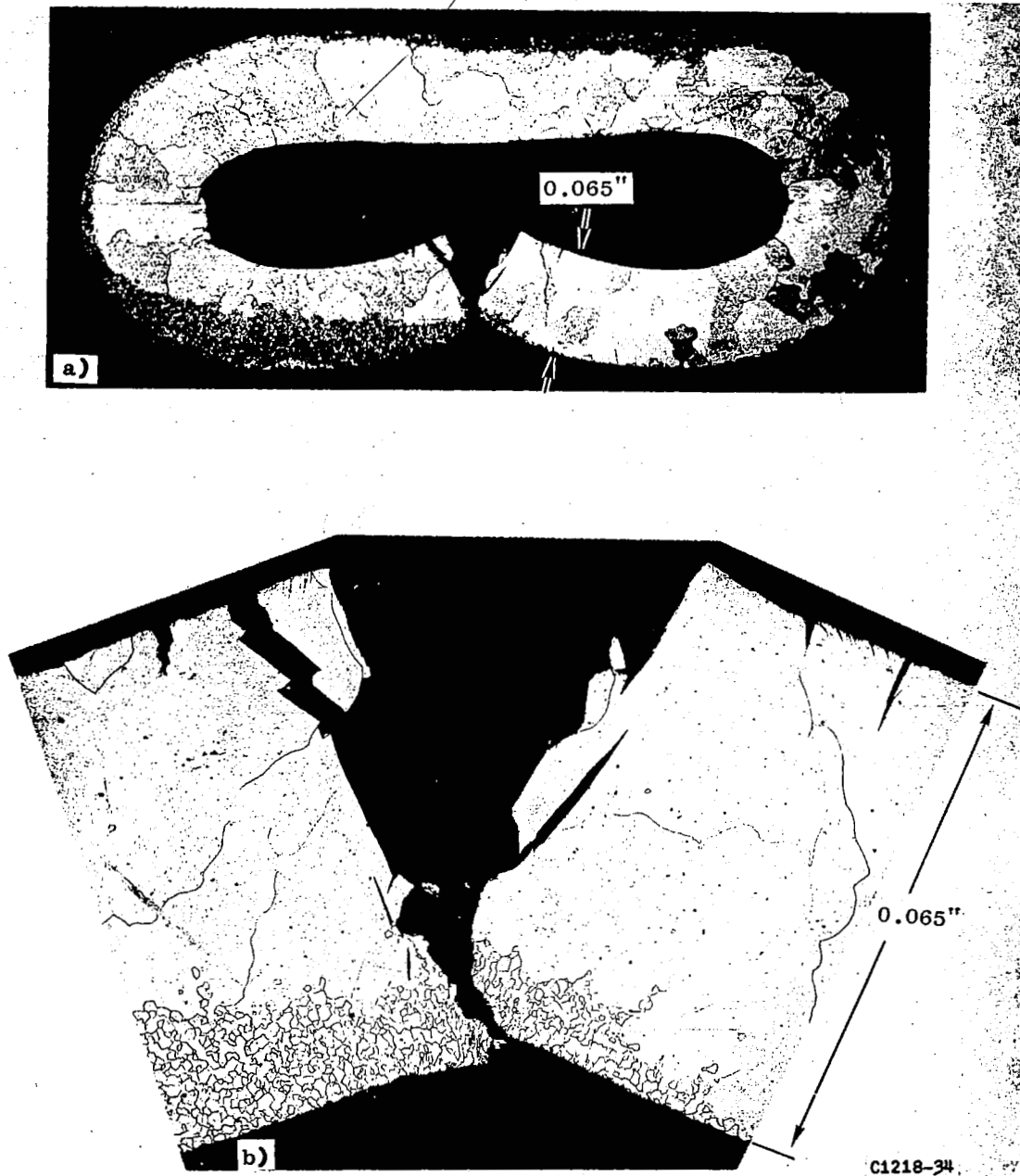


Figure 34. Cross Section of Cb-1Zr Tube Bend Specimen From Region 0 (2075°F) of the Loop. The Transgranular Nature of the Cracking is Very Evident in the Enlarged View.

Etchant: 60mlGlycerine-20mlHF-20mlHNO₃ a) Mag: 10X
b) Mag: 50X

extreme grain growth was responsible for the brittleness observed is afforded by the ductile behavior of large grain specimens from Regions K (Figure 29) and O (Figures 31 and 34).

As mentioned in the previous section describing the results of chemical analysis, different techniques will be used in future tests to remove residual alkali metal in a manner that will not result in hydrogen contamination of the refractory alloy components.

D. Results of Microhardness Survey of Tube Specimens

The results of microhardness surveys across the tube wall of specimens from various regions of the loop are given in Figure 35. The bulk of the hardness values measured (49 of 52 determinations) were in the range 80 to 120 (Knoop Hardness Number) and showed no significant variation from the value of 97 measured on the tubing before test. It is interesting to note that the sudden drop (120 to 90) in the hardness of the specimen from the heater inlet (Region H) at a depth of 17 to 22 mils from the ID corresponds to the termination of the band of fine precipitate previously shown in Figure 32. The slightly higher hardness of the region of the tube wall near the OD of the specimens from the heater inlet and heater exit is attributed to slight subsurface contamination which resulted from the grit blasting of these regions with alumina prior to test to increase the emittance of the tubing. The other variations in the hardness of the various regions are not considered to be significant.

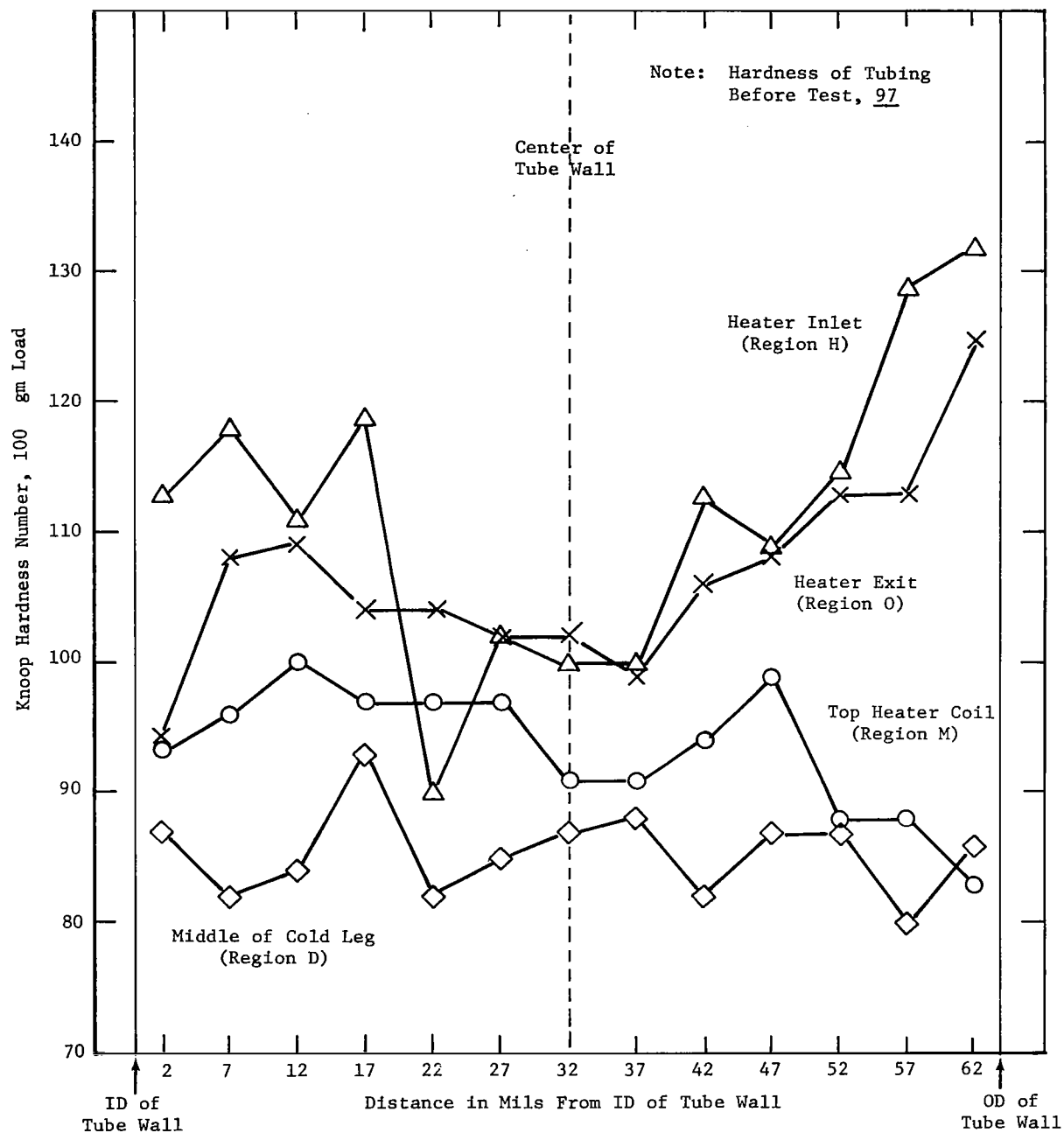


Figure 35. Microhardness Gradients of Cb-1Zr Tube Specimens from Various Regions of the Sodium Thermal Convection Loop.

XI. EVALUATION OF COMPONENT PERFORMANCE AND INSTALLATION PROCEDURES

The objectives of the Sodium Thermal Convection Loop test to prove specific components and instrumentation procedures to be used in succeeding tests of the Potassium Corrosion Test Loop Development Program were realized. The most specific objectives and their evaluations are presented in Table IX.

The 1000-ampere, water-cooled, vacuum feedthrough previously shown in Figure 8 proved to be reliable and rugged component and resulted in no difficulty in either installation or operation. No deterioration of the seal was observed during the test and no indications of leaks were detected by periodic helium leak tests using the partial pressure gas analyzer as the detector. The maximum current used during the test was 564 amperes; however, the 1000-ampere rating appears to be a conservative value since no significant temperature rise was observed in the feedthrough during steady state operation.

The electric resistance heater of the loop proved to be a convenient and reliable method for heating liquid sodium. The heater which consisted of two 4-inch diameter helical coils of 0.375-inch OD x 0.25-inch ID Cb-1Zr tube approximately 36 inches long with a common center electrode and two grounded electrodes operated without difficulty for the entire 1000-hour run. The heat generated in the lower section of the heater was approximately 20% higher than the upper coil due to its lower average electrical resistance as a result of its lower average operating temperature. The thermal unbalance observed in the heater coils of the Sodium Thermal Convection Loop will be negligible in the heater coils of the Rankine System Corrosion Test Loop because of the much higher sodium velocity and the lower temperature rise in the latter system.

The temperature distribution in the top heater electrode was previously shown in Figure 20 and is in agreement with the calculated temperature distribution for a finite rectangular fin with no internal heat generation. The 61 BTU/hr of heat by I^2R electrical losses amounted to only 8% of the 768 BTU/hr of heat radiated by the electrodes and was neglected in determining the calculated temperature distribution. As previously indicated in Section VIII, Test Operation, the electrodes for future test loops will be redesigned to reduce the heat losses from the loop. The lower heat losses and the higher flow

TABLE IX

SUMMARY OF THE PERFORMANCE OF THE PRINCIPAL COMPONENTS
BEING EVALUATED IN THE 1000-HOUR SODIUM THERMAL CONVECTION LOOP TEST

<u>Component</u>	<u>Comment</u>
1. Electrical power feedthroughs; rated current capacity, 1000 amperes	No deterioration of the vacuum seal or air leakage observed. Maximum current during test: 564 amperes
2. Cb-1Zr heater electrodes	Performance satisfactory; however, future electrodes will be modified by drilling holes in the electrodes to reduce heat loss from the heater fluid (Na) and to reduce the temperature at the Cb-1Zr electrode/OFHC copper bus bar interface.
3. Electrical characteristics of the heater	Performance was satisfactory. Resis- tance was within 20% of predicted values at the test conditions.
4. Thermal insulation	Dimpled Cb-1Zr foil was satisfactory in all respects. Four layers on the heater tube and six layers on other regions were readily installed and adequately insulated these portions of the loop.
5. Electrical insulation	The alumina (99.7% Al_2O_3) insulators used on the electrical power leads and the thermocouple wires were not affected by the test environment.
6. Tungsten-rhenium thermocouples	Initial installation procedures resulted both in breakage of the thermocouple leads, particularly the W-3%Re wire, and in the generation of spurious emfs in the thermocouple feedthroughs due to contact of leads with the walls of the nickel feedthrough tubes. The procedures developed and used for the re-instrumenta- tion of the loop after 509 hours of test operation resulted in reliable thermo- couple performance during the second period of loop operation.

rates of the forced convection loops will permit more accurate thermal balances and provide a secondary calibration on the flow rate to be measured by a permanent flowmeter.

The use of multiple layers of metallic foil as thermal insulation proved very effective. No significant change in the insulating effectiveness of the foil was observed during the 1000 hour test. The number of layers of foil on the heater was limited to four to minimize the short circuiting effect of heater coil with the accompanying I^2R heating of the foil. During the test, little heat generation was observed in the foil, probably due to its high electrical resistivity path through the layers of foil. The number of layers in future tests will be increased from four to six on the heater coils which should increase the thermal effectiveness by 40%. The foil did not become embrittled during the test and could be easily removed and reused if required.

Temperature measurement proved to be the greatest problem area in the entire test, both during installation and operation. The use of 0.005-inch diameter tungsten-rhenium thermocouple wire required extremely careful handling of all phases of the installation. The brazing of the thermocouple wires in the nickel tube of the vacuum feedthrough required careful control of the atmosphere and brazing procedure to obtain a leak-free assembly. However, once a leak-free assembly was obtained, no problems were experienced in the re-opening of the brazed joints or failure of the ceramic seals during the test. The extensive use of metallic foil as thermal insulation required careful installation near the exposed thermocouple wires, especially at the junction as previously illustrated in Figure 16, to prevent inadvertent contact which would result in a significant emf output error and would be extremely difficult to detect. The thermocouple installation procedures developed for this test will be quite valuable in the future loop tests in assuring accurate temperature measurements and in minimizing the loss of thermocouples due to breakage and shorts.

XII. SUMMARY AND CONCLUSIONS

Several of the test components and experimental procedures to be utilized in the Cb-1Zr Pumped Sodium Loop and the Cb-1Zr Rankine System Corrosion Test Loop have been experimentally tested. This testing was conducted in a relatively simple thermal convection loop test.

The components to be checked were I²R heaters and the associated high-current electrical feedthroughs. Also, the test gave an opportunity to check temperature measurement procedures and techniques used to monitor vacuum levels and measure partial pressures of residual gases.

In general, the components and techniques performed as anticipated. However, in some areas it was apparent that minor alterations in design or procedures utilized would result in an improved experiment. The major improvements will result from drilling holes in electrodes to reduce conduction heat losses and revised thermocoupling procedures to reduce breakage of thermocouple wires and eliminate spurious emfs generated by contact of leads with nickel feedthrough tubes.

The compatibility of the Cb-1Zr alloy with flowing sodium in a system with a larger temperature differential was substantiated. Although the flow velocity was necessarily quite low in this loop as compared with the subsequent pumped loops of this program, the fact that no corrosion was observed in areas that operated at temperatures 100° to 150°F higher than planned for the pumped systems was reassuring. The results of chemical analyses indicated a possible migration of oxygen from the hotter regions of the loop to the cooler regions. Post-test evaluation of the future loop tests will include detailed chemical analyses and metallographic examinations to determine the extent of interstitial element migration, particularly of oxygen.

The adequacy of the test chamber environment in preventing significant increases in the interstitial element concentration of the loop tubing due to contamination was substantiated.

XIII. PUBLISHED REPORTS

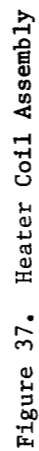
- Report No. 1 - "Purification and Analysis of Helium for the Welding Chamber" by T. F. Lyon, NASA-CR-54158, July 1, 1965.
- Report No. 2 - "Materials and Process Specifications for Refractory Alloy and Alkali Metals" by R. G. Frank, D. N. Miketta, W. H. Kearns, W. R. Young, and R. B. Hand, General Electric Report R66SD3007, December 13, 1965.
- Report No. 3 - "Materials Specifications for Advanced Refractory Alloys" by D. N. Miketta and R. G. Frank, NASA-CR-54761, October 1, 1965.
- Report No. 4 - "Purification, Analysis, and Handling of Sodium and Potassium" by L. E. Dotson and R. B. Hand, General Electric Report R66SD3012, June 13, 1966.

APPENDIX A

DRAWING LIST AND DRAWINGS OF THE Cb-12r SODIUM
THERMAL CONVECTION LOOP TEST

<u>Fig. No.</u>	<u>Title</u>	<u>Drawing No.</u>
36	Sodium Thermal Convection Loop Assembly	SK56131-226
37	Heater Coil Assembly	SK56131-228
38	Heater Coil Installation	SK56131-312
39	Tee	SK56131-230
40	Surge Tank	SK56131-231
41	Valve Tube	SK56131-237
42	Bimetallic Jount Component (Surge Tank Tube)	SK56131-239
43	Bimetallic Joint Component (Valve Tube)	SK56131-237
44	Support Structure Assembly	SK56131-329
45	Electrical Connector	SK56131-331
46	Bus Bar	SK56131-334
47	Washer	SK56131-333
48	Sleeve	SK56131-332
49	Assembly Special Electric Feedthrough	SK56131-326

Figure 36. Cb-Izr Sodium Thermal Convection Loop Assembly



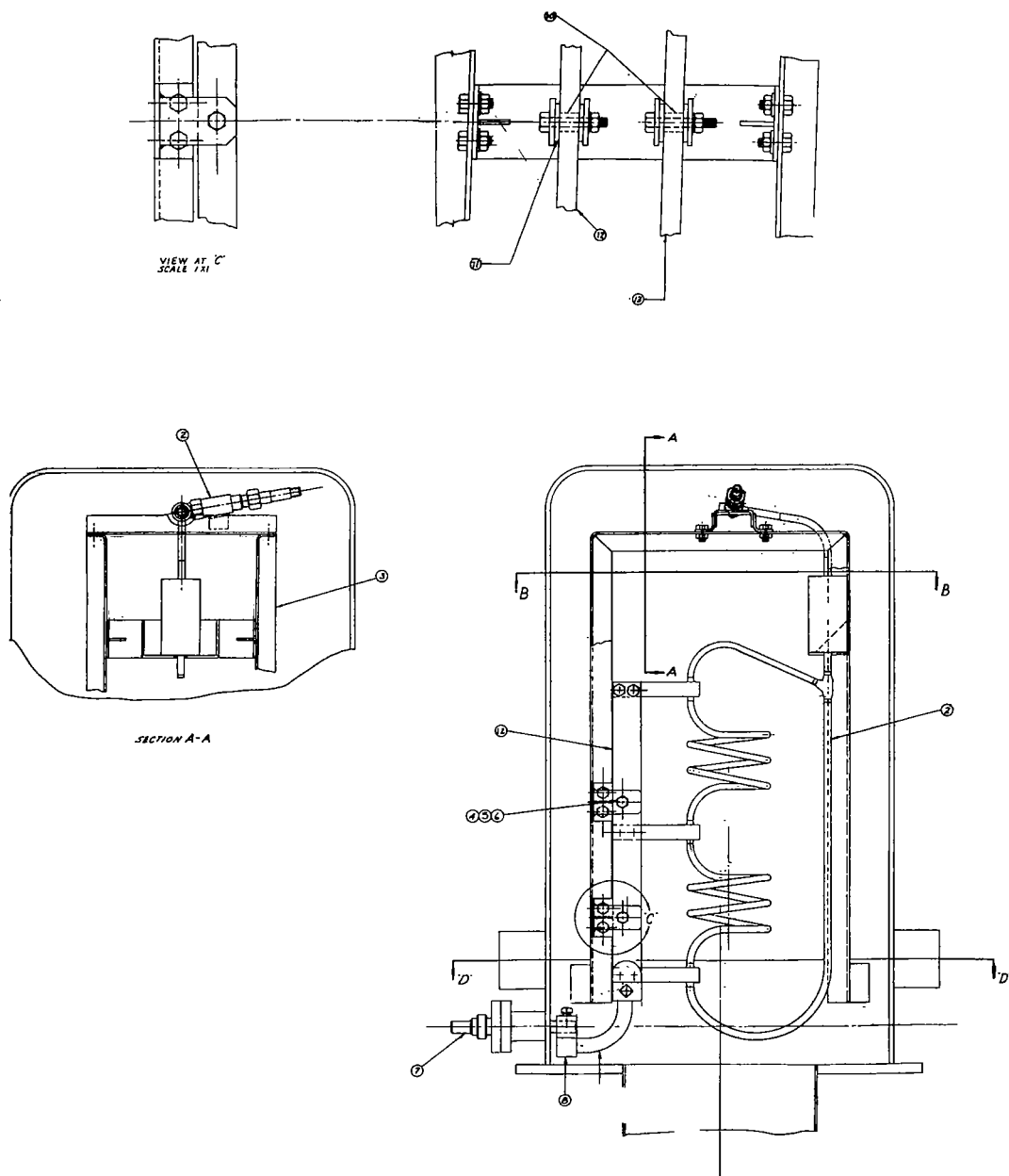
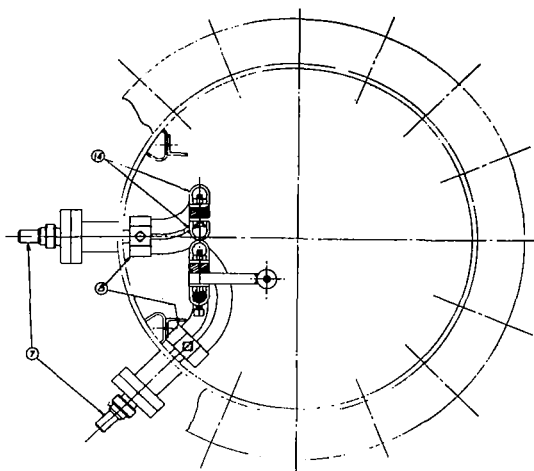
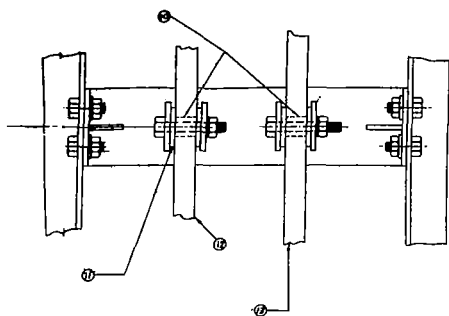
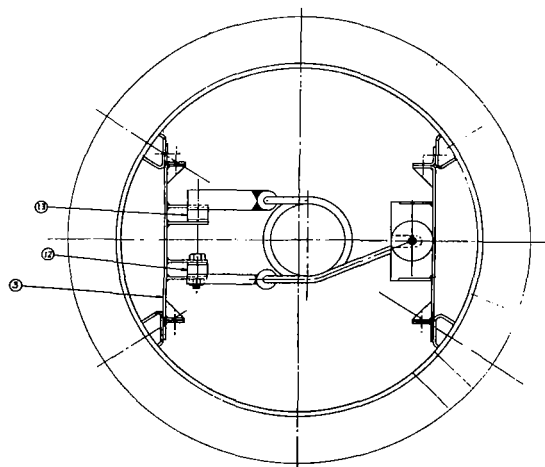


Figure 38. Heater



SECTION D-D



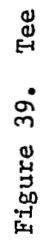
SECTION B-B

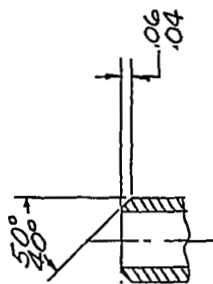
ITEM	DESCRIPTION	QUANTITY	REMARKS
1	SCREW 1/4"	1	
2	SCREW 1/4"	1	
3	SCREW 1/4"	1	
4	SCREW 1/4"	1	
5	SCREW 1/4"	1	
6	SCREW 1/4"	1	
7	SCREW 1/4"	1	
8	SCREW 1/4"	1	
9	SCREW 1/4"	1	
10	SCREW 1/4"	1	
11	SCREW 1/4"	1	
12	SCREW 1/4"	1	
13	SCREW 1/4"	1	
14	SCREW 1/4"	1	
15	SCREW 1/4"	1	
16	SCREW 1/4"	1	
17	SCREW 1/4"	1	
18	SCREW 1/4"	1	
19	SCREW 1/4"	1	
20	SCREW 1/4"	1	
21	SCREW 1/4"	1	
22	SCREW 1/4"	1	
23	SCREW 1/4"	1	
24	SCREW 1/4"	1	
25	SCREW 1/4"	1	
26	SCREW 1/4"	1	
27	SCREW 1/4"	1	
28	SCREW 1/4"	1	
29	SCREW 1/4"	1	
30	SCREW 1/4"	1	
31	SCREW 1/4"	1	
32	SCREW 1/4"	1	
33	SCREW 1/4"	1	
34	SCREW 1/4"	1	
35	SCREW 1/4"	1	
36	SCREW 1/4"	1	
37	SCREW 1/4"	1	
38	SCREW 1/4"	1	
39	SCREW 1/4"	1	
40	SCREW 1/4"	1	
41	SCREW 1/4"	1	
42	SCREW 1/4"	1	
43	SCREW 1/4"	1	
44	SCREW 1/4"	1	
45	SCREW 1/4"	1	
46	SCREW 1/4"	1	
47	SCREW 1/4"	1	
48	SCREW 1/4"	1	
49	SCREW 1/4"	1	
50	SCREW 1/4"	1	
51	SCREW 1/4"	1	
52	SCREW 1/4"	1	
53	SCREW 1/4"	1	
54	SCREW 1/4"	1	
55	SCREW 1/4"	1	
56	SCREW 1/4"	1	
57	SCREW 1/4"	1	
58	SCREW 1/4"	1	
59	SCREW 1/4"	1	
60	SCREW 1/4"	1	
61	SCREW 1/4"	1	
62	SCREW 1/4"	1	
63	SCREW 1/4"	1	
64	SCREW 1/4"	1	
65	SCREW 1/4"	1	
66	SCREW 1/4"	1	
67	SCREW 1/4"	1	
68	SCREW 1/4"	1	
69	SCREW 1/4"	1	
70	SCREW 1/4"	1	
71	SCREW 1/4"	1	
72	SCREW 1/4"	1	
73	SCREW 1/4"	1	
74	SCREW 1/4"	1	
75	SCREW 1/4"	1	
76	SCREW 1/4"	1	
77	SCREW 1/4"	1	
78	SCREW 1/4"	1	
79	SCREW 1/4"	1	
80	SCREW 1/4"	1	
81	SCREW 1/4"	1	
82	SCREW 1/4"	1	
83	SCREW 1/4"	1	
84	SCREW 1/4"	1	
85	SCREW 1/4"	1	
86	SCREW 1/4"	1	
87	SCREW 1/4"	1	
88	SCREW 1/4"	1	
89	SCREW 1/4"	1	
90	SCREW 1/4"	1	
91	SCREW 1/4"	1	
92	SCREW 1/4"	1	
93	SCREW 1/4"	1	
94	SCREW 1/4"	1	
95	SCREW 1/4"	1	
96	SCREW 1/4"	1	
97	SCREW 1/4"	1	
98	SCREW 1/4"	1	
99	SCREW 1/4"	1	
100	SCREW 1/4"	1	

C1218-38

Coil Installation

- 1 PLATE MATL PER SPEC SPPS 1B
- 2 BREAK ALL SHARP CORNERS
- 3 ALL DIA TO BE CONCENTRIC AND
IN LINE WITHIN .010 FIR.
- 4 BAG OR TAG WITH DWG NO. & SERIAL NO.





NOTES:

1. WELDING OF C₆-12R INERT GAS
2. TUNGSTEN ARC PER SPDS-3B
3. X-RAY INSPECTION REQ'D
4. BAR MAT'L PER SPEC SPDS1B
5. BREAK ALL SHARP CORNERS
6. ALL DIA'S TO BE CONCENTRIC WITHIN .010 FIR
7. TAG WITH DWG NO. & SERIAL NO.

-89-

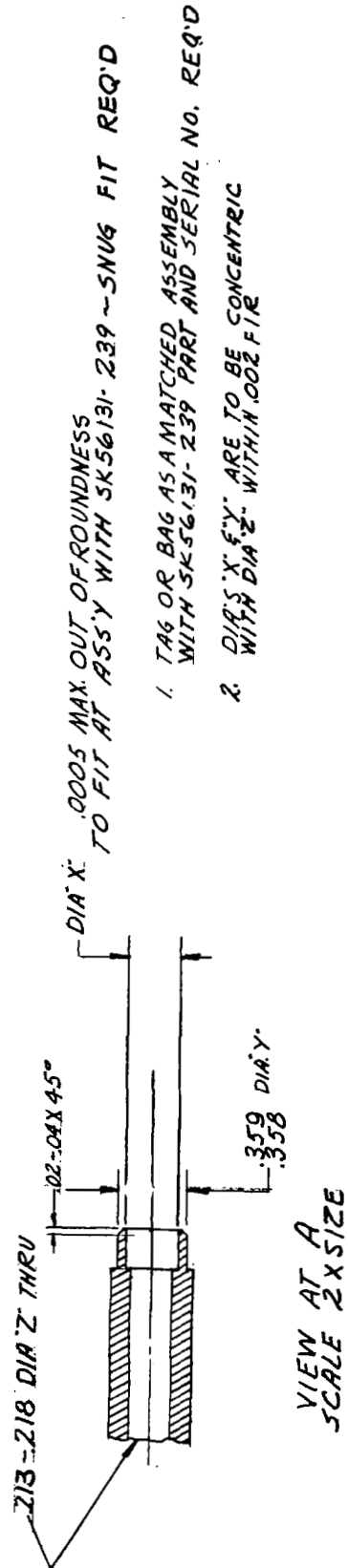
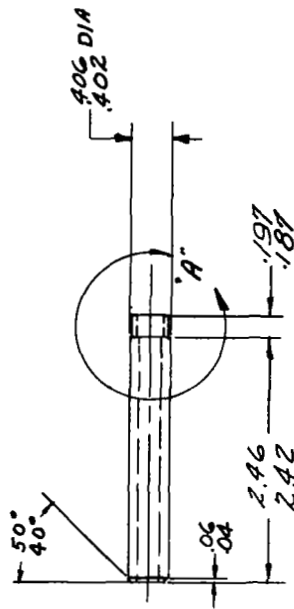
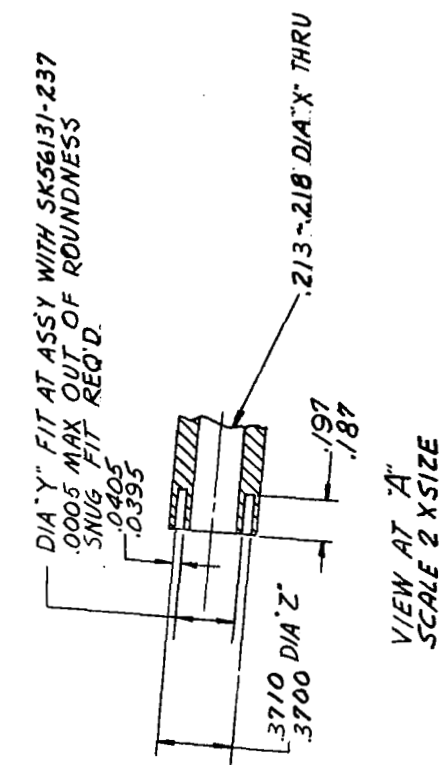
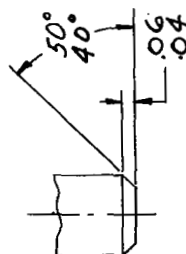
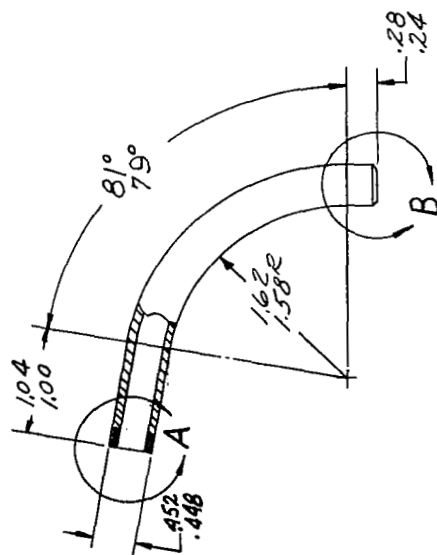


Figure 41. Valve Tube



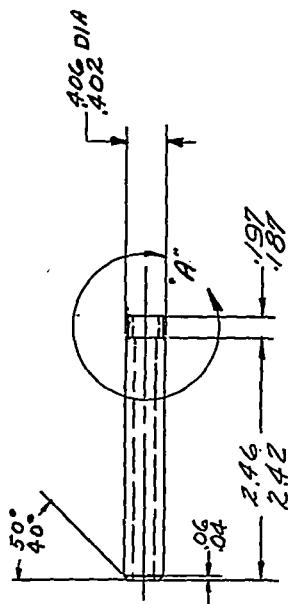
NOTES:

1. BAR MAT'L PER SPEC SPPS 1/B
2. DIA'S "Y" & "Z" ARE TO BE CONCENTRIC WITH DIA "X" WITHIN .002 FIR
3. TUBING MUST BE ROUND, STRAIGHT AND FREE OF ALL KINKS AND ABRASIONS. ONLY BENDING SPECIFIED ON DWG ALLOWED.

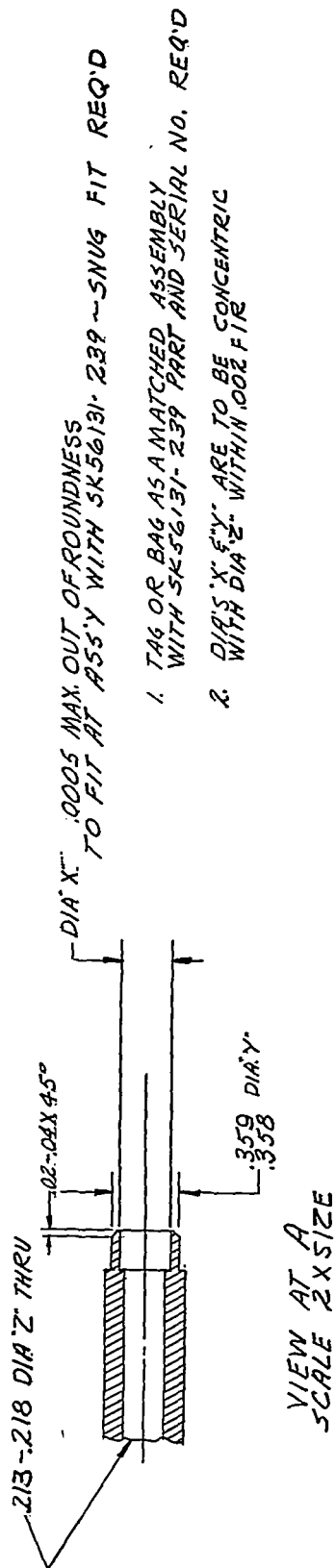


NOTES:
4. TAG OR BAG AS A MATCHED ASSEMBLY WITH SK56131-237 PART # SERIAL NO. REQ'D

Figure 42. Bimetallic Joint Component (Surge Tank Tube)

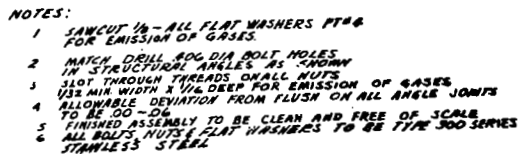
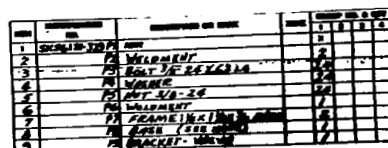


MAT'L - SEAMLESS TUBING
TYPE 316 SS PER
ASTM - A376-61T



1. TAG OR BAG AS A MATCHED ASSEMBLY WITH SK56131-239 PART AND SERIAL NO. REQ'D
2. DIA'S "X" & "Y" ARE TO BE CONCENTRIC WITH DIA "Z" WITHIN .002 FIR

Figure 43. Bimetallic Joint (SK56131-237)



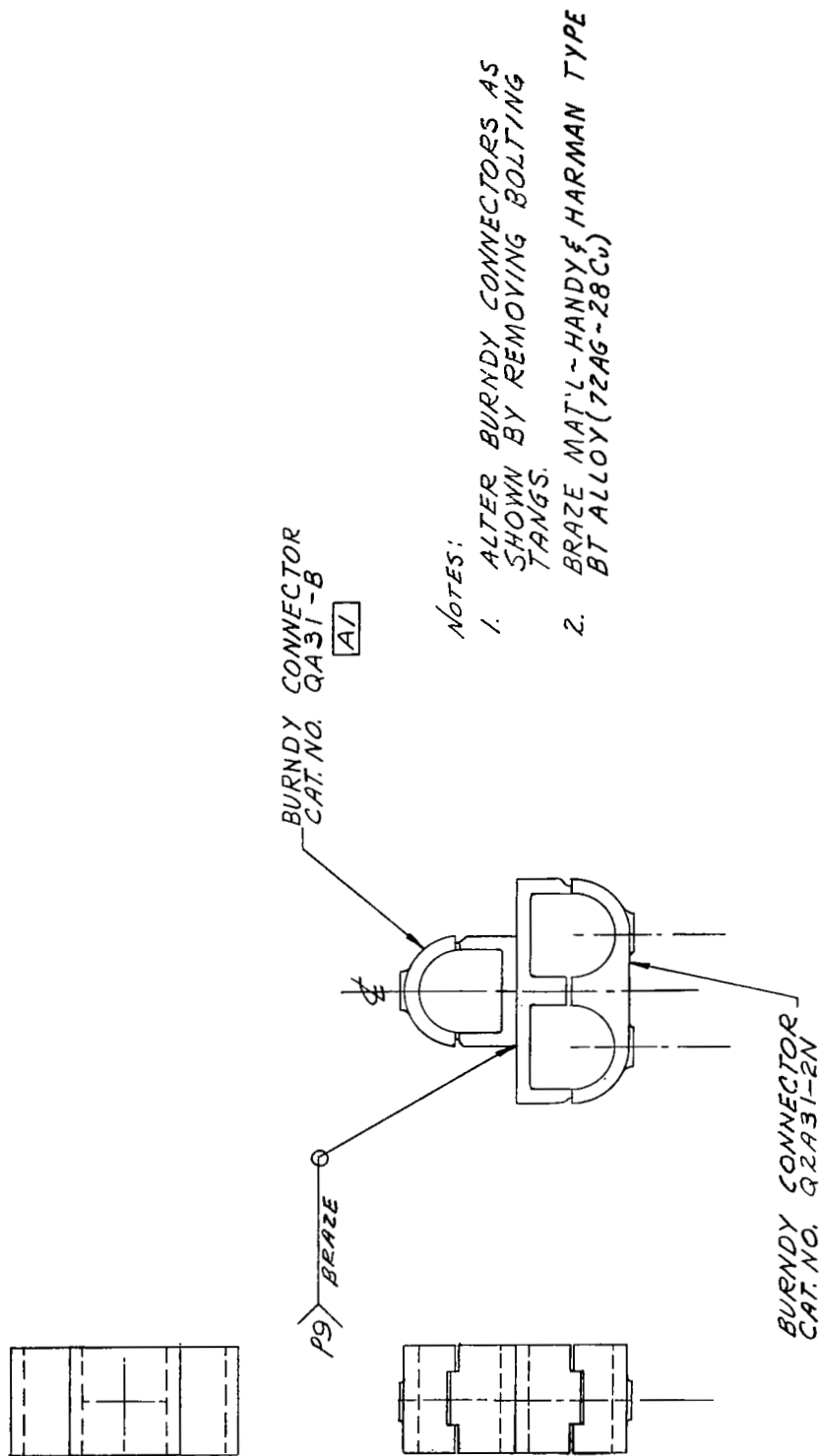
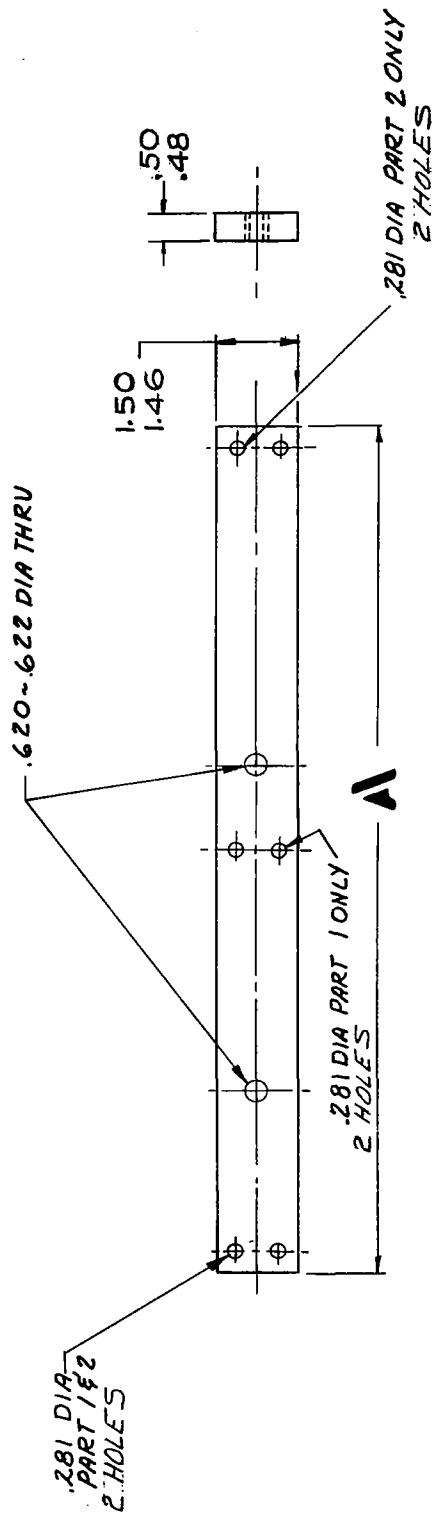
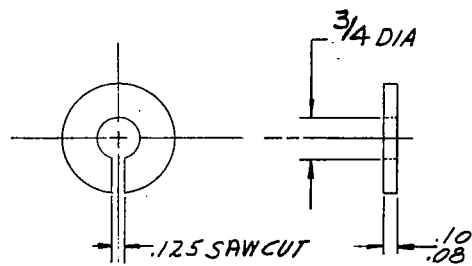


Figure 45. Electrical Connector



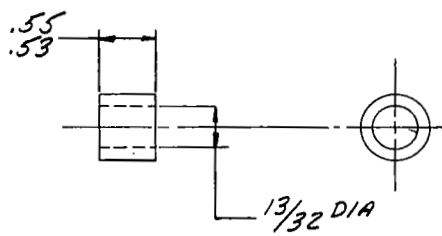
PART NO	1	2
10.12	10.08	16.76
16.72		

Figure 46. Bus Bar



MAKE FROM 99.7% Al_2O_3
 TRIANGLE RR TUBING
 MORGANITE INC.
 LONG ISLAND CITY
 1, NEW YORK

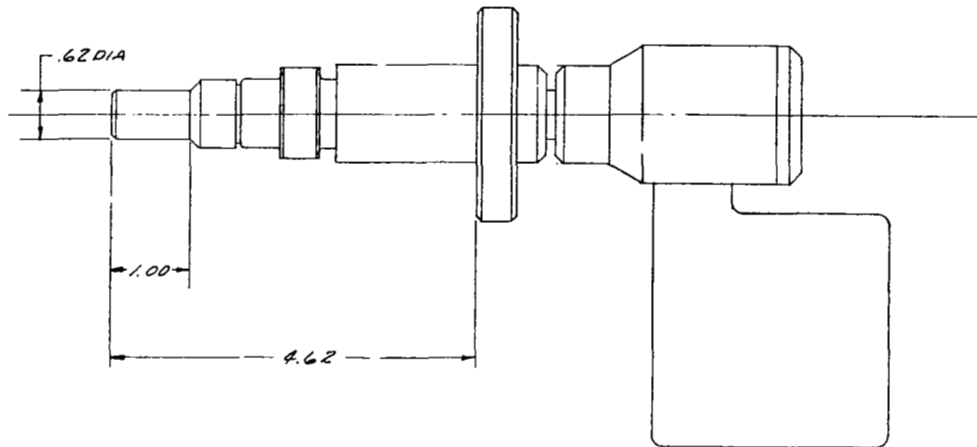
Figure 47. Washer



MAKE FROM 99.7% Al_2O_3
TRIANGLE RR TUBING
MORGANITE INC.
LONG ISLAND CITY
1, NEW YORK

Figure 48. Sleeve

RATING -
1000 AMPS
110 VOLTS



SPECIFICATION CONTROL
NO CHANGE SHALL BE MADE TO THE DESIGN, CONFIGURATION,
MATERIAL, PARTS OR MANUFACTURING PROCESSES WITHOUT
PRIOR WRITTEN APPROVAL OF THE PURCHASING DEPARTMENT
(SPPS)

Figure 49. Assembly Special Electric Feedthrough

APPENDIX B

LOOP DESIGN

1. Nomenclature

Simple Latin Letter Symbols

<u>Symbol</u>	<u>Quantity</u>	<u>Unit</u>
A	Area	ft ²
C	Specific heat	BTU/lb _m -°F
D	Diameter	ft, inch
E	Electric potential	Volts
f	Fanning friction factor	Dimensionless
g	Conversion factor	lb _m /ft ² -sec
I	Electric current	Ampere
k	Thermal conductivity	BTU-ft/ft ² -hr-°F
L	Generalized length parameter, $l \sqrt{\frac{\alpha_E}{kt} \left(\frac{T_o}{1000} \right)^3}$	ft, inch
l	Length	ft, inch
N	Number of shields	Dimensionless
P	Power input	KW
Q	Rate of heat flow	BTU/sec, BTU/hr
S	Perimeter	ft, inch
T	Temperature	°F
t	Thickness	ft, inch
W	Mass flow rate	lb _m /sec
X	Distance	ft, inch
Z	Elevation	ft, inch

Composite Latin Letter Symbols

P_f	Frictional pressure	lb_f/ft^2 , psi
P_B	Buoyancy pressure	lb_f/ft^2 , psi
N_{Re}	Reynolds number DG/μ	Dimensionless
Q_{loss}	Net heat loss from electrode	BTU/sec, BTU/hr
Q_{net}	Net heat rejected from heater	BTU/sec, BTU/hr
Q_o	Heat rejected from uninsulated electrode	BTU/sec, BTU/hr
Q_{Rej}	Heat rejected from hot leg	BTU/sec, BTU/hr
T_{end}	Electrode end temperature	$^{\circ}\text{R}$
T_{in}	Sodium temperature at heater inlet	$^{\circ}\text{R}$
T_{Na}	Sodium temperature	$^{\circ}\text{R}$
T_o	Electrode base temperature	$^{\circ}\text{R}$
T_{out}	Sodium temperature at heater outlet	$^{\circ}\text{R}$
T_e	Surface temperature at length, l	$^{\circ}\text{R}$
T_s	Surface temperature	$^{\circ}\text{R}$
T_s^*	Equivalent sink temperature of environment	$^{\circ}\text{R}$
T_w	Vacuum chamber wall temperature	$^{\circ}\text{R}$
T_x	Temperature at any distance X	$^{\circ}\text{R}$

Greek Letter Symbols

σ	Stefan-Boltzman constant	$0.173 \times 10^{-8} \text{ BTU/hr-ft}^2\text{R}^4$
ϵ	Total emissivity	Dimensionless
μ	Dynamic viscosity	$\text{lb}_m/\text{ft-sec}$
ρ_L	Average sodium density in cold leg	lb/ft^3
ρ_H	Average sodium density in hot leg	lb/ft^3
η	Fin Radiating Efficiency	Dimensionless

2. Flow Rate and Temperature Distribution

The flow rate and temperature distribution in a thermal convection loop can be determined by solving simultaneously the equations relating the flow rate, heat transfer and the heat balance in the system. Although detailed two dimensional, theoretical analyses have been carried out for laminar-free convection in simple, single pipe loops, the small variations in dimensions, operating conditions, and physical properties found in typical test loops result in an extremely difficult analysis with general solutions impractical. Although experimental tests under exact conditions are needed for reliable results, the following analysis was completed to determine the size of the electrical power equipment required to maintain a maximum operating temperature of 2200°F.

The method used in predicting the thermal performance of this loop is based on the procedure outlined by Bonilla⁽¹³⁾. A sodium temperature distribution in the hot and cold leg is assumed and the flow rate is calculated by simultaneously solving the heat balance and heat transfer equations. Using the calculated flow rate, the frictional pressure loss ΔP_F is computed and checked with the available driving head or buoyancy pressure ΔP_B due to the sodium density difference in the hot and cold legs. If the pressure forces do not agree, a new sodium ΔT is assumed until the frictional pressure ΔP_F is equal to the buoyancy pressure ΔP_B .

A schematic diagram of the thermal convection loop is shown in Figure 50. The sodium is heated in the hot leg by an I^2R electrical heater and cooled in the cold leg by thermal radiation to the water-cooled walls of the vacuum chamber. The effective height of the hot and cold legs of the loop is 18 inches.

The heat rejected by radiation from a small increment, dx , of the cooling leg is shown in the sketch below:

(13) Bonilla, Charles F., Nuclear Engineering, McGraw Hill Book Co., Inc., New York, 1957, p. 452.

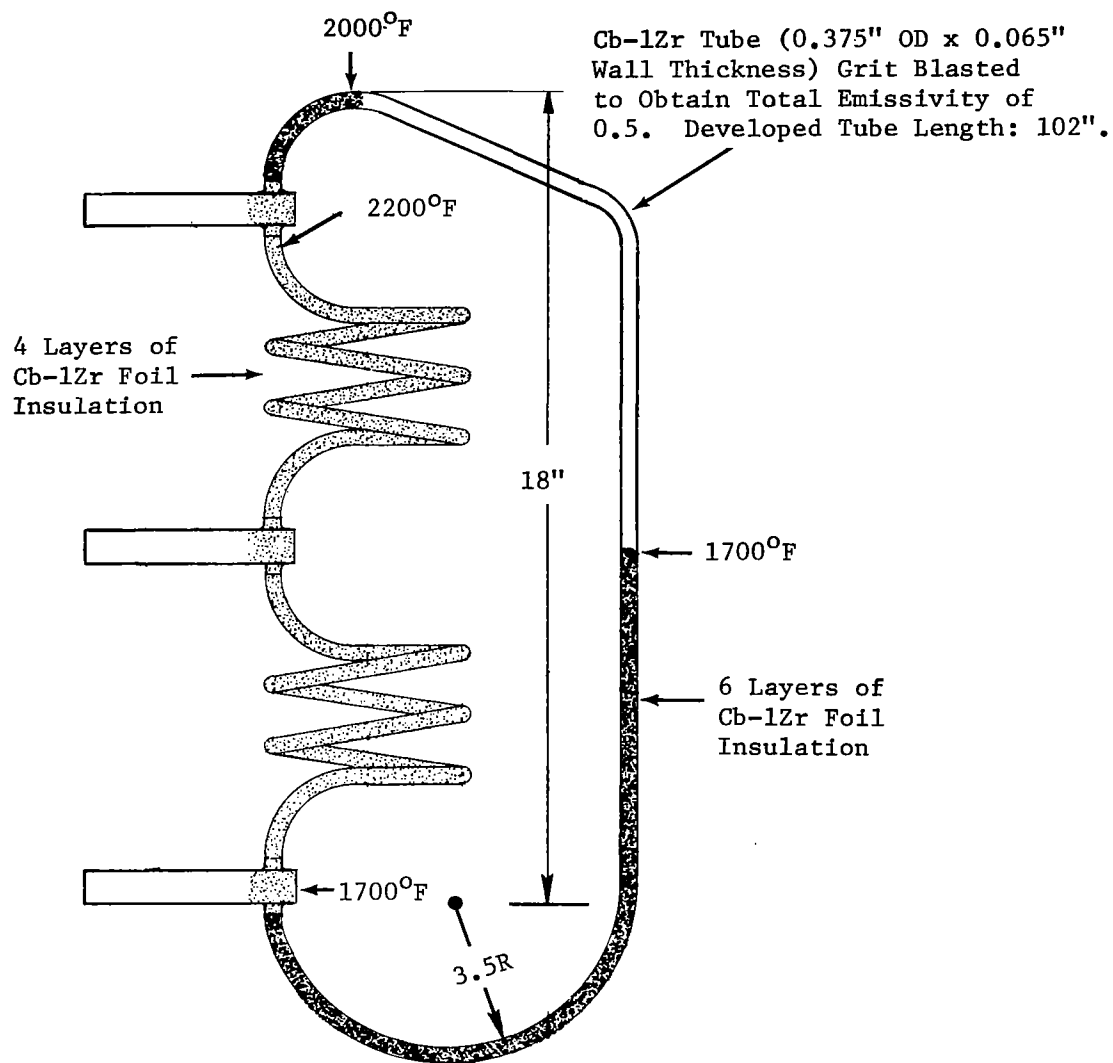
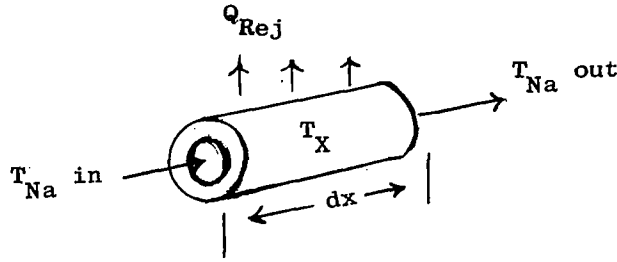


Figure 50. Schematic Diagram of Thermal Convection Loop.



$$Q_{Rej} = \sigma \epsilon A (T_s^4 - T_w^4) \quad (1a)$$

where:

T_s = temperature of tube wall

T_w = temperature of chamber wall

for $T_s^4 \gg T_w^4$

$$Q_{Rej} \cong \sigma \epsilon A T_s^4 \quad (1b)$$

Differentiating equation (1b), we find that the heat rejection rate for an incremental radiating area, dA , is equal to

$$dQ_{Rej} = \sigma \epsilon T_s^4 dA \quad (1c)$$

$$\text{For a tube, } dA = \pi D dx \quad (1d)$$

and substituting for dA in equation (1c), we obtain

$$dQ_{Rej} = \sigma \epsilon T_s^4 \pi D dx \quad (1e)$$

During steady state conditions, the heat rejected from the incremental area, dA , is also equal to the heat loss of the sodium in passing through the incremental length, dx .

$$dQ_{Na} = dQ_{Rej} = WC dT_{Na} \quad (1f)$$

Equating equations (1e) and (1f), we obtain

$$WC dT = \sigma \epsilon T_s^4 \pi D dx \quad (1g)$$

which can be rearranged to

$$\frac{dT}{T_s^4} = \frac{\pi \sigma \epsilon D}{W C} dx \quad (1h)$$

Upon integrating equation (1h), we obtain

$$\frac{1}{T^3} = \frac{3 \sigma \epsilon \pi D x}{W C} + \text{const} \quad (1i)$$

Upon evaluating equation (1i) when $x = 0$, $T = 2660^\circ\text{R}$, we obtain

$$\frac{1}{T^3} - 53.2 \times 10^{-12} = \frac{3 \sigma \epsilon \pi D x}{W C} \quad (1j)$$

where:

T = temperature at x , $^\circ\text{R}$

x = distance along cooling leg, ft

W = flow rate, lb/hr

D = OD of tube = 0.0313 ft.

C = specific heat of Na = $0.32 \frac{\text{BTU}}{\text{lb}^\circ\text{F}}$ at 1950°F (average temperature assumed for heat rejection section)

ϵ = total emissivity = 0.5 (grit blasted)⁽¹⁴⁾

σ = Stefan Boltzman constant = $0.481 \times 10^{-12} \frac{\text{BTU}}{\text{sec-ft}^\circ\text{-R}^4}$

Substituting the above values in equation (1j) and for the first trial assume a 500°F temperature drop, we calculate a flow rate of 16.5 lb/hr.

The temperature distribution along the cooling leg can now be estimated by substituting the calculated flow rate in equation (1j) and computing the temperature for any location along the cooling leg. The temperature distribution for a sodium flow rate of 16.5 lb/hr is shown in Figure 51. The

(14) Dotson, L. E., "Emittance Coating Studies on Cb-1Zr Alloy," General Electric Company Report, R61FPD571, March 15, 1962.

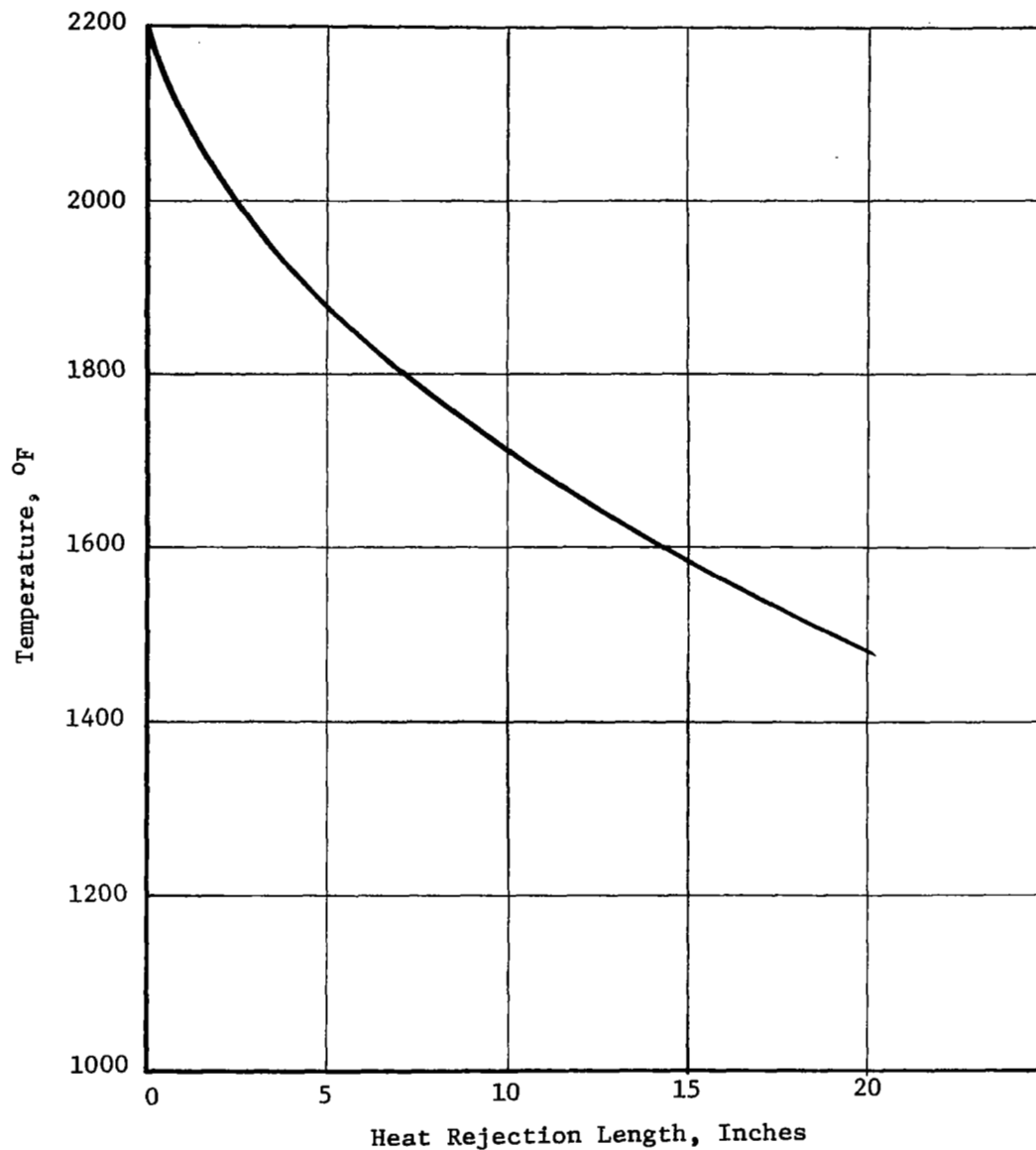


Figure 51. Temperature Distribution of the Cold Leg of the 0.375-Inch Diameter Cb-12r Tube (Emittance = 0.5) of the Sodium Thermal Convection Loop as a Function of the Heat Rejection Length.

average hot leg temperature can now be estimated and used in obtaining the buoyancy pressure ΔP_B which is used in checking the calculated flow rate based on the thermal balance and heat transfer relationships.

The computed flow rate of 16.5 lb/hr based on an assumed ΔT of 500°F must now be checked with the frictional pressure loss equation and the available head.

Reynolds number

$$N_{Re} = \frac{D W}{A} \quad (1k)$$

$$N_{Re} = 3,120 \text{ for sodium at } 1900^\circ\text{F}$$

For smooth commercial pipe, the friction factor, (f), for sodium at a Reynolds number of 3,120 is equal to 0.012⁽¹⁵⁾.

The frictional pressure loss can now be computed (neglect expansion and turning losses). The developed length of the loop is approximately 102 inches.

$$\Delta P_f = 4f \frac{L}{D} \frac{\rho V^2}{2g} \quad (1l)$$

or

$$\Delta P_f = 4f \frac{L}{D} \frac{W^2}{2\rho g A^2} \quad (1m)$$

where:

L = developed length, 102 inches

D = tube ID, 0.245 inch

ρ = density of sodium, 44 lb/ft³

A = flow area of tube, 0.000327 ft²

W = sodium flow rate, 0.00458 lb/sec

$$\Delta P_f = \left[4 (0.012) \frac{102}{0.245} \right] \left[\frac{0.00458^2}{2(44)(32.2)(3.27 \times 10^{-4})^2} \right]$$

$$\Delta P_f = 1.38 \text{ psf}$$

(15) McAdams, W. H., Heat Transmission, p. 118, McGraw Hill Book Co., Inc., New York, 1942.

The available head is the net buoyant force due to the difference in the density of the sodium in the hot and cold legs which have an overall height of 18 inches. The average temperature of the hot leg was estimated to be 1950°F. The average temperature of the cool leg was assumed to be 1745°F. The net available head ΔP is therefore equal to

$$\Delta P_B = Z (\rho_c - \rho_H) \quad (1n)$$

where:

Z = effective height of loop, 18 inches

ρ_c = density of sodium in cold leg, 45.5 lbs/ft³ at 1745°F

ρ_H = density of sodium in hot leg, 44.2 lbs/ft³ at 1950°F

For steady state conditions

$$\Delta P_B = \Delta P_F$$

$$1.8 \text{ PSF} \approx 1.38 \text{ PSF} + \text{turning losses} \quad (1o)$$

3. Power Requirements

Net Power Input - The net power input for the thermal convection loop can now be computed on the basis of the calculated flow rate of 0.00458 lb/sec (16.5 lbs/hr) and a temperature rise of 500°F.

$$Q_{\text{net}} = W C \Delta T \quad (2a)$$

$$Q_{\text{net}} = 0.00458 \frac{\text{lb}}{\text{sec}} \times 0.318 \frac{\text{BTU}}{\text{lb}^\circ\text{F}} \times 500^\circ\text{F}$$

$$Q_{\text{net}} = 0.72 \text{ BTU/sec}$$

$$Q_{\text{net}} = 0.78 \text{ KW}$$

In addition to the net heat input to the sodium, the heat losses from the heater and the electrodes must be added to give the gross electrical power input.

Heater Losses - The longitudinal temperature distribution in the heater for uniform power generation is a linear rise equal to

$$T_x = (T_{out} - T_{in}) \frac{x}{L} + T_{in} \quad (2b)$$

where:

L = total heater length, 73 inches

T_{out} = sodium temperature out, 2200°F

T_{in} = sodium temperature in, 1700°F

$$T_x = \left(\frac{(2200 - 1700)}{73/12} \right) x + 1700^\circ\text{F}$$

or differentiating

$$dT = 82.3 \, dx \quad (2c)$$

The heat loss from the uninsulated or bare heater can be estimated by

$$dQ_o = \epsilon \sigma T_s^4 \pi D \, dx \quad (2d)$$

Substituting equation (2c) into equation (2d), we obtain

$$dQ_o = \epsilon \sigma T_s^4 \pi D \frac{dT_s}{82.3} \quad (2e)$$

Integrating (2d) and evaluating, we obtain

$$Q_o = \left[\frac{\sigma \epsilon D T_x^5}{82.3 \times 5} \right]_{2160^\circ\text{F}}^{2600^\circ\text{F}}$$

$$Q_o = 2.08 \text{ BTU/sec for } \epsilon = 0.2^{(14)} \text{ (polished Cb-1Zr)}$$

The most effective type of insulation used in vacuum is a highly reflective, multiple shield assembly. For closely wound layers of dimpled foil with the same emittance as the heat source, the effectiveness of the assembly will be inversely proportional to one plus the number of shields.

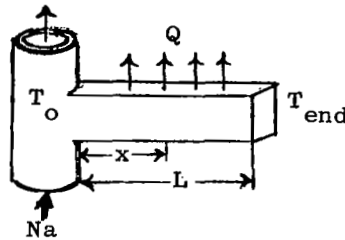
Therefore, the heat loss for the heater with four layers of columbium foil will be:

$$Q_{\text{loss}} = \frac{Q_o}{N+1} \quad (2f)$$

$$Q_{\text{loss}} \approx \frac{2.08}{4+1}$$

$$Q_{\text{loss}} \approx 0.4 \text{ BTU/sec}$$

Electrode Temperature Distribution and Heat Loss



Assuming the electrode acts as a finite fin with one dimensional heat conduction along the length; then for an element of length, dx , the change in the heat conducted along the fin can be expressed as

$$dQ_{\text{cond}} = \left[-k A \left(\frac{dT}{dx} \right)^2 \right] dx \quad (3a)$$

where A = cross section area.

The heat rejected from the surface of the incremental length, dx , is

$$dQ_{\text{rad}} = \sigma \epsilon S (T_o^4 - T_s^4) dx \quad (3b)$$

where S = circumference of electrode

Equating (3a) and (3b), we obtain

$$k A \left(\frac{dT}{dx} \right)^2 dx = \sigma \epsilon S (T_s^4 - T_w^4) dx \quad (3c)$$

or

$$\frac{d^2 T}{dx^2} = \frac{\sigma \epsilon S}{k A} (T_s^4 - T_w^4) \quad (3d)$$

Equation (3d) is the same equation that is solved by Lieblein⁽¹⁶⁾ with $\frac{\epsilon_s}{A}$ instead of $\frac{\epsilon}{t}$ for the generalized length parameter

$$L = \ell \sqrt{\frac{\sigma \epsilon}{k t} (10^9) \left(\frac{T_o}{1000} \right)^3}$$

Using equation (3d) and Figures 52 and 53, the following end temperatures and heat losses were calculated for the electrodes:

<u>Electrode</u>	<u>T_o</u>	<u>T_{end}</u>	<u>L</u>	<u>η</u>	<u>Q Loss</u>
3/4" x 1/2" x 5" LG	2200°F	1002°F	1.87	0.32	0.1 $\frac{\text{BTU}}{\text{sec}}$
3/4" x 1" x 5" LG	1950°F	1045°F	2.64	0.25	0.14 $\frac{\text{BTU}}{\text{sec}}$

Total Power Input Required - The total thermal input to the loop heater may be determined by summation of the net heat input to the sodium and the heat loss from the electrodes and the heater.

Heater input to sodium	0.7 BTU/sec
Heat loss from electrodes	0.35 BTU/sec
Heat loss from heater	<u>0.4 BTU/sec</u>
Total Power	1.45 BTU/sec
Total Power	1.53 KW

4. Electrical Characteristics of the I²R Heater

The heat input to the thermal convection loop is by electrical resistance heating of the hot leg of the loop. Heat generation occurs in both the tube and the sodium as a function of local temperature and geometry. The heater consists of two coils in series with a common center electrode and both ends grounded. The difference in the power generated between the upper and lower coil as a result of the difference in average electrical resistance

(16) Lieblein, S., "Analysis of Temperature Distribution and Radiant Heat Transfer Along a Rectangular Fin of Constant Thickness," TND-196, NASA, November, 1959.

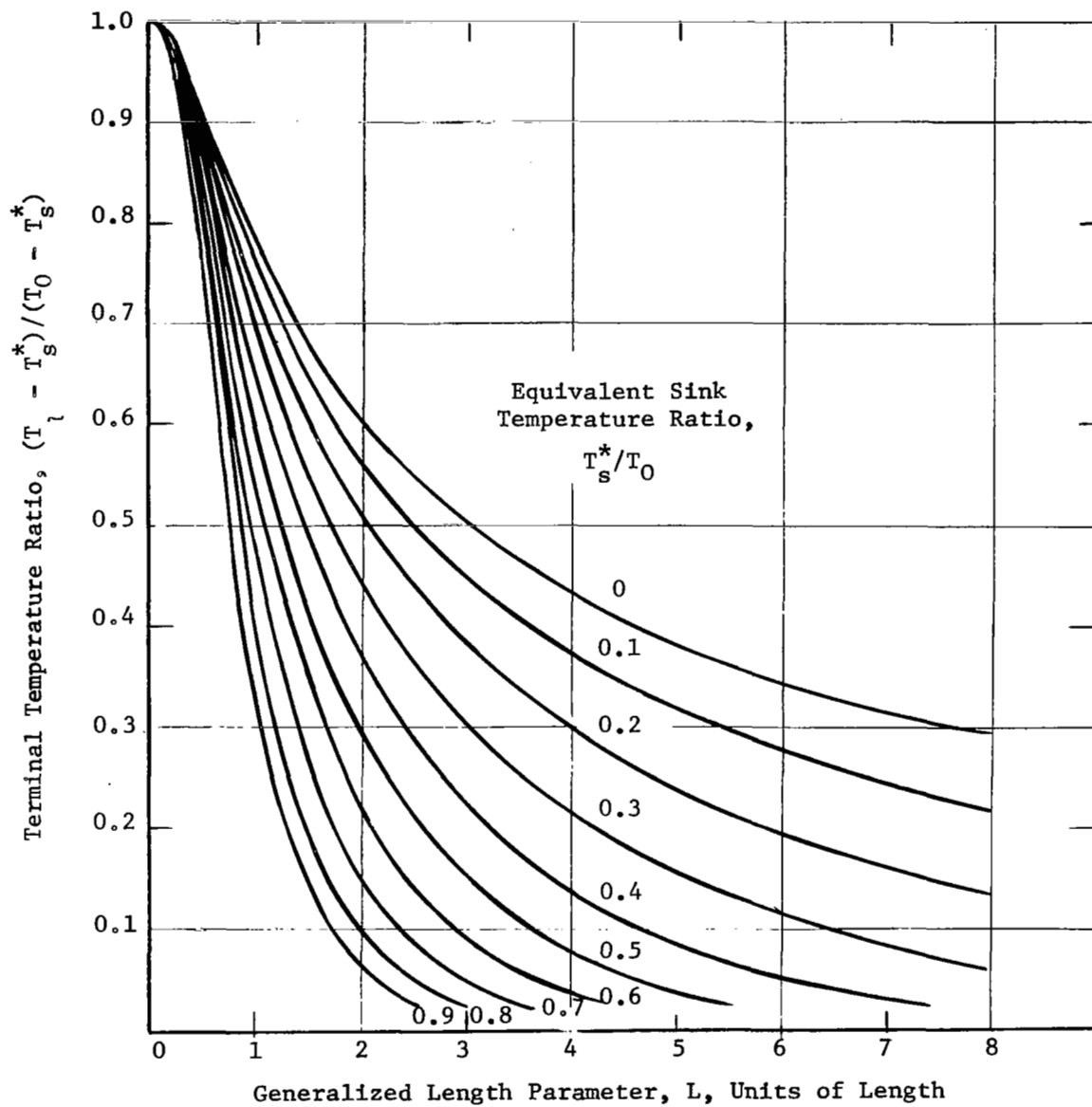


Figure 52. Variation of Terminal Temperature Ratio with Fin Plate Length.

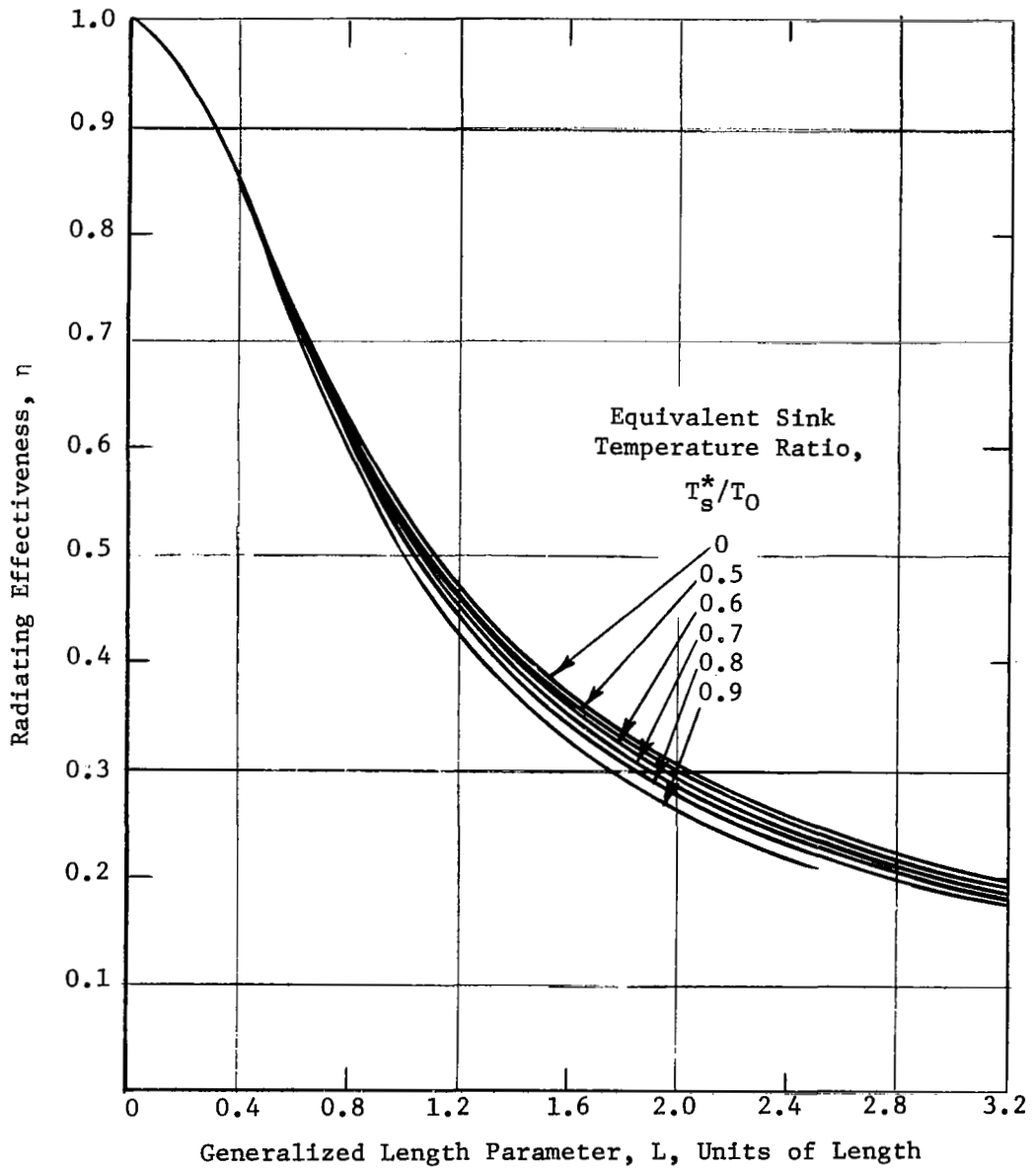


Figure 53. Variation of Radiating Effectiveness with Fin Plate Length.

which is a function of the temperature, will be neglected. It will be assumed that each coil dissipates one-half of the total power input.

Sodium heater

No. of coils	2
Material	Cb-1Zr
Electrical resistivity of Cb-1Zr	56×10^{-6} ohms-cm @ 2050°F
Electrical resistivity of sodium	74.8×10^{-6} ohms-cm @ 2050°F
Total length	73 inches
Tube ID	0.375 inch
Tube OD	0.245 inch

Resistance of one coil (tube only)

$$\text{Resistance of coil} = 1/2 \left(\frac{\rho_L}{A} \right) \quad (4a)$$

$$\text{Resistance of coil} = 1/2 \left(\frac{56 \times 10^{-6} \times 73}{\frac{\pi}{4} (0.375^2 - 0.245^2) \times 2.54} \right)$$

Resistance of coil = 0.0126 ohms

$$\begin{aligned} \text{Resistance of sodium in one coil} &= 1/2 \frac{\rho_L}{A} \quad (4b) \\ &= 1/2 \left(\frac{74.8 \times 10^{-6} \times 73}{\frac{\pi}{4} 0.245^2 \times 2.54} \right) \end{aligned}$$

Resistance of sodium in one coil = 0.0229 ohms

$$\begin{aligned} \text{Total resistance of each coil} &= \frac{1}{\frac{1}{R_{Na}} + \frac{1}{R_{Cb}}} \quad (4c) \\ &= \frac{1}{\frac{1}{0.0229} + \frac{1}{0.0126}} \end{aligned}$$

Total resistance of each coil = 0.00815 ohms

Assuming each coil will contribute 1/2 of the 1.74 kilowatts required, the current in each coil will be

$$I = \sqrt{\frac{P}{R}} \quad (4d)$$

$$I = \sqrt{\frac{870 \text{ watts}}{0.00815 \text{ ohms}}}$$

$$I = 326 \text{ amps}$$

The voltage drop across each leg will be

$$E = IR \quad (4e)$$

$$E = 326 \text{ amps} \times 0.00815 \text{ ohms}$$

$$E = 2.65 \text{ volts}$$

The total input current to the heater will be

$$I_{\text{Tot}} = 2 I = 652 \text{ amps} \quad (4f)$$

5. Internal Pressure Stress

The maximum pressure stress in the loop system is in the loop tubing.

$$S_H = \frac{P}{t} (r_i + 0.6 t) \quad (5a)$$

where

P = internal pressure, 190 psia

D = inside tube diameter, 0.25 inch

t = wall thickness, 0.065 inch

r_i = inside tube radius, 0.122 inch

$$S_H = \frac{190}{0.065} [0.122 + 0.6(0.065)]$$

$$S_H = 370 \text{ psi}$$

The stress required to produce 1% creep in 10,000 hours at 2200°F is reported to be approximately 1200 psi ⁽¹⁷⁾.

(17) Moss, Thomas A., "Materials Technology Presently Available for Advanced Rankine Systems," Nuclear Applications, Volume 3, No. 2, February 1967, p 74.

APPENDIX C

GRAIN GROWTH STUDIES ON Cb-1Zr TUBING

1. Previous Studies

Early in the program it was realized that the design of certain of the loop components, such as heater coils which required fabrication by bending, followed by test operation in the temperature range of interest, 2000-2300°F, might result in critical strain grain growth in the Cb-1Zr tube walls. The most pertinent previous research in this area was conducted by Murphy and his co-workers⁽¹⁸⁾

This study at Los Alamos was concerned with critical strain grain growth in three materials: unalloyed tantalum, tantalum plus 0.1 per cent tungsten, and tantalum plus 3 per cent tungsten. Varying amounts of deformation were introduced into the recrystallized fine-grained, 1/8-inch thick sheet material by rolling. Specimens of the three materials were then heat treated for one hour at their normal annealing temperatures (Ta, 1100°C; Ta-0.1%W, 1200°C; and Ta-3%W, 1600°C) and examined metallographically to determine the extent of critical strain grain growth in each. The grain size was plotted versus the per cent reduction, and the strain corresponding to the maximum grain size which developed during the heat treatment was defined as the critical strain. The critical strain values obtained for the three materials were as follows: Ta, 18%; Ta-0.1%W, 13%; and Ta-3.0%W, 9.5%. A typical example of the effectiveness of the critical strain in producing giant grains in this study may be seen in the results obtained for the Ta-0.1%W alloy. The grain size of the specimen which received 13% reduction was 400 microns, while a similar specimen with 40% reduction has a post-heat treat grain size of 50 microns.

2. Critical Strain Grain Growth Tests on Cb-1Zr Tubing Used to Construct the Sodium Thermal Convection Loop

It was concluded that the strain gradient introduced in the tube walls of the Cb-1Zr tubing for the Sodium Thermal Convection Loop during bending might result in even more exaggerated grain growth than observed in the sheet

(18) Murphy, D. J., Ferguson, W. E., and Hanks, G. S., "Critical Strain in High Purity Tantalum and Tantalum-Tungsten Alloys," LA-2871, Los Alamos Scientific Laboratory, June 24, 1963.

specimens of the study cited above which had no strain gradient. A plot of the maximum strain in 0.375-inch OD x 0.065-inch wall tubing as a function of bend diameter is given in Figure 54. This figure illustrates the outer fiber strains which develop when tubing of this size is plastically deformed in bending. Elementary bending theory would indicate that the cross section of the tubing remains unchanged and that maximum outer fiber stress in tension and compression are equal. In actual tube bending, the tube flattens slightly, the neutral axis moves closer to the forming die, and compressive strain is decreased from the simple theoretical value while the tensile strain is increased.

A modest test program was formulated to evaluate the critical strain grain growth problem in the 0.375-inch OD Cb-1Zr loop tubing using two bend diameters, 2.6 inches and 3.5 inches. These diameters were chosen as they were representative of the heater coil diameters selected in preliminary design layouts for the Sodium Thermal Convection Loop. The recrystallized Cb-1Zr tubing used in this study had an ASTM grain size of 6-8 and analyzed as follows: 1%Zr, 0.0136%O, 0.0009%N, 0.0020%C, and 0.0004%H. Twelve-inch lengths of the tubing were formed manually over the 2.6-inch diameter and 3.5-inch diameter dies. As may be seen in Figure 54, these bend diameters yielded maximum outer fiber strains of approximately 9% and 12%. Two transverse sections were carefully cut from the center of the bend of the formed tubing so as to obtain as uniform an amount of strain from sample to sample within a single bend as possible. After a pickling treatment, one sample of each bend diameter was wrapped in tantalum foil, placed in a tantalum container, and exposed for 165 hours at 2200°F in a vacuum of 1×10^{-5} torr. A second set of specimens was exposed to 2000°F for the same length of time and similar environmental conditions.

Metallographic examination of the heat treated samples revealed significant preferential grain growth over a considerable area on both the tension and compression side of the bends. Figure 55 shows a macrograph and a 100X micrograph of the sample formed over the 3.5-inch diameter die and heat treated for 165 hours at 2200°F. As is quite apparent in this illustration, the sharp strain gradient in the tube wall resulted in a very abrupt change in the grain size.

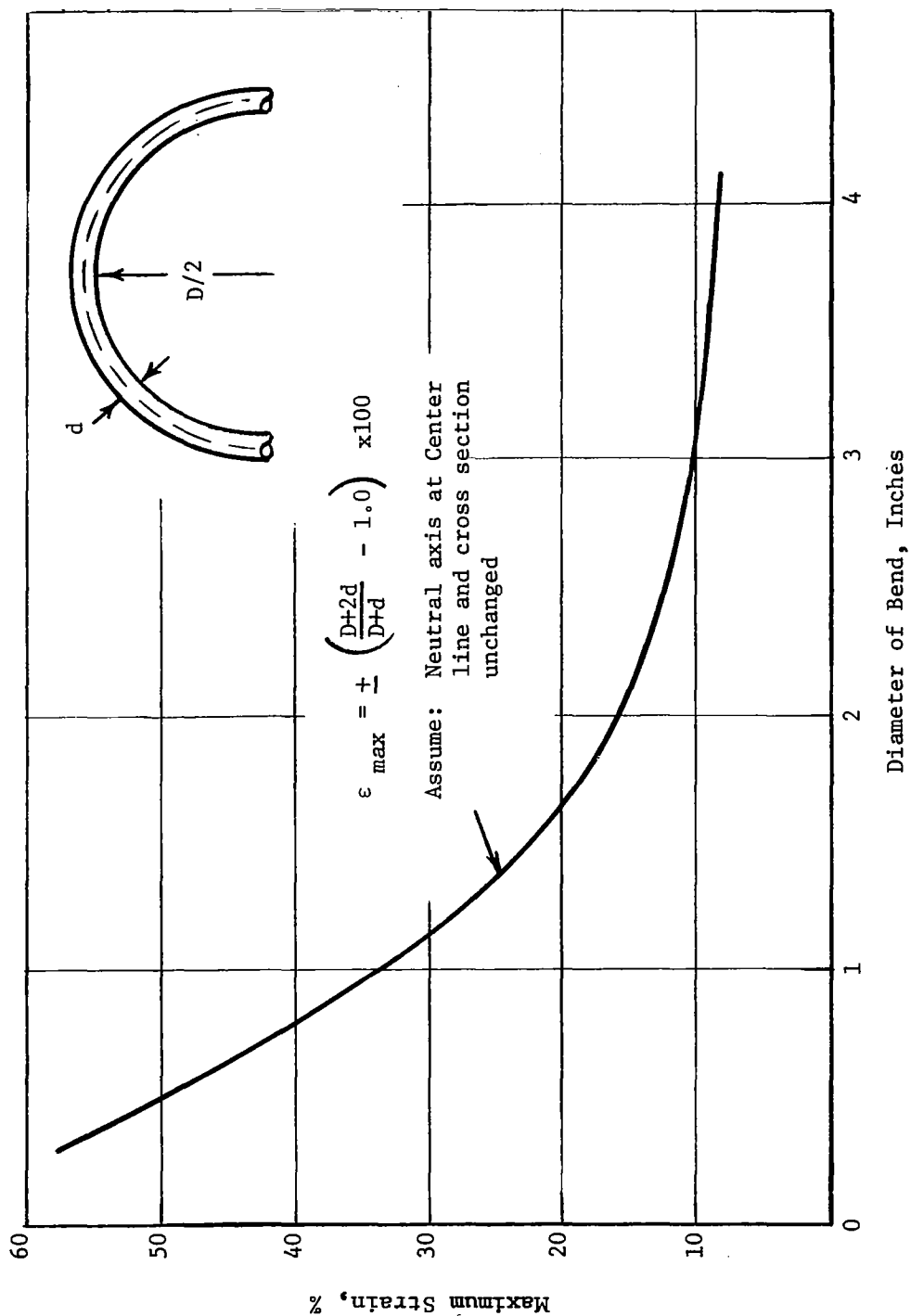


Figure 54. Effect of Bend Diameter on the Maximum Fiber Strain in 0.375-Inch OD x 0.065-Inch Thick Wall Tubing.

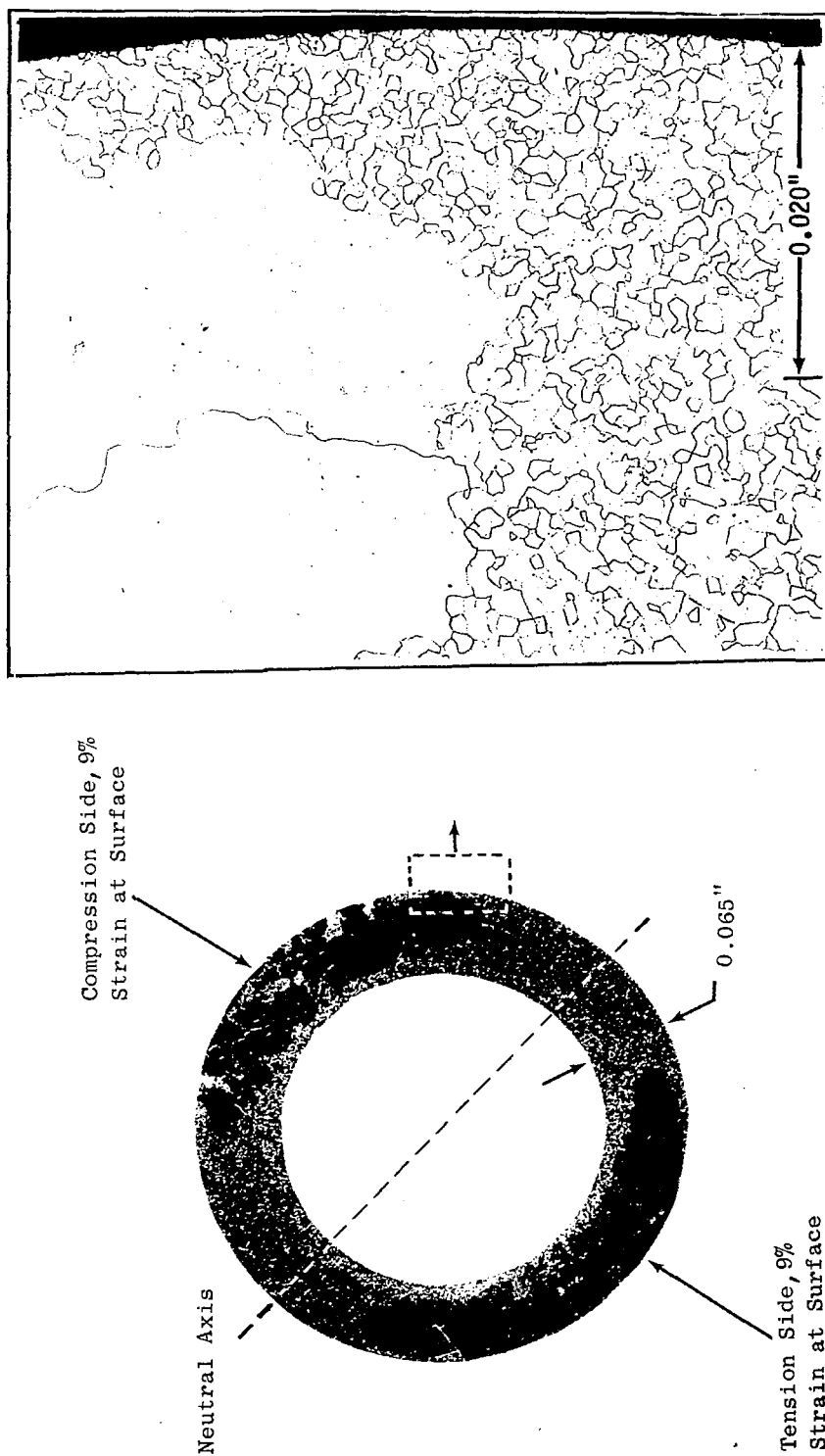


Figure 55. Cross Section of 0.375-Inch OD x 0.065-Inch Wall Cb-1Zr Tube. The Recrystallized Tube was Bent Around a 3.5-Inch Diameter Die and Subsequently Annealed for 165 Hours at 2200°F.

There was little difference in the magnitude of the grain growth between the specimens with the two bend diameters at a given temperature. However, the total volume of grain growth was less in those samples exposed at the lower temperature. The fine-grained structure, shown in Figure 55, is representative of the structure of the recrystallized tubing.

In order to determine whether this condition exists after a short time at elevated temperatures, one section of each bend diameter was vacuum heat treated for one hour at 2200°F and examined for evidence of grain growth. Initiation of growth was found only on the tension side of the sample formed over the 2.6-inch diameter die, as illustrated in Figure 56. This is not surprising since, as was pointed out earlier, the amount of strain on the tension side of the tube wall would be slightly greater than on the compression side.

As a result of these studies, it was anticipated that a considerable amount of critical strain grain growth would be observed in the hotter regions of the Sodium Thermal Convection Loop which were formed by bending, even though a slightly larger bend diameter (4 inches) was specified for the design than was used in the study described above. The 4-inch bend diameter gave a maximum strain of 8 per cent. The considerable grain growth that did occur is well illustrated in Figures 29, 30, and 31 of this report where some of the grains were observed to have grown to a size of 30 mils (760 microns).

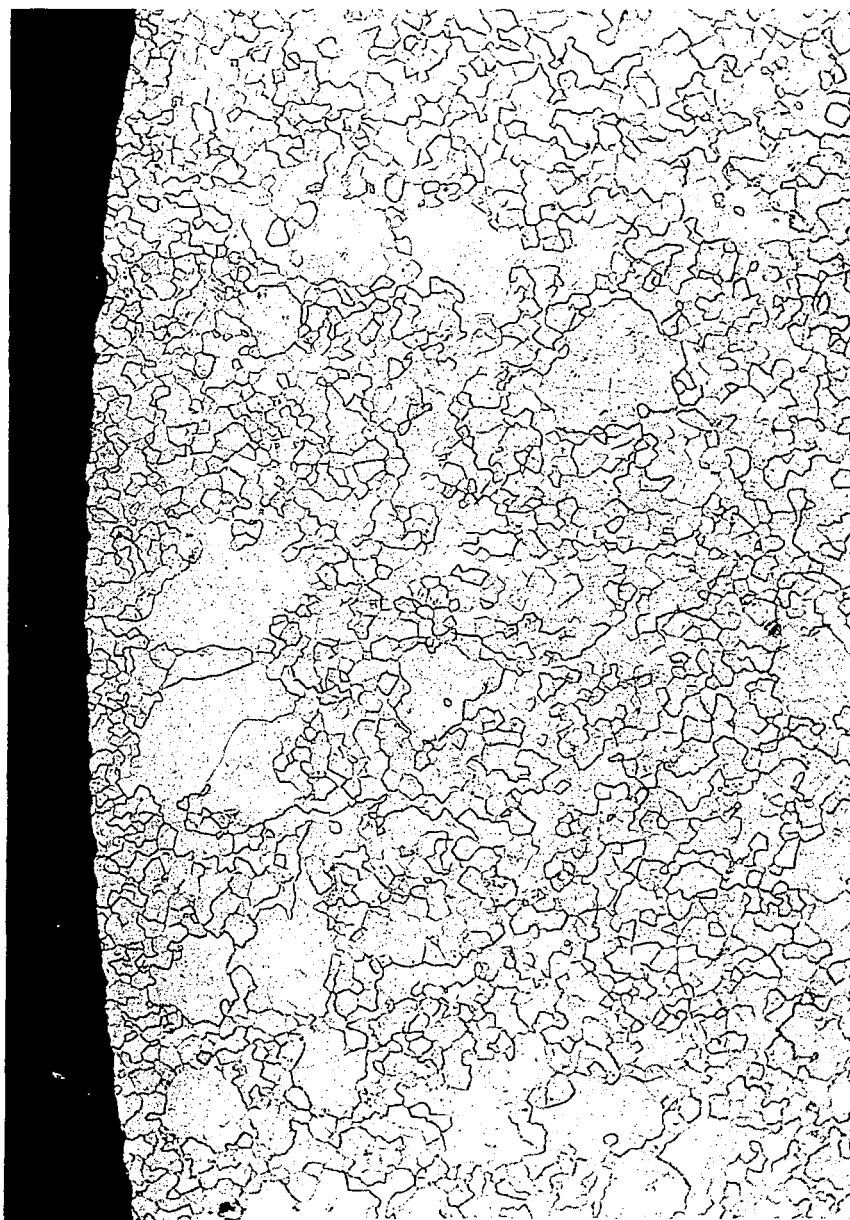


Figure 56. Micrograph of a Cross Section of 0.375-Inch Diameter x 0.065-Inch Thick Wall Cb-1Zr Alloy Tubing. The Recrystallized Tubing was Bent Around a 2.6-Inch Diameter Die and Subsequently Annealed for 1 Hour at 2200°F.

Etchant: 60%Glycerine-20%HF-20% HNO_3 Mag: 100X

XV. REFERENCES

- (1) Frank, R. G., et al., Potassium Corrosion Test Loop Development Topical Report No. 2: Material and Process Specifications for Refractory Alloy and Alkali Metals, General Electric Report R66SD3007, December 13, 1965.
- (2) Dotson, L. E. and Hand, R. B., Potassium Corrosion Test Loop Development Topical Report No. 4: Purification Analysis and Handling of Sodium and Potassium, General Electric Report R66SD3012, June 13, 1966.
- (3) Hendricks, J. W. and McElroy, D. L., High Temperature High Vacuum Thermocouple Drift Tests, ORNL-TM-833, August 1964.
- (4) Potassium Corrosion Test Loop Development, Quarterly Progress Report No. 4, for Period Ending June 15, 1964, NASA Contract NAS 3-2547, NASA-CR-54167, p. 65.
- (5) Personal communication, J. H. DeVan, Oak Ridge National Laboratory.
- (6) Albrecht, W. M., Mallett, M. W., and Goode, W. D., "Equilibria in Niobium-Hydrogen System," J. Electrochemical Society, 105 (1958) 219, pp 461-453.
- (7) Katz, O. M. and Gulbransen, E. A., Discussion Section, J. Electrochemical Society, 105/12 (1958) 756, p. 462.
- (8) Personal communication, C. E. Sessions, Oak Ridge National Laboratory.
- (9) Frank, R. G., et al., Potassium Corrosion Test Loop Development Topical Report No. 2: Material and Process Specifications for Refractory Alloy and Alkali Metals, R66SD3007, General Electric Company, Cincinnati, Ohio, December 13, 1965, p. 281.
- (10) Murphy, D. J., et al., "Critical Strain in High Purity Tantalum and Tantalum-Tungsten Alloy," LA-2871, Los Alamos Scientific Laboratory, June 24, 1963.
- (11) Rostoker, William and Dvorak, James R., "Interpretation of Metallographic Structures," Academic Press, New York, 1965, p. 28.
- (12) McCoy, H. E. and Douglas, D. A., "Effect of Various Gaseous Contaminants on the Strength and Formability of Columbium," Columbium Metallurgy, Interscience Publishers, New York, 1961, p. 112.
- (13) Bonilla, Charles F., Nuclear Engineering, McGraw Hill Book Co., Inc., New York, 1957, p. 452.
- (14) Dotson, L. E., "Emittance Coating Studies on Cb-1Zr Alloy," General Electric Company Report, R61FPD571, March 15, 1962.

- (15) McAdams, W. H., Heat Transmission, p. 118, McGraw Hill Book Co., Inc., New York, 1942.
- (16) Lieblein, S., "Analysis of Temperature Distribution and Radiant Heat Transfer Along a Rectangular Fin of Constant Thickness," TND-196, NASA, November, 1959.
- (17) Moss, Thomas A., "Materials Technology Presently Available for Advanced Rankine Systems," Nuclear Applications, Volume 3, No. 2, February 1967, p. 74.
- (18) Murphy, D. J., Ferguson, W. E., and Hanks, G. S., "Critical Strain in High Purity Tantalum and Tantalum-Tungsten Alloys," LA-2871, Los Alamos Scientific Laboratory, June 24, 1963.

06U OCT 42 51 305 68243 00903
AIR FORCE WEAPONS LABORATORY/AFWL/
KENTLAND AIR FORCE BASE, NEW MEXICO 87111

WILLIAM L. GARDNER, ACTING CHIEF TECH. LIAISON

POSTMASTER: If Undeliverable (Section-15
Postal Manual) Do Not Return

"The aeronautical and space activities of the United States shall be conducted so as to contribute . . . to the expansion of human knowledge of phenomena in the atmosphere and space. The Administration shall provide for the widest practicable and appropriate dissemination of information concerning its activities and the results thereof."

—NATIONAL AERONAUTICS AND SPACE ACT OF 1958

NASA SCIENTIFIC AND TECHNICAL PUBLICATIONS

TECHNICAL REPORTS: Scientific and technical information considered important, complete, and a lasting contribution to existing knowledge.

TECHNICAL NOTES: Information less broad in scope but nevertheless of importance as a contribution to existing knowledge.

TECHNICAL MEMORANDUMS:
Information receiving limited distribution because of preliminary data, security classification, or other reasons.

CONTRACTOR REPORTS: Scientific and technical information generated under a NASA contract or grant and considered an important contribution to existing knowledge.

TECHNICAL TRANSLATIONS: Information published in a foreign language considered to merit NASA distribution in English.

SPECIAL PUBLICATIONS: Information derived from or of value to NASA activities. Publications include conference proceedings, monographs, data compilations, handbooks, sourcebooks, and special bibliographies.

TECHNOLOGY UTILIZATION PUBLICATIONS: Information on technology used by NASA that may be of particular interest in commercial and other non-aerospace applications. Publications include Tech Briefs, Technology Utilization Reports and Notes, and Technology Surveys.

Details on the availability of these publications may be obtained from:

SCIENTIFIC AND TECHNICAL INFORMATION DIVISION
NATIONAL AERONAUTICS AND SPACE ADMINISTRATION
Washington, D.C. 20546